Implications of direct contacts between mule deer (*Odocoileus hemionus*) on transmission of chronic wasting disease

by

Maria Angelica Dobbin

A thesis submitted in partial fulfillment of the requirements for the degree of

Master of Science

in

Ecology

Department of Biological Sciences
University of Alberta

Abstract

Chronic wasting disease (CWD) is a fatal, prion disease of cervids that was first detected in Alberta in 2005. Transmission of CWD occurs by direct contact with an infected individual or via contaminated environments. I investigated the seasonal effects of landscape heterogeneity on direct, sex-specific (same or mixed sex) contacts of individuals within and between groups of mule deer (*Odocoileus hemionus*) in central eastern Alberta. Using data from collared deer, I determined group membership based on simultaneous movement, pair-wise relatedness from genetic sampling at capture, contact rates based on proximity loggers, and habitat characteristics of dyad (pairs) in space-use overlap based on GPS telemetry. I found that within-group contact rates were several orders of magnitude higher than between-group contacts, contact rates were unrelated to genetic relatedness, and within-group contacts rates were more dependent on the sex of individuals, between-group rates were more influences by habitat. I also determined where seasonal contacts were most likely to occur by comparing habitat characteristics of contact locations to random locations within areas of shared space use. In winter, contacts occurred in areas with higher use by deer, whereas in summer contact locations were less constrained and were more varied between sexes. The exceptions were that contacts were more likely to occur than expected by use in areas of limited woody cover in both winter and summer, less likely to occur in forest-open edges in winter, and closers to roads in summer. Predictions of where contacts occur among within and between-group male dyads in winter and between-group female dyads in summer were the best predictors of CWD risk derived from hunter-harvested infected deer detected during Alberta's CWD surveillance program. My results suggest that the pattern of CWD risk on the landscape is related to areas of deer contact, and that the seasonal, sex-specific

contact rates may better inform transmission in spatially explicit models to help guide management strategies for an emergent wildlife disease.

Preface

This thesis is an original work by Maria A. Dobbin. The research project, of which this thesis is a part, received research ethics approval from the University of Alberta Research Ethics Board for both time periods, project name “Chronic Wasting Disease: Mule Deer Contact Rates”, AUP00001461 and AUP00001369, 2007-2011 and 2017-2021.

To date, no manuscripts have been submitted for publication

Acknowledgements

Thank you to my supervisor Evelyn Merrill for being my mentor and motivator throughout this process. I am so grateful to have had this opportunity. I'd also like to thank Kathreen Ruckstuhl and Viktoria Wagner for serving on my committee and providing me with valuable feedback.

To the members of the CWD team, Kelsey Gritter, Peter Smolko, Laurens Put and Jingjing Xu, thank you for all your input and hard work. It's been great to see the project grow, and I am lucky to have been a part of it.

A very special thank you to Johanna Thalmann for your work on the project and for being the best field partner I could have asked for. I'd also like to thank all the hard-working research technicians that have contributed to various aspects of this project including Liam Horne, Gary Elaschuk, Greg Melvin, Alia Schamehorn and our various other volunteers.

I'd like to thank my parents, Mark and Sandra, for their endless support and frequent care packages and my siblings, Megan and Michael, for always being there when I need it. Thank you to Maria for being my number one supporter throughout this process, it means the world to me. Thank you, Liam, for your love, support and endless energy that kept me positive and reminded me to be excited about science.

Thank you, Sam, and Heather Seim, for opening your home to a couple of ridiculous biologists you knew nothing about. Your continued hospitality and generosity made all the difference during my field seasons. My time at the farmhouse was the first place I can remember where Alberta felt like home. I am happy to have met you and am eternally grateful to Sam for helping me to dislodge mud stuck field trucks on more than one occasion.

Final shout out to Steve Irwin for being my original inspiration for choosing a career in wildlife biology.

Table of Contents

List of Tables

List of Figures

CHAPTER 1 – INTRODUCTION

Emergent wildlife diseases have attracted significant interest in ecological and public health disciplines as the effects of climate change and human land use exacerbate the consequences of epizootic incidents (Daszak et al. 2001; Epstein 2001; Altizer et al. 2013; Hoque et al. 2022). Disease-related impacts in wildlife populations can include loss of biodiversity (Grogan et al. 2014), population declines and extinction (Daszak et al. 1999; De Castro and Bolker 2005; McCallum 2009), and emergence of zoonotic diseases (Daszak et al. 2007; Meurens et al. 2021). Effective management of emergent wildlife disease depends on the ecology of the host-pathogen system, the stage of pathogen invasion (Langwig et al. 2015), as well as public and stakeholder support (Carstensen et al. 2011). Thus, identifying appropriate management action can be challenging and requires sufficient knowledge of specific host-pathogen systems and an understanding of underlying mechanisms that facilitate the spread of disease.

Disease transmission is a key process that drives host-pathogen dynamics. Typically, epidemiological models describe the rate of change in number of infected individuals (I) as

$$dI/dt = \beta Sp$$

where the transmission parameter (β) is the product of *c,* contact rate, and *v,* the probability of successful disease transmission given a contact, *S* is the number of susceptible individuals and *p* is the probability that the contact occurs with an infected individual (Anderson and May 1979; May and Anderson 1979; Begon et al. 2002a). The transmission parameter can be modeled as density-dependent (DD), which assumes that contact rate increases linearly with population density and takes the form:

$$dI/dt = \beta SI/A$$

in which A is the area that contains the population and contact rate increases with the overall density of hosts. Alternatively, frequency-dependent (FD), assumes contact rate is independent of density:

$$dI/dt = \beta' SI/N$$

where N represents the total number of hosts and β' is adjusted because rate of contact is constant irrespective of host density (Begon et al. 2002a). However, empirical studies have demonstrated that contact rates can follow non-linear relationships with host density, where contacts increase linearly at relatively low densities but eventually become saturated at high densities (Ji et al. 2005; Smith et al. 2009b; Habib et al. 2011). Thus, appropriate transmission functions can represent an intermediate between DD and FD formulations resulting from contact heterogeneities facilitated by social grouping patterns (Habib et al. 2011), seasonal behaviours (Smith et al. 2009b), and landscape features (Tardy et al. 2018a).

Quantifying contact dynamics relevant to disease transmission is required to accurately parametrize models of transmission. However, the frequency and nature of interactions among hosts are difficult to observe in nature and, as a result, are usually extrapolated from behaviour recorded between pairs of monitored individuals (Whitehead 2008). In recent years, advancements in bio-logging technology have allowed for more thorough quantification of pairwise contacts. For example, proximity loggers record contact events at a predetermined distance threshold to record relevant interactions between individuals and, in recent years, even record the GPS location associated with each encounter. However, pairwise sampling techniques are subject to sampling biases because monitoring all individuals in a population is not feasible. Alternatively, estimations of pairwise rates between classes, such as age, sex, and species, can be

used to populate models that quantify total per capita contacts, particularly when the population composition is known (Habib et al. 2011; Cross et al. 2013; Tardy et al. 2018b). Estimations of per capita contact rates describe contact dynamics and are useful for inferring mechanisms of spread such as DD vs FD transmission. However, incorporating parameters for simulating disease transmission is computationally expensive, particularly when accounting for distinct host classes. Alternatively, mathematical compartmental susceptible-infected (SI) models are frequently used in disease ecology to describe the spread of epidemics. Potapov et al. (2013) estimated plausible routes of disease transmission using continuous-time population SI models where different β parameters were derived between host classes that represented differences in direct contacts between different sex and age types. The models were used to describe possible explanations for patterns of chronic wasting disease (CWD) prevalence observed in free-ranging deer populations but did not account for heterogeneity driven by variable landscapes. Thus, knowledge of landscape factors affecting contacts dynamics could offer useful insights into mechanisms of CWD transmission.

CWD is an invariably fatal, transmissible spongiform encephalopathy (TSE) that has been detected in free-ranging mule deer (*Odocoileus hemionus*), white-tailed deer (*O. virginianus*), elk (*Cervus canadensis*), and moose (*Alces alces*) throughout North America, including three Canadian provinces and 28 US states (Miller and Vaske 2022). In recent years, CWD has also been detected in free-ranging moose, reindeer (*Rangifer tarandus*), and red deer (*Cervus elaphus*) across Finland, Norway, and Sweden (Mysterud and Edmunds 2019a; Vikøren et al. 2019). Prions, the infectious agents of CWD, collect in the nervous system of infected individuals, are shed through bodily fluids such as saliva, blood, urine, and feces (Haley and Hoover 2014), and are capable of persisting in the environment for years (Miller et al. 2004). As

a result, CWD can be transmitted either by direct contact between individuals or by contact with contaminated environments. CWD is of growing concern among management agencies because of the potential to cause population declines (Edmunds et al. 2016; Devivo et al. 2017) and fiscal repercussions such as management costs for herd reductions and surveillance efforts, and loss of hunting revenue (Bollinger et al. 2004; Uehlinger et al. 2016). Further, as there is currently no vaccine or cure, the management of CWD is largely limited to targeted removal of potential hosts (Miller et al. 2020). Thus, it is essential to understand how the disease is spread throughout populations to make timely management decisions that prevent or slow the spread of CWD into new regions.

Simulated models of CWD dynamics are largely dependent on transmission parameters, which are notoriously difficult to estimate. Thus, quantifying contact rates is a useful tool to infer mechanisms explaining spatial and demographic patterns of disease prevalence. Since it was first detected in 2005, over 3500 cases of CWD have now been recorded in free-ranging deer throughout Alberta with the highest prevalence (14.8%) in mule deer relative to (5.0%) white-tailed deer and is more frequent in males than females in both species (Alberta Government 2022). The patterns of prevalence observed in Alberta persist across multiple jurisdictions, which could indicate that behavioural differences between host classes are influencing transmission dynamics via heterogeneous contact rates (Miller et al. 2000; Rees et al. 2012). Similarly, spatial structuring in the distribution of CWD has been attributed to host movements and aggregations that could reflect elevated rates of direct contact. For example, forested habitats have consistently been identified as relevant predictors of CWD prevalence (Storm et al. 2013b; Evans et al. 2016; Hefley et al. 2017). In the northeastern United States, forested landscapes were inversely related with CWD prevalence which researchers attributed to greater dispersal distance

by white-tailed deer when forest cover was limited (Evans et al. 2016). In Alberta, risk of CWD was greatest in agricultural areas that facilitate the formation of isolated patches of woody cover and potentially cause deer to aggregate and come in contact with individuals from different social groups (Smolko et al. 2021).

In this thesis I investigated the influence of inherent deer characteristics and landscape factors on pairwise contacts then related them to published prediction of CWD risk in the same area. I used GPS collars enabled with proximity loggers to collect contact data from mule deer collared in 2019-2020. Recent advancements in bio-logging technology allow for fine scale location and association data on highly mobile wildlife, thereby providing new opportunities to measure frequency and specific locations associated with direct contact events. In Chapter 2, I quantified seasonal pairwise contacts rates between conspecific mule deer in east-central Alberta. These estimates will eventually be used to parameterize hunter harvest models in a collaborative project centered on CWD management. I first established criteria for biologically relevant seasons and delineated dyads (deer pairs) as members of the same or separate social groups based on correlated movements and shared space use. I measured differences in contact rates between group types (within, between), season (winter, summer, rut) and dyad type (female-female, male-male or mixed sex) to quantify the effect of seasonal grouping patterns. Then, I modelled seasonal, pairwise contact rates as a function of genetic relatedness, shared space use, landscape covariates and dyad type to determine the relative influences of social and environmental factors while accounting for group membership and overlapping space use. In Chapter 3, I use the same classifications of deer groups, and dyad types to predict the seasonal probability of direct contacts between deer across heterogeneous landscapes. I modelled contact location as a function of landscape covariates by comparing known contact locations to random

points generated within areas of home range overlap. I used my predictions of contact probability from the best supported model to create predictive surfaces that I related to maps of CWD risk in the same areas (Smolko et al. 2021). Finally, in Chapter 4, I used the information in the previous Chapters to discuss the significance of my findings, some limitations and how my work can advance CWD management.

CHAPTER 2 - CLOSE ENCOUNTERS: EFFECTS OF GENETIC RELATEDNESS AND LANDSCAPE ON MULE DEER CONTACT RATES

INTRODUCTION

Wildlife diseases pose a significant threat to free-ranging populations across the globe, especially as they interact with ongoing habitat degradation and climate change (De Castro and Bolker 2005; McCallum 2009; Altizer et al. 2013). For many wildlife diseases, a major route of pathogen transmission is through direct contact between infected and susceptible individuals (Craft 2015; VanderWaal and Ezenwa 2016; Arthur et al. 2017). The variable contributions by hosts to disease dynamics depend on the frequency and types of interactions with conspecifics. Host transmission has been related to sex, age, social affiliations, and to the spatial configuration of habitat that influence host distributions and aggregations (Gudelj and White 2004; Ostfeld et al. 2005a). The resultant heterogeneity in contact rates between individuals leads to differential rates of disease transmission. Thus, understanding the sources and dynamics of contact heterogeneity is key in epidemiological modeling to better predict rates of disease spread and inform management strategies (Cross et al. 2012; Manlove et al. 2017; Pepin et al. 2021).

In gregarious species, conspecific contact rates occur within and between social groups at different rates, where within-group contacts are typically more frequent (Altizer et al. 2003). For example, within-group contact rates in wild boar (*Sus scrofa;* Podgórski et al. 2017) and cervids (Schauber et al. 2007, 2015) have been reported as 5-20 times higher than between-groups. Contact rates within social groups have been related to seasonal changes in the attraction of group members, familial ties, and sex-based behavioural differences (Bansal et al. 2007; Herrera and Nunn 2019). Sexual segregation is hypothesized to have evolved to improve reproductive performance through reduced sexual harassment, foraging dynamics, and sex-based differences

in predation risk, that ultimately reduces intraspecific competition (Chapman et al. 2003, Main et al. 1996; Ruckstuhl and Neuhaus 2000; Pérez-Barbería et al. 2005). However, mixed evidence exists for the role of sexual segregation in host-disease dynamics. Parasite impacts in simulated populations of alpine ibex (*Capra ibex*) were lower when the degree of sexual segregation was increased (Ferrari et al. 2010). Further, some research suggests that sexual segregation can lead to differential sex-specific prevalence levels resulting from high frequencies of infectious contacts within sexually segregated groups (Härkönen et al. 2007; Potapov et al. 2012; McDonald et al. 2014). In polygamous mating systems, which is common among mammals, infectious, mixed-sex contacts during breeding seasons may comprise major routes of disease spread between groups (Garvin et al. 2003; Ji et al. 2005; Uchii et al. 2011). For example, epidemiological modeling of chronic wasting disease (CWD) showed that the high CWD infection levels reported in male deer across jurisdictions at the beginning of an CWD epidemic (Miller and Conner 2005; Osnas et al. 2009; Smolko et al. 2021) were lost when the effects of sexual segregation were omitted (Potapov et al. 2012, Orby et al. 2014).

Genetically related individuals also may contribute to disease transmission within and between groups if genetically related conspecifics interact more frequently (Real and Biek 2007). In some species, relatedness among individuals is a key driver of social structure, such as dolphins (*Tursiops aduncus*) where genetic relatedness was positively correlated with association strength in females (Wiszniewski et al. 2010) or in elephants (*Loxodonta africana*), where males were more likely to associate with related individual than their non-related counterparts (Chiyo et al. 2011). Although relatedness is not always a reliable predictor in socially structured species, Vander Wal et al. (2012) found close-contact interaction rate and duration did not covary with genetic relatedness in elk (*Cervus canadensis manitobensis*). Contacts within family groups can

have quantifiable patterns in disease dynamics such as white-tailed deer *(Odocoileus virginianus*), where individuals infected with bovine tuberculosis were more genetically related than non-infected deer (Blanchong et al. 2007). In wild boar (*Sus scrofa*), infection risk of African swine fever was positively correlated with genetic relatedness and spatial proximity to nearby infected individuals (Podgórski et al. 2021). Researchers concluded that risk of infection was dependent on the mechanisms of transmission, where genetic relatedness was more influential for infections occurring by direct contact between hosts when compared to those resulting from contamination by infected carcasses. In matriarchical societies, related inidividuals often reside in close proximity, where interactions between kin may be correlated with increased shared space use (Mathews and Porter 1993; Grear et al. 2010; Carter et al. 2013; Podgórski et al. 2021). Indeed, Cullingham et al. (2011) found strong spatial correlation in relatedness between mule deer at small spatial scales (2km) and determined pairwise relatedness was greater between CWD infected deer than in sympatric noninfected deer. However, when inferring rates of infection, it is possible that interaction between individuals is confounded with space use overlap.

Space use overlap has been positively correlated with contact rates across some taxa (Robert et al. 2012; Best et al. 2014; Sanchez and Hudgens 2015; Pepin et al. 2021). However, the relationship is not always linear, suggesting other factors such as resource composition and configuration may also affect contact dynamics (Habib et al. 2011; Hernández et al. 2020). Contact rates may be elevated where animals are attracted to high quality resources (Ostfeld et al. 2005a; Real and Biek 2007; Tardy et al. 2018) including those that are ephemeral or seasonally variable (i.e., salt licks (Plummer et al. 2018), water sources (Dudley et al. 2016), and artificial feed sites (Bradley and Altizer 2007)). For example, contact rates between elk were 2.6

times greater during periods of supplemental feeding, compared to the baseline rate in winter, as animals clustered around food sources (Janousek et al. 2021). Meanwhile, overall prevalence of avian influenza virus was greatly increased in spring, compared to estimates throughout the rest of the year, during the migration of ruddy turnstone (*Arenaria interpres*), when the density of birds is inflated because of large aggregations foraging on the eggs of horseshoe crabs in Delaware Bay (Krauss et al. 2010). Regardless of whether habitat attractions are resulting from artificial sources, seasonal variability or natural landscape heterogeneity, the resultant increase in rates of direct contact can influence heterogeneity in transmission of infectious wildlife diseases.

CWD is an emerging disease that has the potential to reduce populations of cervids (Edmunds et al. 2016; Devivo et al. 2017). The disease is an invariably fatal transmissible spongiform encephalopathy (TSE) that has been detected in free ranging cervids in 28 US states and 3 Canadian provinces (Miller and Vaske 2022). CWD is spread through infectious prions transmitted by direct contact between hosts or environmental contact in contaminated areas (Miller and Wild 2004). Patterns in CWD prevalence have emerged where mule deer (*Odocoileus hemionus*) and white-tailed deer (*Odocoileus virginianus*) are sympatric, that indicates CWD infection are 1.6 to 4.2 times higher in mule deer (Rees et al. 2012; Smolko et al. 2021; Colorado Parks and Wildlife 2022) and 2-3 times higher in males relative to females (Miller and Conner 2005; Osnas et al. 2009; Jennelle et al. 2014). Although the primary routes of CWD transmission are not fully understood, there is evidence to suggest that disease dynamics in the early stages of an epizootic are driven by direct contacts rather than environmental transmission (Ketz et al. 2019), indicating behavioural differences between host classes are likely to dictate early transmission routes (Potapov et al. 2013a; Storm et al. 2013b).

In this thesis we quantify seasonal contact rates between individual pairs of mule deer (hereafter referred to as dyads) within sex-specific group types and assess the influence of social, genetic and environment influences on contact rates. Specifically, we measured daily contact rates based on proximity loggers and compare these seasonal changes to the same trends using contacts derived from GPS locations. We then related seasonal contact rates within and between groups of sex-specific dyads to extent of overlap, genetic relatedness, and landscape covariates within the overlap between home ranges. We modelled within and between-group contacts separately because we expected higher within group contact (Schauber et al. 2007), and used a two-component hurdle model to model between group contacts because many groups had zero contacts. We expected 1) the extent of space-use overlap to be the strongest predictor of contact rates, but where overlap was low, contact rates would increase with genetic relatedness, 2) within-group contact rates would be highest and least variable seasonally compared to between-group rates. However, in summer, within-group contact rates of male dyads would be lower than females due to lower cohesion of bachelor groups (Lingle 2003, Mejia-Salazar et al. 2017), and 3) between-group contact rates would be highest in winter because deer are most concentrated, and contacts would be higher in areas of space use overlap when the extent of quality deer habitat, such as woody cover (Nixon et al. 1991; McClure et al. 2005) and agricultural areas (Carrollo et al. 2017), was high. We focused on mule deer because they had the highest CWD prevalence in Alberta (Smolko et al. 2021).

MATERIALS AND METHODS

Study area

The study area was located southeast of Edgerton, Alberta in the east-central portion of the province within the prairie-parklands ecoregion (Fig. 2.1). Deer collaring took place in a Heritage Rangeland Natural Area called Cresthill Grazing Lease (CGL). The area is characterized by rolling hills and sand dunes with elevation ranging from 546 to 782 m. Landcover consisted of a matrix of agricultural fields (48%), pastures and native grasslands (19%), interspersed with woody cover (20%). Agricultural cover is composed of annual crops such as canola (*Brassica* spp.), wheat (*Triticum spp*.) and alfalfa (*Medicago* spp.) or perennial crops and tame grasses for pasture. We defined woody cover to include deciduous tree stands (*Populus spp*.), and tall shrubland *(Elaeagnus commutata*, *Salix* spp., *Prunus* spp., and *Amelancier alnifolia*). Human development (1%), wetland (7%), water (3%), and exposed land (1%) make up the remaining coverage. Landcover was mapped based using a a multi-temporal remote sensing approach, combining Landsat 5 TM satellite imagery and field verification (Merrill et al. 2013). Land use included cattle pasturing between 1 June – 31 October to graze the native grasslands, and human development consisted of paved and gravel roads as well as clearings for oil and gas, development of seismic lines, pipelines, access roads, OHV trails, and well-sites. Other land uses include recreation areas such as a golf courses and campgrounds.

The study area falls within Wildlife Management Unit (WMU) 234, which has been among the mandatory units for submission of harvested mule deer and white-tailed deer heads for CWD testing since 2006. In 2019, prevalence of CWD in male mule deer ranged from 31 to 55% (Alberta Government 2022). Other ungulates commonly found within the study area include elk (*Cervus canadensis*) and moose (*Alces alces*). Hunting season with rifle runs between

1 November to 30 November (mule deer, white-tailed, and moose) and 1 November to 20 January (elk). The coyote (*Canis latrans*) is the primary predator of deer within the study area, with possible but rare predation by black bears (*Ursus americanus*) and cougars (*Puma concolor*).

Deer capture, collaring, and monitoring

We collared mule deer on the CGL January 23 - 30 in 2019 and 2020 (Appendix A). Deer were located by helicopter, captured using a net gun, and immobilized with xylazine or Butorphanol-Azaperone-Medetomidine. We collected 4-mm ear samples using biopsy punches that were stored in 95% ethanol, and or blood from the jugular vein from all individuals for genotyping. Both sample types were refrigerated at -20°C before analysis. Deer were fitted with Lotek Litetrack 420 collars (Lotek Wireless Inc., Newmarket, ON) equipped with a proximity logger (PL) and global positioning unit (GPS). GPS schedules were programed to record deer locations at 2-hour intervals on even hours throughout the day. If GPS relocations could not be recorded instantaneously, collars would reattempt to record locations for three minutes then end telemetry efforts until the next scheduled upload. Overall fix rate success ($\mu \pm SD$) in this relatively open environment was 94.9% ± 8.6. The VHF signal from PL devices were programed to transmit 20 bpm and thus, had the potential to communicate with another PL every three seconds. We selected a RSSI threshold of -100 dBm after conducting a series of preliminary distance trials (Appendix B) to assess the value at which PLs record proximity of other devices to obtain contact events within approximately three meters. Once PLs passed outside the RSSI threshold for a minimum of five minutes, the ongoing contact event was terminated.

Biological seasons

We defined three biological seasons (winter, summer, rut) based on rates of change in pairwise movements of deer dyads to reflect potential changes in social grouping that would correspond to distinct, seasonal contact rates (van Beest et al. 2013). We modeled changes in pairwise, nearest neighbor distances across collared deer each year and delineated inflection point demarcations between seasons. Nearest neighbour distances were calculated as the distance between each dyad when both deer were sampled simultaneously and were reported as the average daily pairwise distance (m day $^{-1}$). We set a time threshold for simultaneous locations of 3 minutes and included only nearest neighbor distances for those with a volume of intersection (VI) value greater than zero. We predicted the changes in nearest neighbor distances with general additive mixed-effects model analysis (GAMM) as a function of Julian day, smoothing with a cubic regression spline and using dyad ID as a random effect based on the restricted maximum likelihood (REML) method in the mgcv package (Wood 2004, RStudio Team 2019). The start of a season was delineated at inflection points along the first derivative of the predictive curve produced by GAMM. We used the first derivative to identify inflection points from periods of increase to decrease that we interpreted as start dates for summer and rut seasons. This approach did not identify a clear change in movements between November and late January to reflect winter movements, therefore we used winter start dates delineated by Silbernagel (2010; Appendix C).

Within and between-group membership

We modified the general approach of Schauber et al. (2007) and distinguished whether two deer were considered in the same or different groups at the time of the contact based on two metrics: 1) space-use overlap and 2) direction and displacement between simultaneous timesteps of a deer dyad. We quantified space-use overlap using volume of intersection (VI; Millspaugh et al. 2004)

where the seasonal utilization distributions of both deer intersected. Movement displacement and direction was based on the global dynamic interaction index (DI; Nelson and Long, 2013), where simultaneous consecutive fixes were compared for each deer pair. We ordered the values of DI and VI from lowest to highest by season and modeled each metric as a function of dyad rank order along the X axis to confirm a broken stick regression of each metric performed better than the linear model using the segmented package (Muggeo 2017) in R (R Core Team 2019). If the values for both metrics were above the corresponding threshold, we considered that dyad to be in the same (within) group, if one or both metric values were below the corresponding threshold the dyads would be considered as members of different (between) groups (Appendix D).

Genetic Relatedness

Genetic relatedness of dyads was based on tissue samples collected from all collared deer during capture. We used Qiagen DNeasy® Blood & Tissue column kits, following standard protocol for DNA extractions as outlined by the manufacturer (Qiagen, Mississauga, Ontario, Canada). Samples were amplified for each individual in three multiplexes for a total of 16 loci per sample. The samples were then diluted before running on a 3730 ABI sequencer (Cullingham et al. 2011a). Alleles were assigned using GeneMapper (Currie-Fraser et al. 2010). We quantified pairwise relatedness using the relationship coefficient R estimated according to Queller and Goodnight (1989) using the related package (Pew et al. 2015) in R (RStudio Team 2019). Queller and Goodnight relatedness estimator values are hereafter referred to as QG estimates. Next, we compared values between seasons for within and between-group types separately using a Mann-Whitney U test. We used a Kruskal-Wallis test and a Dunn post-hoc test for multiple comparisons with adjusted p-values to compare between dyads types in each group type and season, separately. We calculated seasonal VI for each dyad based on seasonal UDs, where VI is

a 3-dimensional overlap index of joint space use of a dyad with values ranging between zero (no overlap in space use) to 1 (identical overlap in space use, (Seidel 1992; Millspaugh et al. 2004) and compared mean VI and QG estimates between group types across seasons and dyad types.

Seasonal contact rates

We determined daily contact rates for sex-specific dyads (female-female, F; male-male, M; mixed-sex, Mix) within and between groups by season. We first tested for differences in contact rates within and between group types across all seasons and dyad types, and then for differences in contact rates between seasons by group types using a Mann-Whitney U test. Finally, we compared daily contact rates between dyad types within season and group type using a non-parametric Kruskal-Wallis test and a Dunn post-hoc test for multiple comparisons with p-values adjusted by the Benjamini-Hochberg method (Dunn 1964; Benjamini and Hochberg 1995). We modelled contact rates between all dyads with overlapping utilization distributions as a function of VI for each group type, season, and dyad type. After visually assessing the relationship between contact rates and VI, we compared three model structures using generalized linear models (GLMs) to determine the shape of the relationship including 1) linear regression, 2) GLM with an inverse link, and 3) GLM with a gamma distribution. We determined best model fit using Akaike's Information Criterion (AIC) model selection.

Comparison of Concurrent GPS and PL Derived Seasonal Contact Rates

To assess the reliability in the trends of proximity logger (PL) based contact rates, we also derived daily contact rates using concurrent GPS locations for the same sample of deer. We defined a contact event when the simultaneous locations of two GPS-collared deer were within ≤ 25 meters using the package spatsoc (Robitaille et al. 2018) in R (R core team 2019). We chose the 25-meter criterion to account for collar error (6.2 ± 1.0 m) in the study area and a ≤ 3-minute

window to reflect active periods of satellite search time for collars (Appendix E). We also summarized contact rates as the average number of daily contacts. We compared trends in daily contact rates recorded by PL and GPS rates using Kendall rank correlations for the same dyad within and between-group types by season.

Modeling seasonal contact rates

We assessed factors influencing daily contact rates within and between groups by modeling them as a function of dyad type, genetic relatedness, volume of intersection (VI), and metrics of environmental characteristics measured within the dyad's UD overlap (Table 2.1; Appendix F). We used distinct modeling approaches for modeling dyad-specific contact rates within and between-group because of the differences in frequency of contact rates. For between-group dyads, we used hurdle models. A hurdle model has two parts, whereby the first model uses logistic regression to determine whether contacts between dyads were likely to occur, and a gamma general linear models (GGLM) with a log link to predict daily contact rates when contacts occurred. Because all within-group dyads had at least one contact, we used only the GGLM to predict within group daily contact rates. There was a limited number of dyads (n = 25) available to calculate within-group summer contacts rates, so we assessed only simple models with one or two covariates to ensure the number of predictor variables did not exceed the required number of observations in each model (Harrell 2017). We determined the top competing models predicting contact rates by model selection using AIC corrected for small sample size (AICc) and a threshold of $\Delta AICc \leq 2$. We derived median values of distance to anthropogenic features, percent landcover and topography indices within the areas representing the UD overlap of a dyad during a season (Table 2.1). We assessed collinearity between all other covariates and did not include correlated variables $r > |0.6|$ in the same model (Appendix G).

RESULTS

We delineated dates for winter (16 December – 9 May), summer (10 May – 12 November), and rut (14 November – 16 December; Fig 2.2). Deer dyads were monitored on average 131.4 ±12.0 days (F =128, M = 34, Mix = 147) in winter, 151.8 ± 60.5 (F =103, M = 48, Mix = 130) days in summer and 9.2 ± 9.9 (Mix = 9) days during the rut (Fig.2.2).

Genetic relatedness

Three individuals were not sampled for genetics (female = 2, male = 1) resulting in missing relatedness estimates for 35 dyads (female-female = 14, male-male = 7, mixed-sex = 14) of the 389 dyads. Genetic relatedness ranged from -0.46 to 0.58 with no differences in pairwise genetic relatedness among group types ($w = 17606$, $p = 0.10$), seasons for within ($w = 758$, $p = 0.9$) and between-group dyads ($w = 25271$, $p = 0.9$) or dyad types ($p > 0.5$) (Fig.2.3; Appendix H).

Space use overlap

Mean VI values were higher ($w=1727$, $p < 0.05$; Fig 2.4) in within-group dyads (VI = 0.5 ± 0.02) than between-group (VI = 0.05 ± 0.004) and were higher in winter for both group types ($w_{between}=17800$, $p < 0.05$, $w_{within}=182$, $p < 0.05$; Appendix I). Within each season, mean VI values did not vary among dyad types except for between-group, female dyads in the winter which had the highest VI values relative to the other dyad types ($x^2=8.0$, $p< 0.05$). We found no statistical correlation between VI and QG estimates (Fig 2.5; Appendix J)

Seasonal Contact Rates

We found an overall 4.6 times higher frequency in PL-based daily contact rates than GPS-based contact rates but similar trends in seasonal and group contact rates based on the rank order existed between methods (tau > |0.5|) (Fig. 2.6; Appendix K). Between group contacts averaged

1.5 times higher in winter relative to summer ($w=22035$, $p < 0.05$). Within-group contact rates were 95 and 110 times larger than between-group rates across winter and summer seasons ($w = 669$, $p<0.05$; Table 2.2). Female ($z = 2.5$, $p < 0.05$) and male ($z = 2.5$, $p < 0.05$) dyads had higher between-group contact rates than mixed-sex dyads in the winter. In summer, between-group female contact rates were larger than both mixed-sex ($z = 2.7$, $p < 0.05$) and male ($z = 3.1$, $p < 0.05$) between-group dyads (Appendix L). In contrast, within-group contact rates stayed more consistent in winter and differed between dyad types in summer ($x^2=4.2$, $p < 0.05$), where male dyads had significantly lower rates than female dyads. We modelled contact rates as a function of VI for each group type, season, and dyad type and determined that gamma distributed GLMs with a log link were the best fit for out data (Fig. 2.7 Appendix M).

Models of contact rates within groups

All dyads considered to be within-group had at least one recorded contact. Model uncertainty among top models for dyads was high for winter and summer seasons (Table 2.3). Genetic relatedness between individuals was not associated with rates of contact in either season, and there was considerable uncertainty in whether contact rates were influenced by the extent of woody cover. In winter, contact rates increased with volume of intersection, was higher among females, and when dyads were far from streams. VI was not found in the top models in summer; nevertheless, contacts were higher between females and in areas with lower percent woody cover.

Models of contact rates between groups

Of the dyads with home range overlap, 68% had no between group contacts and 32% had 1 – 180 contacts. Degree of VI and percent woody cover within 500m were consistently present in the top winter and summer models predicting the probability of at least one contact occurring,

whereas generic relatedness was not. There was marginally more uncertainty in the models for summer than winter (Table 2.3, Appendix N). In winter, the probability of at least one contact occurring declined as the extent of woody cover declined, although this was less true at high levels of VI (Fig.2.8). In the summer, the probability of at least one contact occurring was higher for females and increased when deer were far from streams and near well sites.

VI extent was also consistently in the top models predicting pair-wise contact rates when contacts occurred, but model uncertainty was greater in winter than in summer (Table 2.3). In winter, pairwise contact rates were not higher between genetically related individuals but were higher in males than in female or mixed-group dyads, higher in less rugged areas and areas with higher woody cover, and higher when dyads were far from streams. In summer, contact rates increased with genetic relatedness among between-group dyads, were higher in less rugged areas, lower in areas of intermediate cover, and higher when dyads were far from streams.

DISCUSSION

The spread of CWD across North America is of great concern among management agencies because of its potential to cause cervid population declines (Edmunds et al. 2016; Devivo et al. 2017), and the costs required for surveillance and management to limit CWD spread (Bollinger et al. 2004; Uehlinger et al. 2016). Outcomes of epidemiological models of CWD that guide management strategies often disregard the effects of transmission heterogeneity (Osnas et al. 2009; Jennelle et al. 2014; Russell et al. 2015), yet patterns in transmission can be crucial to both characterize long-term dynamics and evaluate opportunities for disease management (VanderWaal and Ezenwa 2016b). We quantified pairwise, direct contact rates of mule deer, the cervid species with the highest CWD prevalence in Alberta, to help understand the spatiotemporal factors that potentially influence disease exposure. These contact rates will serve

as a basis to derive spatio-temporal and demographic weighting factors of CWD transmission in epidemiological models (e.g. Belsare et al. 2021, Xu et al in press).

Overall, our findings were consistent with past studies that showed contact rates between deer increased non-linearly with increasing overlap in space use (Schauber et al. 2007; Tosa et al. 2015), which is consistent for within-group contact rates being several orders of magnitude higher than between groups (Habib et al. 2011; Schauber et al. 2015). Indeed, we found contact rates among within-group dyads remain almost 100 times higher across seasons than between groups. Higher contact rates in deer in the same group have been reported for both mule deer (Mejia-Salazar et al. 2017) and white-tailed deer (Schauber et al. 2007, 2015), as well as a number of other mammals such as raccoons (*Procyon lotor*; Robert et al. 2012) and foxes (*Urocyon littoralis*; Sanchez and Hudgens 2015). Consistent with our hypotheses, we found that within-group female contact rates were higher than within-group male contacts and ~3-4 times higher in summer than winter. Post-parturient female mule deer show relatively high cohesiveness in their groups (Haskell et al. 2010), which may be related to participation in cooperative antipredator behaviour, where females band together to defend fawns (Griffith 1988; Lingle 2001; Lingle et al. 2005). In contrast, bachelor groups formed by male deer during summer are less cohesive than their female counterparts (Forand and Marchinton 1989; Lingle 2003). As expected, between-group contact rates were higher in winter compared to summer because mule deer form larger mixed-sex groups in winter motivated by limited availability of winter habitat (Lingle 2003; Habib et al. 2011, Smith et al. 2015). Between-group winter contacts also are more likely to occur between male dyads when accounting for VI and habitat covariates. In winter seasons, white-tailed deer have been observed engaging in aggressive behaviours when in large groups around areas of felled browse (Ozoga 1972). Similar agonistic

behaviour has been observed in male red deer (*Cervus elaphus*) around supplemental feed sites in winter (Schmidt et al. 1998). Limited resources on winter ranges and elevated local density could increase aggressive interactions, particularly between male mule deer, resulting in greater instances of close physical contact between overlapping males in different social groups. Mixed-sex, between-group contact rates in both winter and summer seasons were low, consistent with previous findings that reported preferential associations between same-sex deer pairs (Silbernagel et al. 2011; Mejia-Salazar et al. 2017).

We also expected that pairwise contact rates would reflect genetic relatedness because of matrilineal social structures recorded in mule deer and established patterns in prevalence of CWD. For example, Grear et al. (2010) determined that risk of infection was over 100-times greater among genetically related female white-tailed deer and assumed prevalence among sampled females was the result of direct transmission within matrilineal groups. Meanwhile, studies across other taxa have found positive correlations between interactions among conspecifics and genetic relatedness (Wiszniewski et al. 2010; Chiyo et al. 2011; Best et al. 2014). Contrary to our predictions, higher contact rates did not occur between more genetically related mule deer of either sex either within or between groups. We propose two alternative reasons for this outcome. First, if the nature of the social relationship (e.g., parent-offspring vs. cousins) is more important than the degree of relatedness, adding age or kinship may have shown a stronger genetic relationship (Magle et al. 2013). Second, mule deer, like white-tailed deer exhibit matrilineal group structure (Hawkins and Klimstra 1970; Bowyer 1985), and form social clusters on the landscape based on kinship (Mathews and Porter 1993; Grear et al. 2010). The spatial dependence of relatedness in mule deer has been documented within 2 km in female mule deer (Cullingham et al. 2011b), while other studies demonstrate genetic and geographic distances

between mule deer were positively correlated (Cullingham et al. 2011b; Colson et al. 2012; Noble et al. 2016). Magle et al. (2013) reported that relatedness in white-tailed deer increased with volume of intersection. Overlap in spatial use (VI) was the most consistent variable predicting contact rate and could have confounded effects of genetic relatedness on pairwise contact rates. However, we did not find a similar correlation between space use and genetic relatedness, eliminating the possibility that these two variables are confounded in our analysis.

We found evidence for the rates of contacts varying with environmental conditions. Woody cover within common space use areas had the most persistent influence on contact rates across group types and seasons. Individuals in the same group increased their contact rates as cover increased in winter, when individual's space use overlap was highest. The high within-group contact rates as woody cover increased likely reflects the close association of individuals, particularly for females, because they use the same woody cover areas at the same time. In contrast, between-group contact rates generally increased in areas of low woody cover, which may reflect the strong selection by mule deer for woody cover (Nixon et al. 1991; McClure et al. 2005) that puts individuals in close proximity when cover is limited in their areas of overlap. Such patterns were also reported by Habib et al. (2011) using data from GPS-collared mule deer, particularly for individuals in different groups. The explanation behind the relationship we found between contact rates and proximity to streams is less clear. An increase in contact rates of individuals within groups in winter and between groups in summer when deer are farther from streams may reflect simultaneous use of preferred habitat such as agriculture far from riparian areas (Yoder 2002; Long et al. 2009; Carrollo et al. 2017) or avoidance of cattle in summer (Mackie 1970; Loft et al. 1991). In contrast, in winter when deer distribution is constrained, increased contact rates between-group may be limited to use of areas adjacent to stream that are

more rugged and associated with shallow snow (Walter et al. 2011; Smith et al. 2015; Coe et al. 2018). Mule deer are known to select for rugged areas as escape terrain in response to predation (Bowyer et al. 2001; Lingle 2001). We found that within group contact rates were unaffected by ruggedness, and that between-group contract rates were lower in rugged areas, particularly in summer. Reduced between-group rates in rugged areas may be because deer aggregate as an antipredator response in gentler terrain (Mackie 1970; Bowyer et al. 2001; Lingle 2001), resulting in increased between-group contact rates (Silbernagel et al. 2011).

We attempted to account for direct contacts resulting from depredation on agricultural crops by including percent cropland cover in our analyses; however, we did not include data on discreet locations of stored grains. Features such as grain bins and hay bales are considered artificial attractants because they promote aggregations of deer resulting in increased contact rates and greater potential for disease transmission (Thompson et al. 2008; Sorensen 2014; Oja et al. 2017; Escobar et al. 2020). Locations of hay bales are subject to change on a yearly basis and specific to individual landowners. As a result, we did not have access to location data and did not include location of hay bales in our analysis. Thus, it is possible that our estimates of the effect of agriculture on direct contacts between mule deer were underestimated and more detailed data are needed to fully understand how the number and configuration of artificial attractants influences direct contacts between mule deer in our study area (Gritter 2022).

Contacts rates recorded by PLs were 2.1-7.2 times higher than those recorded using concurrent GPS locations, although in most cases the sex and season-specific patterns were similar. The higher contact rate from PL was largely because loggers operate continuously and are not restricted to an intermittent GPS schedule. Fewer GPS contacts also may result from most studies using 10-25m to define contacts (Schauber et al. 2007; Habib et al. 2011; Silbernagel et

al. 2011; Lavelle et al. 2014) yet GPS error can be 4.7-8.8m (Schauber et al. 2007; Lavelle et al. 2014; Tosa et al. 2015, this study). If GPS error is not random, locations that are missed under specific environmental conditions may add to the discrepancy in between approaches (D'eon et al. 2002; Frair et al. 2004). Higher contact rates recorded by PLs likely contribute to the relative magnitude of difference between contacts within and between-groups. For example, Schauber et al. (2007) determined odds of direct contact, defined as the proportion of simultaneous locations within 10m over the total number of simultaneous locations; within-group were ~20 times greater than between-group. Schauber et al. (2015) suggested their contact rates based on GPS locations were likely underestimating effects of group membership, hypothesizing that deer in the same group were more likely to contact each other once they came within the 10m threshold, as opposed to those in different social groups. Meanwhile, Tosa et al. (2015) demonstrated familiarity (degree of overlapping home range) strongly influenced the likelihood that direct contact would be recorded by PL when individuals were within 10m, as defined by simultaneous GPS locations.

We set a 3m distance using the proximity sensors on collared mule deer to identify potential transmission events through direct contact. Errors associated with PL in previous research have largely focused on false negatives, where direct contacts occur but are not recorded by devices resulting from attenuating radio signals due to coarse habitat (Marfievici et al. 2013; Triguero-Ocaña et al. 2019), body encumbrance (Krull et al. 2018) and increasing distance (Rutz et al. 2015). PL and GPS contact rates demonstrated greatest divergence among between-group summer dyads where correlations based on individual deer were moderate (tau = 0.5). Thus, variation in summer rates could be explained by dense summer vegetation affecting both devices which we do not anticipate altering our conclusions particularly when comparing

source of error in GPS contacts. However, false positives can be produced when the maximum range of contact detection exceeds that of the calibrated RSSI threshold when the transmission of radio signals is amplified by surrounding environments (Ossi et al. 2022). Thus, magnitude of difference between group types could be overestimated if within-group deer are frequently near one another and there is more opportunity for false positives to occur. Further, we programmed separation times of 5 minutes, thus if deer were in proximity for prolonged periods of time (i.e., bedded), it is possible that transmission is interrupted by a change in position, and reconnects after separation time is surpassed, and that single proximity event could be overrepresented in contact records. Therefore, between-group contact rates, that are more influenced by habitat, could be biased towards environmental features where deer are bedded, or that amplify PL signals.

Despite the advances in technology, reliable estimates of contact rates remain difficult to obtain in the field (Gilbertson et al. 2021; Long et al. 2021). Knowledge of demographic, seasonal, and landscape patterns in pair-wise contacts can provide relative weights of attraction in epidemiological models to move us beyond random mixing and uniform contact probabilities as model input (Potapov et al. 2013a; Tardy et al. 2018a; Han et al. 2020). Evidence exists that disease transmission is neither frequency-dependent nor density-dependent but is an intermediate between these two concepts resulting from social and spatial dynamics in disease exposure that changes with local population densities, composition, and behavioral dynamics (Smith et al. 2009a; Wasserberg et al. 2009; Ferrari et al. 2011). Determining how pairwise contacts between individuals among demographic segments of populations change through time may allow us to more realistically model disease transmission by including the spatiotemporal heterogeneity in attraction among specific demographic classes (Özmen et al. 2016; Almberg et al. 2022). For

example, in individual-based models where sickness induced lethargy was included, researchers found that total host contacts increase when compared to models that exclude infection status, resulting in elevated spread of the associated pathogen (Franz et al. 2018). In compartmental models, researchers used field data to fit variable transmission parameters among demographic groups and were able to determine that density-dependent models best fit their field data only after explicitly accounting for sex-group, where male-male transmission played a significant role in disease dynamics (Erazo et al. 2021). Therefore, the timing and focus of management actions may also be justified by differences in demographic, seasonal and environmental dynamics (Pybus 2012; Hedman et al. 2020; Belsare et al. 2021).

Our study highlights that mule deer contacts rates are strongly influenced by group membership and space use overlap, where contact rates within social groups occurred much more frequently, particularly among female dyads. Despite rapid spread within social groups, compartmentalization of contacts can reduce transmission throughout populations within distinct, stable grouping patterns (Blower and McLean 1991; Cross et al. 2005). Our results are consistent with transmission of CWD in mule and white-tailed deer that may be density-dependent in winter, when local density and space use overlap is high, but shifts to reflect frequency-dependent transmission in summer (Wasserberg et al. 2009; Oraby et al. 2014), especially among females. Previous research of socially organized ungulates also suggested that strength of social tries and density effects were sex specific. For example, Webber and Vander Wal (2020) derived social networks from sexually segregated, captive elk that were collared with PLs under varying density treatments (Vander Wal et al. 2012). They reported simulated infections had a linear relationship with density for males, while female infections increased nonlinearly with density. They proposed this was due to sex specific, density-dependent social

behaviours where female connectedness peaks at intermediate densities (O'Brien et al. 2018). Similarly, we found consistent within-group contact rates were greatest among female dyads while between-group rates increase during winter, due to greater local density, especially between male dyads. The effects of sexual segregation on contact structure has direct implications for transmission dynamics resulting in different rates of infections between demographic classes (Ferrari et al. 2011). For example, there is evidence of greater growth rate in CWD prevalence among female mule deer despite overall prevalence being greater in males (Smolko et al. 2021).

We also found that contact rates were dependent on habitat composition within overlap areas between social groups, which may contribute to the spatial spread and structuring in prevalence of CWD that that has been reported across multiple jurisdictions (Garlick et al. 2014; Nobert et al. 2016; Winter et al. 2021, Chapter 3). For example, our results suggest that between-group contact rates occur where deer habitat is limited, thereby aggregating individuals within smaller, desirable areas. In Alberta, agriculturally dominated landscapes generate isolated patches of cover away from major rivers that have been associated with greater risk of a harvested deer being CWD positive (Smolko et al. 2021). Habitat configurations that result in greater between-group contact rates could act as disease hotspots by increasing transmission through direct contact or by accumulating prions and acting as a source of environmental transmission (Almberg et al. 2011). However, distinguishing transmission mechanisms that result in spatial patterns of prevalence is complex and further research is required to attribute spatially explicit models of direct contact with prevalence of CWD. Regardless, the contact dynamics explored in our study support mechanisms of disease transmission by direct contact that reflect observed patterns of CWD prevalence.

TABLE 2. 1. Definitions for landscape and dyad-specific covariates used in contact rate analysis of collared mule deer in central eastern Alberta, Canada (2019-2020).

Covariate	**Symbol**	**Units**	**Description**
Volume of Intersection	VI		3-dimensional index (range 0 to 1) indicating overlap in utilization distributions (Millspaugh et al. 2004)
Genetic Relatedness	QG		Pairwise measure of genetic relatedness (range -1 to 1) using allele identities across multiple individuals (Queller and Goodnight 1989).
Dyad Type	F	0/1	Binary variables representing female-female dyads (Fem) as 1 and other dyad types as zero or male-male (Male) dyads as 1 and other dyad types as zero.
	M	0/1	
Woody Cover	Cov	%	Percent woody cover in a circular buffer (500m). Woody cover included deciduous, deciduous/conifer mix and tall shrubland (*Elaeagnus* sp., upland mix) landcover categories (Merrill et al. unpublished data; Appendix F).
Edge Density	Edge	km/km^2	Linear density of edge in a circular buffer (500m). Edge denotes the boundary between woody cover (see above) and open habitats (cultivated/cropland, forage, and grassland (Merrill et al. unpublished data; Appendix F).
Cropland Cover	Crop	%	Percent of agricultural cover in circular buffer (500m) that consisted of cultivated/cropland landcover categories (Merrill et al. unpublished data; Appendix F).
Distance to Streams	Stream	km	Euclidean distance to streams fit with a decay function $e(-\alpha*distance)$, $\alpha = 0.01$ by Gritter et al. (2022). Streams data retrieved from Altalis (2018).
Distance to Roads	Road	km	Euclidean distance to roads fit with a decay function (see above). Road data retrieved from (Altalis 2020).
Distance to Wells	Well	km	Euclidean distance to wells fit with a decay function (see above).Well data retrieved from Alberta Energy Regulator (2020)
Terrain Ruggedness	Rugg		Terrain ruggedness index (Riley et al. 1999), derived from digital elevation model (Altalis 2018b)

TABLE 2. 2. Mean daily contact rates derived from proximity loggers deployed on 69 (n = 21 males, 48 females) mule deer collared in central eastern Alberta, Canada (2019-2020) summarized by group type, season, and dyad type (female-female F; male-male M; mixed-sex Mix). Letter superscripts denote statistical differences in group specific (a,b) daily contact rates across seasons (a, b) and among dyad types within a season (a,b).

Group	**Season**	**Dyad**	**n**	**Contact rate** ($\bar{x} \pm SE$)
Between (0.05 ± 0.01)[a]	Winter (0.06 ± 0.02)[b]	F	82	0.09 ± 0.03^{b}
		M	23	0.06 ± 0.03^{b}
		Mix	134	0.02 ± 0.01^{a}
	Summer (0.04 ± 0.01)[a]	F	84	0.05 ± 0.01^{b}
		M	42	0.02 ± 0.02^{a}
		Mix	130	0.04 ± 0.03^{a}
Within (5.1 ± 1.0)[b]	Winter (5.7 ± 0.8)[a]	F	46	6.6 ± 1.1^{a}
		M	11	6.4 ± 1.4^{a}
		Mix	13	4.0 ± 2.1^{a}
	Summer (4.4 ± 2.2)[a]	F	19	7.0 ± 1.6^{a}
		M	6	1.7 ± 1.1^{b}
		Mix	0	-- --
Rut		Mix	9	2.8 ± 1.3

TABLE 2. 3. Beta estimates for the top competitive binomial logistic regressions and gamma general linear models modelling within and between-group contact rates as a function of volume of intersection, genetic relatedness (QG), dyad type (female-female F; male-male M; mixed-sex Mix), and median environmental covariates values measured in areas of overlap between utilization distributions (Table 2.1). Contact rates were derived using proximity logger data recorded from mule deer collared in central eastern Alberta, Canada (2019-2020). Asterisk denotes estimates with 95% confidence intervals overlapping zero and null models are represented by grey rows.

VI	**QG**	**F**	**M**	**Cov**	**Cov²**	**Stream**	**Rugg**	**Road**	**Crop**	**Well**	**VI* Cov**	**df**	**Δ**	***w***
Within-group (*GGLM*)														
Winter														
5.0		0.5				-86.2						5	0.0	0.2
5.2		0.5*		1.1*		-86.3						6	0.8	0.2
5.2				1.4*		-76.1						5	1.3	0.1
												2	34.7	0.0
Summer														
		1.3										3	0.0	0.2
		1.1		-2.0								4	0.7	0.1
				-2.5								3	0.7	0.1
												2	1.4	0.1
Between-group (*GGLM*)														
Winter														
7.4			1.0	-1.0*		1.9*	-2.4					7	0.0	0.4
7.2			1.0	-1.2		1.8*	-2.6		-23.1*			8	0.4	0.3
7.6			0.9			1.9*	-2.4					6	2.4	0.1
												2	145.6	0.0
Summer														
8.4	2.4			-15.2	14.3	-94.7	-10.4	1.2				9	0	0.6
7.9	2.4		-0.9*	-14.5	13.8	-94.8	-10.2	1.0				10	0.7	0.4
6.2*				-11.0	10.4	-108.5	-13.8	1.7				8	10.8	0.0
												2	36.6	0.0
Between-group (*BLR*)														
Winter														
46.8				-0.2*							-48.5	4	0.0	0.6
46.7		0.01*		-0.2*							-48.4	5	2.1	0.2
46.7	-0.04*	0.02*		-0.2*							-48.4	6	4.2	0.1
												1	56.4	0.0
Summer														
9.5		0.8		-1.7		-23.9*				0.9		6	0.0	0.4
9.7	1.2*	0.8		-1.9		-25.1*				0.9		7	0.7	0.3
9.0				-1.8		-22.1*				1.0		5	3.3	0.1
												1	21.2	0.0

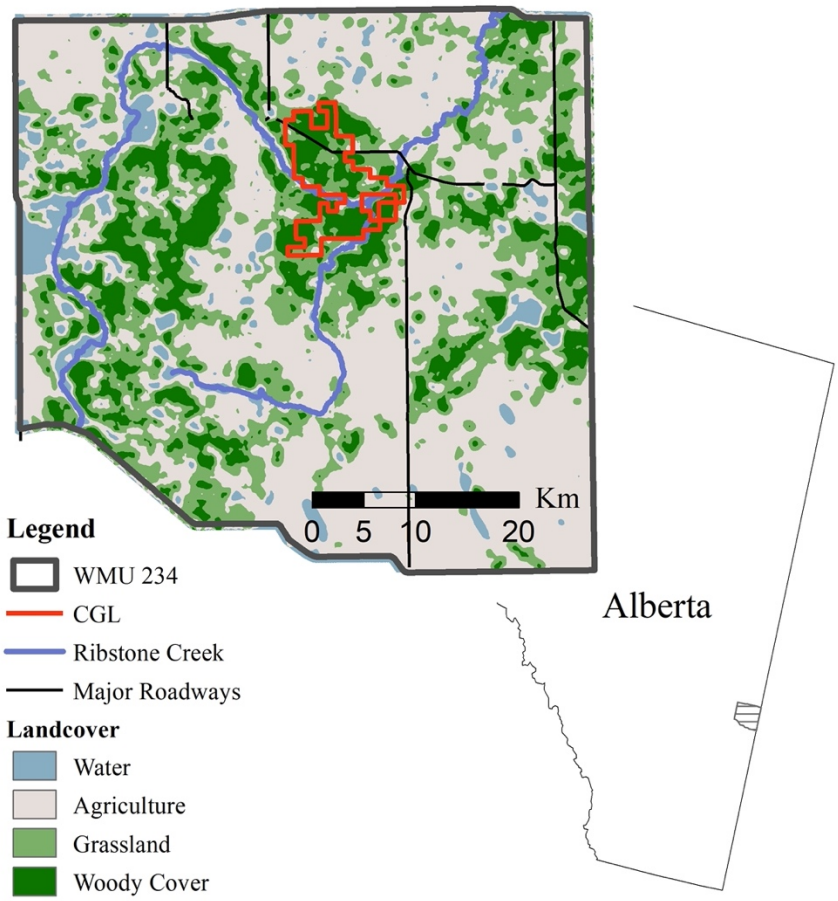

FIGURE 2. 1. Study area located within Wildlife Management Unit 234 in central eastern Alberta, Canada. Mule deer were captured within or immediately adjacent to the Cresthill Grazing Lease (CGL), thereby deer telemetry was also focused around the CGL.

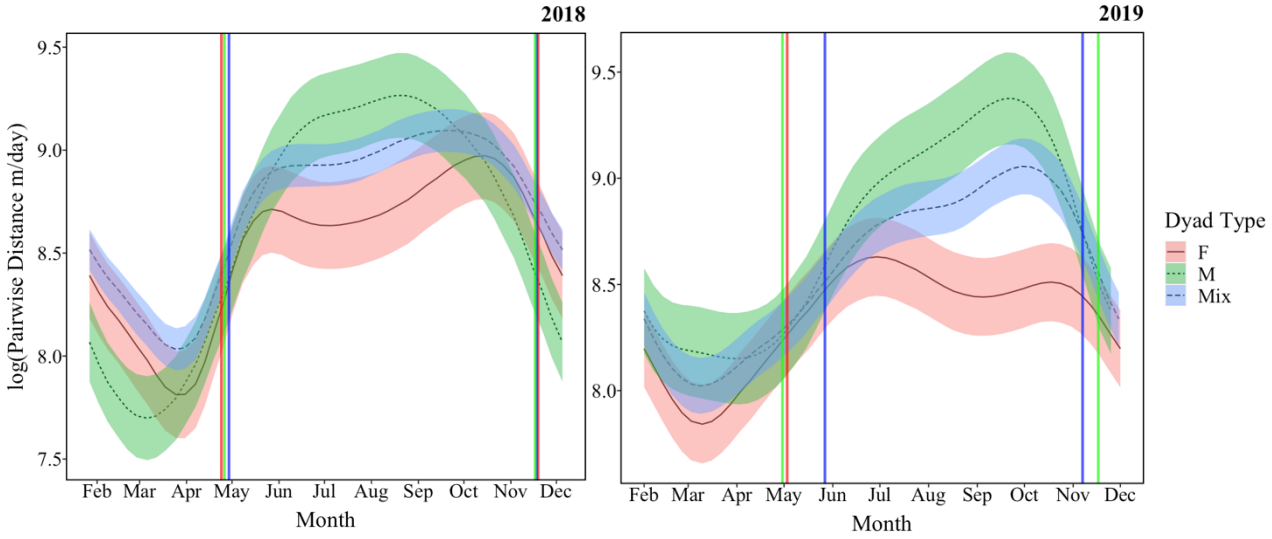

FIGURE 2. 2. Predictive curve produced by general additive mixed models for the logged values of mean daily nearest neighbor distance as a function of Julian day in 2018 and 2019 across dyad types. Infections points derived from first derivative of predictive curves for female-female (F; red), male-male (M; green) and mixed-sex (Mix; blue) dyads denoted by vertical lines. Nearest neighbour distance was derived from mule deer collared in central eastern Alberta, Canada (2018-2019).

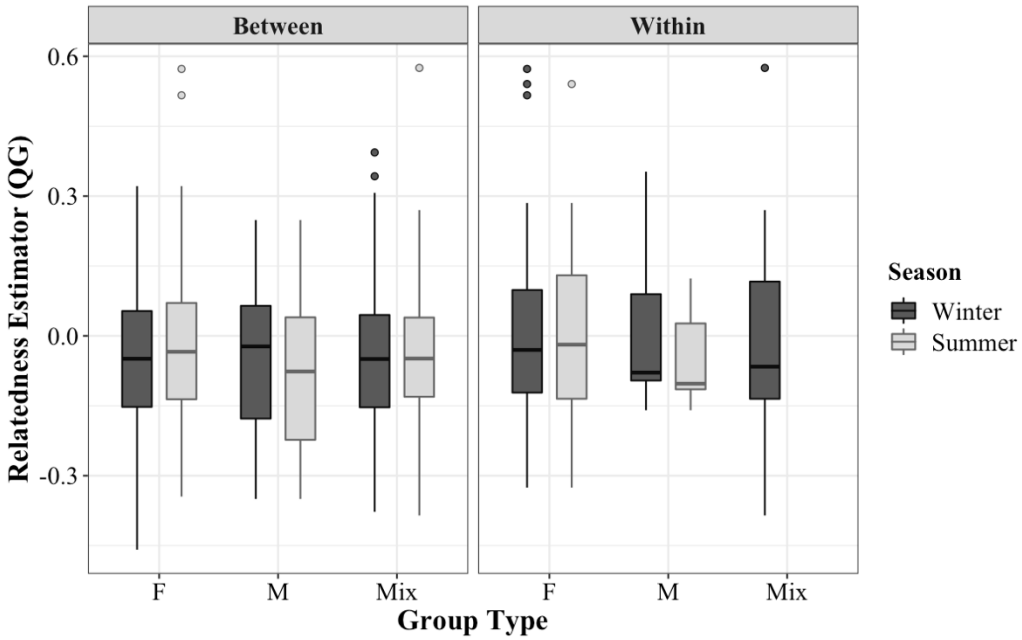

FIGURE 2. 3.Boxplots denoting median values for pairwise genetic relatedness (QG; Queller & Goodnight 1989) between mule deer across season, group, and dyad type (female-female F; male-male M; mixed-sex Mix). Relatedness estimators were derived using samples from collared mule deer captured in central eastern Alberta, Canada (2019-2020). There were no significant differences between QG estimates (Mann-Whitney U test), given $\alpha = 0.05$.

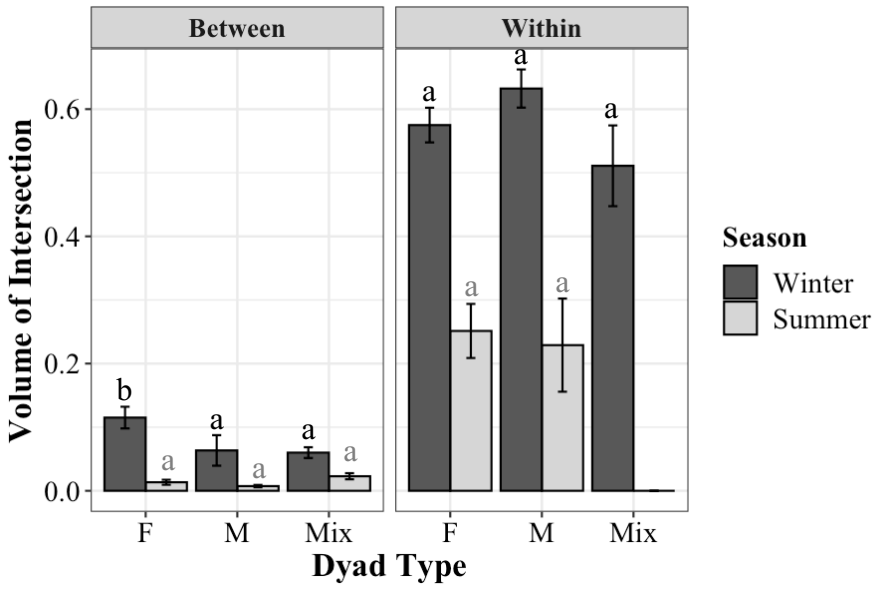

FIGURE 2. 4. Comparison of seasonal volume of intersection values across group type and dyad type (female-female F; male-male M; mixed-sex Mix). Utilization distributions were derived using data from mule deer collared in central eastern Alberta, Canada (2019-2020). Error bars represent standard error. Letter superscripts denote statistical differences in group specific (a,b) mean volume of intersection across seasons (a, b) and among dyad types within a season (a,b).

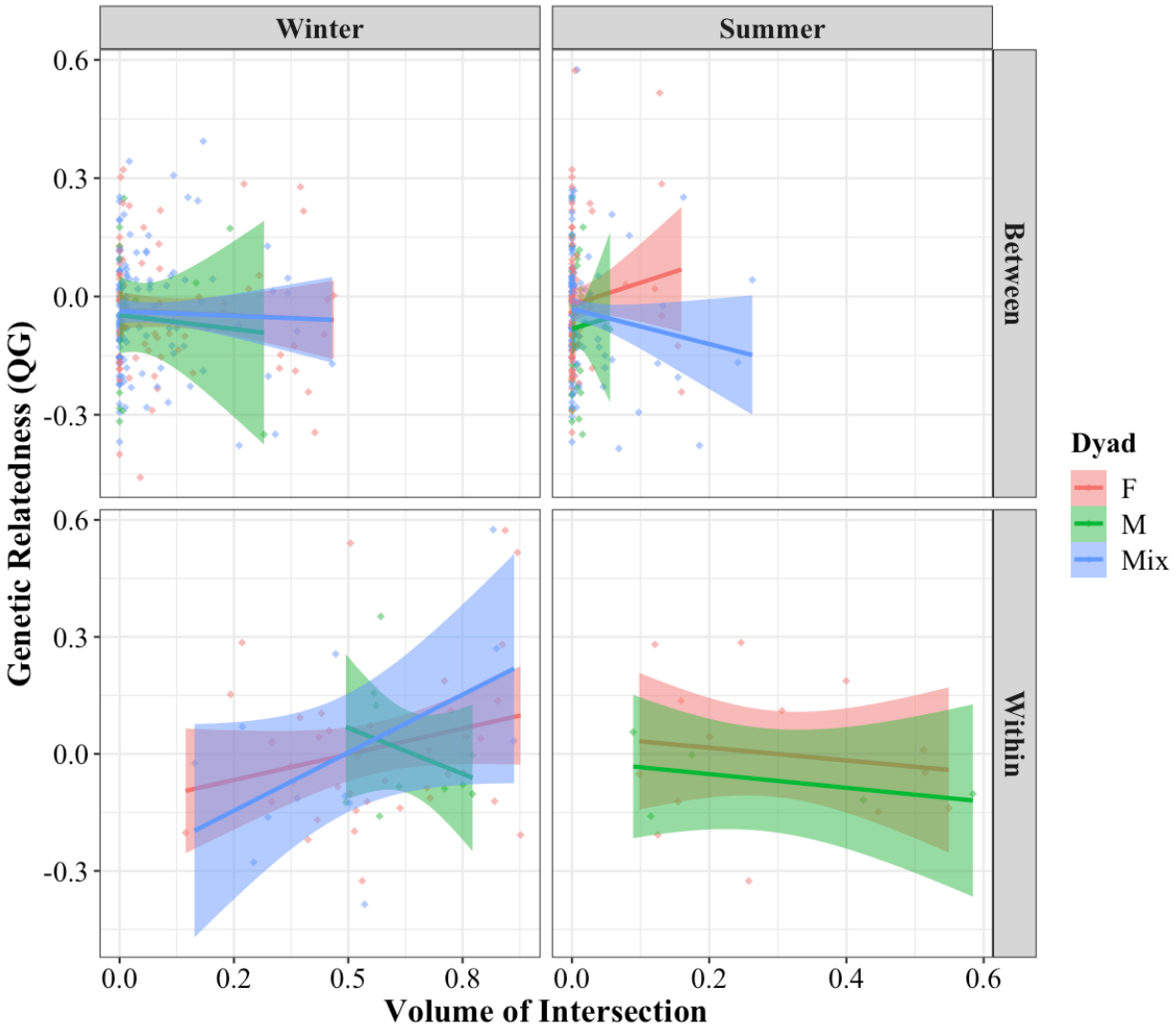

FIGURE 2. 5. Relationships between values of genetic relatedness (QG; Queller and Goodnight 1989) and volume of intersection of mule deer dyad types for deer collared in central eastern Alberta, Canada (2019-2020) by season, group and dyad type (female-female F; male-male M; mixed-sex Mix). There were no significant Pearson's correlation (r) values, given $\alpha = 0.05$.

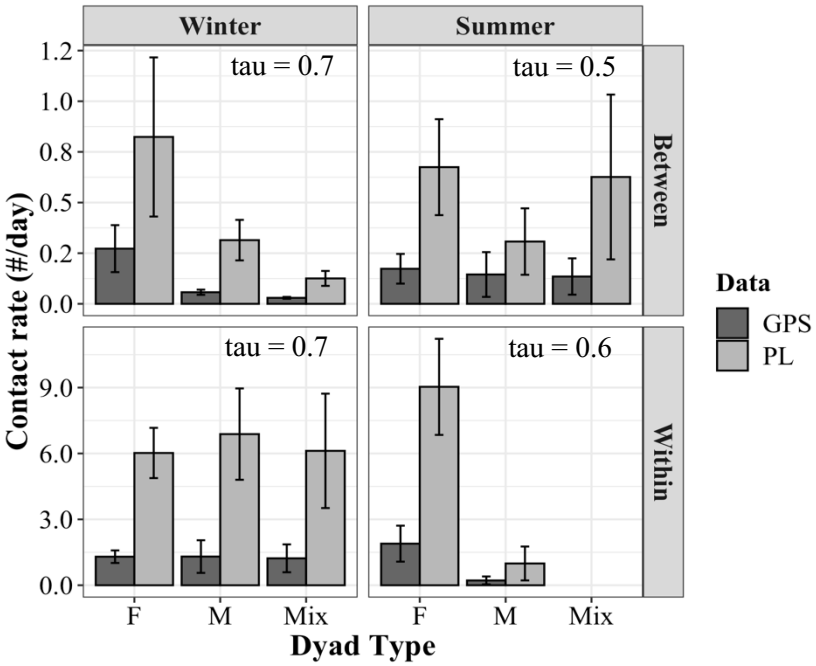

FIGURE 2. 6. Comparison of mean daily contact rates for within and between-group dyads in winter and summer seasons. Contacts derived from collared mule deer, using either concurrent GPS locations within 25 meters or recorded by proximity loggers when deer came within 3 meters with data from the same individuals and results of Kendall's rank correlation test (tau) where all p-value are significant, given $\alpha = 0.05$. Mule deer were collared in in central eastern Alberta, Canada (2019-2020). Error bars represent standard error.

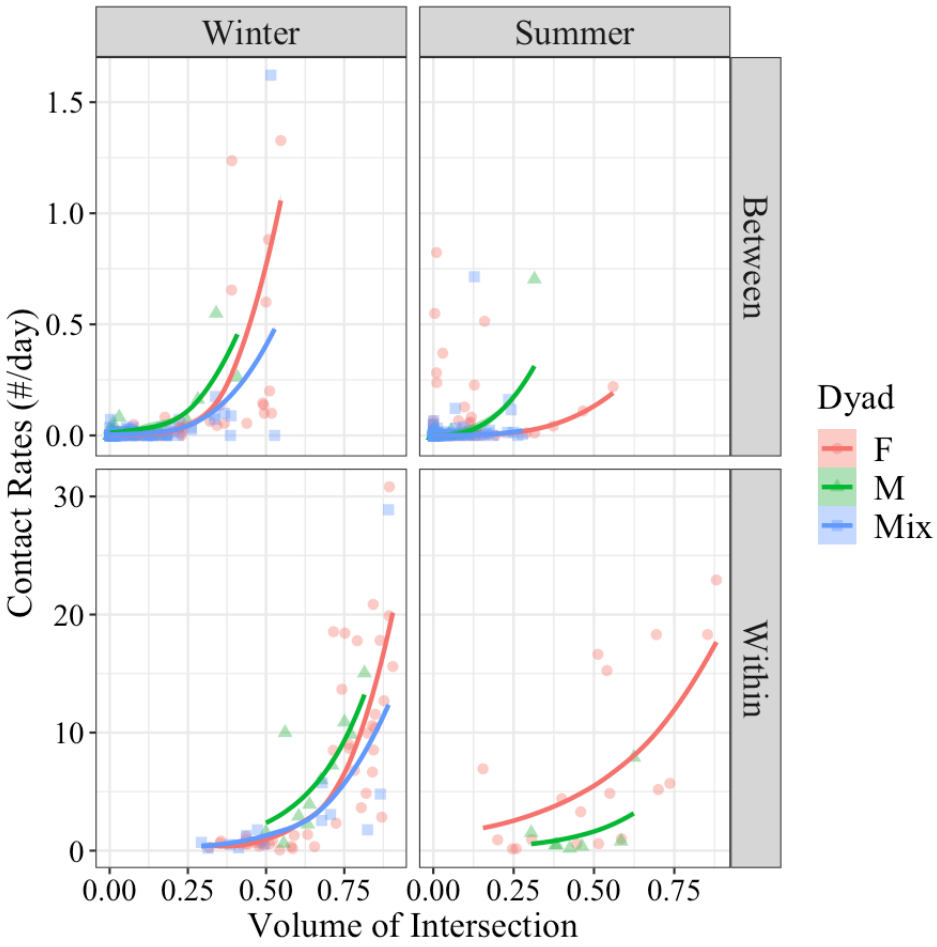

FIGURE 2. 7. Predicted exponential relationship between mean daily contact rates and volume of intersection for within and between-group dyads in winter and summer seasons by GAMMA distributed general linear models with a log link. Contacts derived from collared mule deer in female-female (F); male-male (M); mixed-sex (Mix) dyads in central eastern Alberta, Canada (2019-2020).

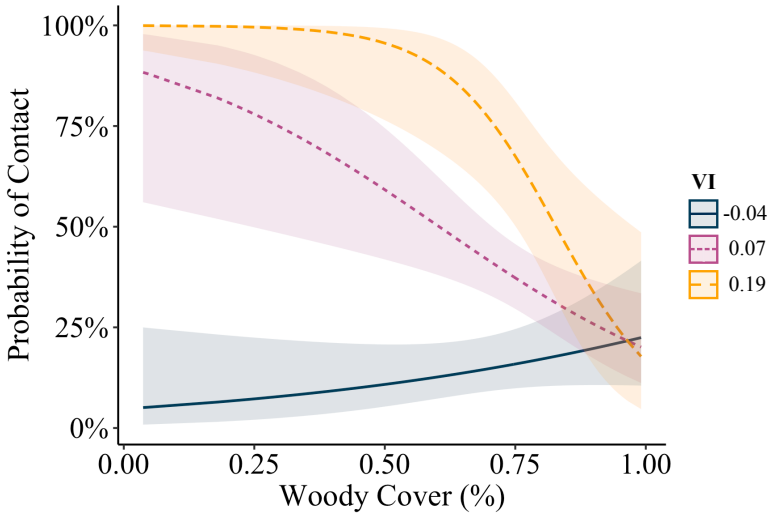

FIGURE 2. 8. Relationship between probability of direct contact among between-group winter dyads and percent woody cover within a 500m circular buffer at varying levels of volume of intersection (mean ± SD) as predicted by binomial logistic regression. Volume of intersection calculated from seasonal utilization distribution of mule deer collared in central eastern Alberta, Canada (2019-2020).

CHAPTER 3 - RISKY BUSINESS: RELATING PROBABILITY OF DIRECT CONTACT WITH DISEASE RISK

INTRODUCTION

Identifying disease transmission among hosts is one of the primary challenges associated with managing and controlling wildlife diseases (Lloyd-Smith et al. 2005). Disease transmission is typically thought to result from two major processes: contact with infectious vectors and the probability of disease transmission given that contact (Begon et al. 2002b). Transmission probabilities are influenced by exposure associated with contact rate and duration, and host susceptibility (VanderWaal and Ezenwa 2016b). Contact with disease vectors is disease-specific and can result from intra-species interactions or contact with the disease in a secondary host or environment (Paull et al. 2012). For example, the route of transmission for devil facial tumor disease in Tasmanian devils (*Sarcophilus harrisii*) is primarily through biting behaviour between infected and susceptible hosts (Hamede et al. 2013). Alternatively, exposure to contaminated water sources has been hypothesized as a major pathway for amphibian chytrid fungus (*Batrachochytrium dendrobatidis*), resulting in global declines in amphibian populations (Kilpatrick et al. 2010; Wilber et al. 2017). However, determining the probability of transmission in wildlife diseases is difficult without direct experimentation (Kirkeby et al. 2017) and is often assumed to be constant in epidemiological models (Caley and Ramsey 2001; Bansal et al. 2007; Ferrari et al. 2011; Craft et al. 2011; Potapov et al. 2013b). More recently, there has been more focus on quantifying the heterogeneity in host exposure in wildlife diseases studies, especially given the new technologies available to monitor contact rates among individuals (Craft and Caillaud 2011; Kappeler et al. 2015; Arthur et al. 2017).

Heterogeneous spatial patterns in host prevalence across landscapes suggest that environmental conditions such as host density, space use, and conspecific interactions influence contacts between infected and susceptible individuals (Conner and Miller 2004; Ostfeld et al. 2005b; Paull et al. 2012). Habitat quality and configuration can alter disease transmission by increasing local host density (Joly et al. 2006a; Habib et al. 2011; Ehrmann et al. 2018), while connectivity between suitable habitats can affect the spread and persistence of disease between infected and susceptible subpopulations (Page et al. 2001; Nobert et al. 2016a; Miller et al. 2020c). For example, in eastern Europe, African swine fever is more likely to occur in forested areas due to elevated wild boar (*Sus scrofa*) densities and, thus, infectious contacts (Podgórski et al. 2020). In the northeastern United States, topographic features strongly influence the connectivity between hibernacula in populations of little brown bats (*Myotis lucifugus*), which directly influence population structure and distributions of white nose syndrome (Miller-Butterworth et al. 2014). Human land use can affect patterns of wildlife disease by fostering environments that are more suitable for pathogens (Jackson et al. 2006; McGinnis and Kerans 2013), artificially aggregating hosts, or altering movements of infected hosts (Becker et al. 2018; Fountain-Jones et al. 2021; Janousek et al. 2021). Understanding what landscape features influence direct contacts among conspecifics and how this differs among segments of the population may help explain patterns of disease prevalence on the landscape to help focus surveillance and management of wildlife diseases.

Chronic wasting disease (CWD) is a fatal, prion encephalopathy of cervid populations that has been recorded in free-ranging white-tailed deer (*Odocoileus virginianus*), mule deer (*O. hemionus*), elk (*Cervus canadensis*), and moose (*Alces alces*) populations in three Canadian provinces, 26 American states, as well as reindeer (*Rangifer tarandus tarandus*), moose, and red

deer (*Cervus elaphus*) in Scandinavia (Mysterud and Edmunds 2019a; Vikøren et al. 2019). All cervids are susceptible to CWD, but there is a higher prevalence in adult age classes (Ketz 2019) and males for both white-tailed deer (Heisey et al. 2010) and mule deer (Miller and Conner 2005). CWD is transmitted through bodily fluids such as saliva, urine, blood, and feces and is spread by direct contact between individuals or by contact with contaminated environments where infectious prions can persist for many years (Miller and Wild 2004; Mathiason et al. 2009). Direct contacts between individuals are likely the primary transmission route in the early progression of the disease, whereas environmental transmission becomes more substantial after prions begin to build up in the environment in the later stages of an epidemic (Almberg et al. 2011). CWD is considered a serious threat because of resulting declines of free-ranging cervid populations (Edmunds et al. 2016; DeVivo et al. 2017), the associated cultural and ecological impacts (Maraud and Roturier 2021; Parlee et al. 2021), and the increased costs for managing the disease (Arnot et al. 2009; Zimmer et al. 2011).

Spatial patterns in CWD are heterogeneous and likely reflect social dynamics and attraction to habitats. In Wisconsin and Illinois, high percent deciduous forest and edge density represent high-quality deer habitat and were associated with increased prevalence of CWD in white-tailed deer (Joly et al. 2006b; Kelly et al. 2010; Storm et al. 2013a). In the Northeastern United States, where forested landscapes are typically homogenous, the risk of harvesting a deer infected with CWD was greatest in areas with relatively small amounts of forest cover resulting from greater dispersal distances by deer in low cover areas (Evans et al. 2016). In agriculturally dominated landscapes, CWD was found in deer occupying isolated patches of woody cover due to this relatively high-quality habitat facilitating aggregations of deer and increasing infection risk (Farnsworth et al. 2005, Smolko et al. 2021). Finally, Nobert et al. (2016) also found that

areas facilitating deer movement between patches had a higher probability of being CWD-infected, suggesting habitat connectivity is a key driver of patterns of CWD on the landscape.

Ongoing CWD surveillance in Alberta, Canada over the period 2005-2018 has documented spatial patterns in disease that have been linked to landscape features (Smolko et al. 2021). We hypothesized that spatial patterns of CWD prevalence during this initial period of disease progression were associated with high direct contact areas, which vary by sex and season. We assessed this hypothesis by determining the locations of direct contacts between pairs of mule deer (hereafter referred to as dyads) of sex-specific or mixed-sex individuals within and between deer groups. To do this, we first determined group membership of collared deer based on pairwise movement metrics and classified deer dyads as within or between-group dyads. Second, we modelled the relative probability of a contact (RCP) occurring in a location based on landscape characteristics for each sex-specific dyad and group type in three seasons and compared it to deer use. Finally, we compared our seasonal predictions of RCP to the spatial risk of a harvested deer being CWD positive derived from 14 years of hunter-based CWD surveillance (Smolko et al. 2021).

In winter, we expected that locations of contacts would be most associated with woody cover and consistent between group and dyad types because of the high selection for woody cover by mule deer at this time of year (Silbernagel et al. 2011; Morano et al. 2019) and concentrations of individuals due to snow accumulation (Drolet 1976; McRoberts et al. 1995; Gilbert et al. 2017). In summer, we expected that areas where female deer contacted each other would also be highest in woody cover or edge because of their high use to avoid predation of fawns (Gulsby et al. 2017; McGovern et al. 2020), whereas contacts between male dyads would reflect selection for forage abundance such as agriculture and grasslands. In addressing how

seasonal and sex-specific contact locations were related to disease risk on the landscape, we proposed five non-mutually exclusive hypotheses predicting which type of contact would have the strongest association with risk of a deer from an area being CWD infected (Table 1). We hypothesized that winter contact locations (H_1) would be most associated with where the disease was found because of high overlapping home ranges and increased group sizes (Wood et al. 1989; Lingle 2003) of mule deer in the winter. In contrast, we hypothesized locations of contacts with males across seasons would have the greatest association with the risk of deer being CWD infected (H_2) because male deer have the highest prevalence and exhibit greater home range size and longer dispersal distances (Robinette 1966; Walter et al. 2018; Smolko et al. 2021). Next, we hypothesized that locations where the probability of a female contact was high (H_3) would be most closely associated with areas of high CWD risk because of the higher social interactions among females, especially within groups (Schauber et al. 2007; Grear et al. 2010). Because males have a high prevalence along with elevated mixed-sex contacts due to polygynous mating structure (Bowyer and Kie 2004; Mejia-Salazar et al. 2017), we expected a close association between locations of rut contacts and where the risk of the disease is high (H_4). We also hypothesized that locations of a contact made by a deer with an individual from a different group (i.e., between-group contact locations) regardless of sex would increase CWD exposure and would be associated with where the risk of CWD was highest (H_5). Finally, we assessed a global model representing all of the above mechanisms. We used the magnitude and direction of the β coefficients to explain the importance of the mechanisms to spatial patterns in CWD risk. Models were compared to the null model (H_{null}) that reflect no relationship between risk of direct contact and disease risk.

MATERIALS AND METHODS

Study Area

The study area (1440 km^2) was in the prairie-parklands of east-central Alberta, approximately 4 km southeast of Edgerton, AB; and bisected by the Ribstone River in the First Nations lands of Treaty 6 (Fig. 3.1). The topography is made up of rolling hills with an elevation ranging from 546 to 782 m. The landscape consists primarily of a matrix of agricultural fields, pastures, and native grasslands interspersed with woody cover. Landcover was mapped based on data collected in 2006 using a multi-temporal remote sensing approach combining Landsat 5 TM satellite imagery and field observations (Merrill et al. 2013). Land cover in the study area was dominated by agriculture cropland (48.0%), followed by grassland (18.9%), deciduous cover (20.1%), human development (1.03%), wetland (7.27%), water (2.63%), and exposed land (1.37%). Croplands were commonly planted with annual crops such as canola (*Brassica* spp.), wheat (*Triticum spp*.) and alfalfa (*Medicago* spp.), or perennial crops and tame grasses for pasture. Native grasslands are made up of drought-tolerant forbs and grasses including (*Stipa* spp., *Bouteloua* spp., *Calamovilfa* spp., and *Artimisia* spp). We defined woody cover to include deciduous tree stands (*Populus spp*.) and tall shrubland *(Elaeagnus commutata*, *Salix* spp., *Prunus* spp., and *Amelancier alnifolia*). Mean daily temperatures recorded at the Edgerton AGCM station ranged between -17.7 − 23.3°C ($\bar{x}$ = 10.7) in summer (10 May – 12 November), -34.3 – 15.2°C ($\bar{x}$ = -6.13) during winter (16 December – 9 May), and -7.2 − 21.2°C ($\bar{x}$ = -7.16) in rut (13 November – 15 December) during 2019 - 2020. Summer precipitation averaged 88.1 mm (range: 13.1 - 220.6) per month. Total monthly snowfall during fall and winter ranged between 12.0 and 22.8 cm. The growing season extends from mid-April through September, when temperatures are above 5°C (Walter et al. 1975).

Approximately 95% of the study area is private land with the remaining lands (5%) under the jurisdictions of the Cresthill Grazing Association (69%), the Dunn Lake Cattle Association (16.8%), and the Municipality of Wainwright (14.2%). Human development includes paved and gravel roads and clearings for oil and gas, development of seismic lines, pipelines, access roads, OHV and well-sites. The study area included the Cresthill Grazing Lease (CGL), which is a 76-km^2 area classified as a Heritage Rangeland Natural Area. During 1 June – 31 October, local landowners use the native grasslands within CGL to graze cattle. Other land uses include recreation areas such as a golf courses, and campgrounds.

Mule deer, white-tailed deer, elk, and moose comprise the large herbivores in the area. All four ungulate species are harvested in WMU 234 with rifle seasons for mule deer, white-tailed and moose from 1 November to 30 November, and elk from 1 November to 20 January. Since 2006, WMU 234 has been among the mandatory units where hunters are required to submit the heads harvested from deer for CWD testing. During this study, CWD prevalence in WMU 234 ranged from 31% to 55% in male mule deer in 2019. Density estimates in WMU 234 for mule deer in 2021 were 2.15 deer/km^2 according to aerial surveys (Government of Alberta 2021). The coyote (*Canis latrans*) is the primary predator of deer within the study area, with possible, but rare, predation by black bears (*Ursus americanus*) and cougars (*Puma concolor*).

Deer capture, collaring and monitoring

Movement data used in this study were collected in 2019 – 2020 from a local deer population collared within, or immediately adjacent to, the Cresthill Grazing Lease (Appendix A). Deer were captured by helicopter using a net gun from January 23 to 30th each year. We targeted capture efforts to collar deer within and between groups based on their spatial distribution during

capture. Captured deer were sedated using xylazine or Butorphanol-Azaperone-Medetomidine (BAM) upon capture.

We deployed Lotek Litetrack 420 collars (Lotek Wireless Inc., Newmarket, ON) and determined average ($\bar{x} \pm SE$) positional area in the study area was 6.2 ± 1.0 m (Appendix E). Each device was equipped with a proximity logger (PL) and global positioning unit (GPS). PL devices were programmed to transmit VHF signals at 20 bpm, allowing PL to record the presence of another collar every 3 seconds. The relative RSSI threshold was set to -100 dBm, which we determined to equate to approximately 3 meters (Appendix B). We used the default separation time of 5 minutes which dictates the amount of time collars could pass outside the RSSI threshold before the contract was ended. Loggers recorded and logged the reciprocal ID of the contacted collar (proximity ID), the start time, the end time, and the duration of contact. GPS locations were scheduled to record locations at 2-hr intervals when no contacts were made. When the PL begins to record a contact event, the GPS schedule will change and collars begin recording locations at 15min intervals on the hour (i.e., 0, 15, 30 and 45min; Fig. 3.2).

Biological seasons

We defined biological seasons based on changes in pairwise, nearest neighbor distance of collared mule deer, to reflect dynamics in social grouping and the potential for distinct seasonal contact rates. First, we modeled changes in pairwise, nearest neighbor distance across collared deer in different dyad types in each year and delineated seasonal inflection points as breaks between seasons. Nearest neighbour distances were calculated as the distance between each dyad whenever both deer were sampled simultaneously, then we averaged daily pairwise values (m day^{-1}). We set a time threshold of 5 minutes for simultaneous location and only included nearest neighbor distance measures for dyads with a volume of intersection (VI) value greater than zero.

Initial start dates of collar data were one-week after collar deployment to account for variation in behaviours after capture. Similarly, final collar sampling days indicated when collar drop-offs were activated. As a result, there was insufficient data available between November and late January to delineate seasons using the generalized additive mixed model analysis (GAMM) approach so we used dates modified from Silbernagel et al. (2011).

We used GAMM with Julian day as the smoothing function and dyad ID as a random effect using the package mgcv (Wood 2004) in R. We used cyclic cubic regression splines with the smoothing parameter estimated using the restricted maximum likelihood (REML) method. We determined seasonal start dates each year by defining inflection points along the predictive curves produced by GAMMs. Inflection points were estimates using the first derivative of the predictive curve where seasonal start dates were inferred when the curve of the derivative changed from increasing to decreasing. We averaged the start date across all dyad types and years (see Chapter 1 for more detail; Appendix C).

Within and between group membership

We distinguished whether two deer were considered to be in the same, or different, group at the time of the contact based on two metrics: 1) space-use overlap and 2) direction and displacement between simultaneous timesteps of a deer dyad (Schauber et al. 2007). We quantified space-use overlap using volume of intersection (VI; Millspaugh et al. 2004) where the seasonal utilization distributions of both deer intersected. Movement displacement and direction was based on the global dynamic interaction index (DI; Nelson and Long, 2013), where simultaneous consecutive fixes were compared for each dyad. We calculated the 2 metrics for all dyads of collared animals in a season. We ordered the values from lowest to highest along the X axis and modeled DI and VI as a function of dyad order along the X axis to assess whether a break point could be

determined using a broken stick regression using the segmented package (Muggeo 2017) in the program R (R Core Team 2019; Schauber et al. 2007). When an inflection point was indicated, we used the corresponding threshold value for a season to split the values for both metrics into those associated with within- and between-group dyads (Appendix D). Between-group dyads were those fit by the first regression line, and within-group dyads were fit by the second regression for both DI and VI values.

Contact Locations

We quantified dyad-specific contacts and identified locations using data from onboard PL and associated GPS locations. We defined a contact event as a time period during which two deer were within 3 m of each other and not separated for more than 5 min. We used data from the PL, rather than simultaneous fixes of GPS collars (Schauber et al. 2007; Habib et al. 2011; Tosa et al. 2015), to quantify contact rates because PL data provides finer scale temporal and spatial data on direct contacts. Trends that are reported in PL rates reflect those derived from concurrent GPS locations (see Chapter 2). Thus, rates of contacts reflected the number of contact events recorded by PL where duration represents a continuous interval when 2 deer were not > 3m apart for more than 5 minutes. We defined the location of a contact as the location of the initial point of contact and excluded any subsequent locations occurring within 15-minute intervals corresponding to the same contact event (Fig. 3.2). We also qualitatively compared the distribution of landscape covariates measured across all contact locations for each season, group type and dyad type with used locations from the same deer by sex and season. We defined used locations as points recorded by GPS collars at 2-hour intervals and only included locations that occurred within the same overlap areas used in the spatial contact models (Appendix O).

Spatial modeling of relative contact probability

We used a design similar to selection modeling (Manly et al. 2002, Lele et al. 2013) to assess the relative contact probability between two mule deer at a location within the study area. We compared landscape characteristics at known contact locations (1) to 15 randomly generated locations (0) within the overlap area of the dyads' 95% kernel utilization distributions by season, for within- and between-groups and dyad types. Kernel distributions were based on GPS locations. We used a logistic regression to obtain the parameters of an exponential model using dyad ID as a random effect (Johnson et al. 2006). To evaluate top models, we used model selection based on Akaike's Information Criterion (AIC) using a threshold $\Delta AIC>2$ to identify the best-supported model for each category (season, group, and dyad type) and parsimony.

Landscape covariates included in the model were edge density, distance to roads, distance to wells, distance to streams, percent woody cover, percent agricultural cover and terrain ruggedness (Table 3.2). To allow for intermediate values of cover facilitating direct contacts, we included both woody cover and square-transformed woody cover. We used the mean values of edge density, woody cover, and agricultural cover in 3 buffer sizes between 250 m, 500 m and 1 km buffer radii and selected the buffer size by comparing competing models using a model selection framework based on AIC using a threshold $\Delta AIC<2$ points in a preliminary analysis (Burnham and Anderson 2002; Appendix P). Prior to modeling, we tested for collinearity among variables ($r > |0.6|$) and did not enter correlated variables into the same model.

To evaluate the model, we predicted the RCP for each 100 m^2 cell across the study area and scaled the predicted RCP values at each location across all seasons (winter, summer, rut), groups (within, between) and dyad types (female-female, male-male, female-male) by dividing by the maximum value. We compared the predicted value at all known contact locations (n =

114 - 23451) and at an equal number of randomly generated locations. We compared the mean values using a t-test assuming equal variance at $\alpha = 0.05$.

Relating Contact Probability to CWD Occurrence

We evaluated the support for 5 hypotheses (Table 3.1) to predict RPCs of different sex and dyad types that would be most closely associated with the probability of disease occurrence in deer on the landscape in three steps. First, because predicted RPC values for a location were generally correlated (r_{mean} among RPC = 0.5 ± 0.1 in winter; r_{mean} among RPC = 0.3 ± 0.1 in summer), we first assessed which RPC metrics among those proposed in Table 3.1 best predicted disease occurrence using in a model selection and AIC > 2 and retained the top model for each hypothesis. In step two, we used the top model for each hypothesis and compared the support for the 5 competing hypotheses and a null model (no variables) based on AIC > 2. In the final step, we compared the most supported model in step two to a global model including all variables across the top models.

The probability of disease occurrence at a location (hereafter, CWD risk) was derived by Smolko et al. (2021) as the probability of a hunter-harvested deer removed during the Alberta surveillance program from 2005 – 2019 being CWD positive (1) or negative (0) as a function of characteristics of the removal location using rare-event logistic regression. Environmental variables included terrain ruggedness, soil type, distance to rivers, streams, wells and urban development. The proportion of woody cover and agricultural cover was measured at a resolution of 100 m^2 in a 12-km^2 buffers. Also included in the model was sex, number of years since initial detection of CWD in Saskatchewan (i.e., 2000), and Euclidean distance to nearest positive case in the previous year (see Smolko et al. 2021 for further details). We used sex-weighted (0.70 female, 0.30 male) predictions for CWD risk in mule deer at 5000 random

locations across the study area. We used CWD risk in 2019 because it incorporates the most current hunter-harvest data collected. We used generalized linear models (GLMs) to relate mean CWD risk values to RPC values at the same locations within a 5 km^2 circular buffer. Prior to the analysis, we standardized RCP values (see above). We used Bayesian Information Criterion (BIC) model selection instead of AIC in previous modeling due to the large sample size (n = 5000).

RESULTS

We used movement data from 68 deer (n = 19 males, 49 females) of 75 deer collared in the January of 2019 and 2020 (Appendix A), which resulted in contacts from 244 deer dyads across seasons (Table 3.3). Data were not used from 7 deer (4 males, 3 females) because of collar failure (n = 6) or corrupted data files (n = 1). Only partial data was used from 11 of the collared deer because of mortality events prior to collar drop-off (6 from coyote predation, 2 from train/vehicle collisions, three from hunter harvest).

Season delineations

Within seasons, variation among dyad types in start dates ranged from 0 - 5 days (2.3 ± 0.52) and 10-30 (14.75± 5.56) in 2018 and 2019, respectively (see chapter 2; Appendix C). Generalizing over the two years of movement data, we defined winter (16 December – 9 May), summer (10 May 10 – 12 November), and in rut (13 November – 15 December) as biologically relevant seasons for mule deer.

Within and between-group designations

We determined that dyads required VI values above 0.13 ± 0.01 in winter and 0.09 ± 0.01 in summer as well as DI values above 0.07 ± 0.01 in winter and 0.07 ± 0.02 in summer to be

designated as within-group. There were no mixed sex dyads that met within-group criteria during the summer. Further, we did not delineate deer groups during the rut and assumed that all mixed-sex contacts were the result of mating behaviours between males and females during the breeding season.

Relative contact probability

Number of contact locations for modeling within group contact were considerably higher than between groups, especially for female deer (Table 3.3), in part, because of the larger sample of collared females. We did not find any significant linear relationships covariates among landscape covariates of contact locations (Appendix Q).

We assessed candidate models predicting the relative contact probability (RCP) from landscape covariates for each combination of season, group, and dyad type (Appendix R). There were only two competitive models for each combination of strata and the weight of the top models was > 0.5 with one exception (i.e., winter within-group male, wt = 0.49). There was more similarity in the factors associated with contact locations among dyad types in winter than in summer with the greatest similarity between female and mixed-sex dyads in winter (Table 3.4). In winter, rugged terrain was the most the most consistent factor increasing the probability of contact across all combinations of deer. Female and mixed-sex dyads were also consistent in that RCP decreased where areas were low in croplands and far from streams. There was a negative effect of distance to roads in all winter RCP models except for between-group, mixed-sex dyads. The effects of percent cover varied among group and dyad types, with the RCP of female dyads both within and between-group types showing the highest RCP at intermediate levels of cover, whereas RCP of males both within and between groups decreased with edge density.

In summer, woody cover was present in all top models, but the nature of the relationships differed. Within-group dyads were more likely to contact each other in intermediate cover while same-sex between-group contacts were greater in high cover areas. Lower RCP in areas close to streams is also consistent in all dyad models with RCP of female and mixed group dyad increasing when edge is high (Table 3.4). Contacts among within-group dyads where far from roads while between-group same-sex contacts occurred near roads with between-group female dyads contacting each other near wells. Further, all female dyads contacted each other in more rugged areas while male dyads and between-group females had greater contacts in agricultural areas.

With two exceptions, mean predicted values for the relative probability of contact were higher ($p< 0.05$) at known contact locations than at random points (Table 3.5). Mean contact probabilities at random locations were greater than known contact locations for models predicting winter, within-group male contacts ($p < 0.001$, $t_{stat}=26.1$) and summer between-group female contacts ($p < 0.001$, $t_{stat}=11.6$).

Relating Contact Probability to CWD Risk

The winter within-group male RCP was the top univariate model for both H_1 and H_2, and winter between-group male RCP was the top univariate model for H_5, indicting CWD occurrence increased where the male contacts were high, particularly in winter. In contrast, summer between-females RCP was top model for H_3 with disease occurrence also increasing. Each of these top models were better supported than a null model. RCP for the mixed-sex dyads in rut was the top model for H_4 with disease occurrence decreasing (Appendix S). The best-supported global model included the predictions from the RPC models between and within males in the

winter and between female groups in summer, with between male in winter RPC having an effect size 7 and 16 times greater than within male group size in winter and between female groups in summer, respectively (Appendix T). The β estimates for all RCP covariates were positive and significant (Table 2.7). The top model was 25 BIC points above second-best supported model and 185 points above the null model. The global model explained 4% of the variation in disease occurrence based on an adjusted R^2.

DISCUSSION

Heterogeneity in transmission of infectious diseases produces quantifiable patterns of prevalence throughout populations of hosts and across landscapes (Gudelj and White 2004; VanderWaal and Ezenwa 2016a). When pathogens are spread through direct contact between infected and susceptible individuals, transmission heterogeneity can arise from variable contact patterns among host classes (Manlove et al. 2017; Silk et al. 2019). We quantified where contacts between mule deer were most likely to occur and which habitat features influence the location of those contacts to assess whether the position of CWD infected deer on the landscape corresponded to patterns in direct contacts. We found habitats influencing contacts in winter were similar between group types and dyad types. This is likely because deer habitat in winter is restricted, and deer are contacting each other in the only suitable habitat that is available. In summer, contact locations were more reflective of sex-specific patterns of habitat selection, particularly among female dyads.

Factors influencing relative probability of a contact occurring in a location were more consistent among within- and between-group deer in winter than in summer for both male and female dyad types. Mule deer form large aggregations in winter, especially where habitat is

limited by snow cover and because deer are no longer sexually segregated (Wood et al. 1989; Lingle 2003). In winter, deer contacts were more likely to occur away from roads and in rugged areas far from agriculture. Mule deer select rugged areas as escape terrain and because they are associated with shallow snow in winters (Anderson et al. 2012; Webb et al. 2013; Coe et al. 2018), and they typically avoid roads most strongly when associated with high human activity and noise (Webb et al. 2013; Northrup et al. 2021). Mule deer may also avoid well pads if human activity is high (Sawyer et al. 2006; Northrup et al. 2016) or may use them at night (Lendrum et al. 2012; Northrup et al. 2021) indicating human disturbance may be key to deer responses. These patterns qualitatively correspond with those of individual deer use (Appendix O), indicating that deer were simply contacting each other in the sites they already frequent. In contrast, we found most between-group contacts were more likely to occur in high woody cover relative to their use. Woody cover is often selected for by mule deer because it provides thermal cover, reduced snow depth, and camouflage from predators (Connolly 1981; Nixon et al. 1991; McClure et al. 2005). It is possible that strong attraction of deer to woody cover combined with the insular and fragmented nature of forest stands in the aspen parklands (Shorthouse 2010; Nobert 2012), constrained the distribution of deer in winter. Thereby mule deer are crowding in cover more than would be expected by their overall selection for this preferred habitat alone. We expected a similar effect on where contacts of male dyads occurred in winter but did not find this. Instead, between-group contacts of males decreased with the density of edge more than expected by their use of these areas (Appendix O). Low edge density can correspond with an increase in contiguous open habitat, whereby male deer typically form the largest aggregations (Bowyer 1985; Lingle 2001).

In summer, contact locations of within versus between-group dyads were more distinct than in winter. The seasonal, sex-specific distinctions were likely due to reduced constraint of snow on movements, wider distribution of available forage, and segregation of the sexes that results in shifts of sex-specific, seasonal habitat selection (Pierce et al. 2004; Bowyer and Kie 2004). Same sex between-group dyads, particularly males, were more likely to occur in agricultural areas that provide summer forage (Nixon et al. 2007; Kjaer et al. 2008). However, this reflected areas that deer generally use, such that increased use of these areas may be responsible for contacts in these locations (but see Silbernagel et al. 2011). However, the probability of mixed-sex contacts did not similarly increase, which may reflect either spatial segregation or distinct foraging activities where male and female deer partition their time differently (Ruckstuhl and Neuhaus 2000; Bowyer and Kie 2004; Biggerstaff et al. 2017). Within-group, same-sex dyads were more likely to contact each other when far from roads, which is consistent with general avoidance of roads by mule deer. In contrast, between-group dyads were more likely to contact each other near roads, which may represent attraction to forage along roadsides (Bellis and Graves 1971; Waring et al. 1991). Female dyads, regardless of group type, had a higher probability of contact where edge density and rugged terrain was high, but contacts in these locations also generally reflected the individual use by deer. Edge habitats provide deer forage with the benefit of nearby cover for fawns in post-parturient females (Mysterud and Østbye 1999; Kie et al. 2002; D'Eon and Serrouya 2005; Horncastle et al. 2013), whereas ruggedness provides escape terrain that may be especially beneficial for females with fawns (Lingle 2001; Lingle et al. 2005). Thus, habitat selection influencing contact between females may be influenced by predator avoidance. Finally, in summer, the probability of deer contacting other deer was high in woody cover across all groups, where within-group and

between-group female dyads had a higher probability of contact with increasing amounts of woody cover and between-group male and mixed-sex dyads contacted each other in areas with intermediate cover. Mule deer have demonstrated strong selection towards woody cover, and when cover is limited in isolated patches, this may promote greater contact rates between groups (Habib et al. 2011, Chapter 2).

We found habitat features influencing contact locations among mixed-sex dyads during the rut followed similar patterns to the spatial contact probabilities of between-group female dyads in summer. Although, contact locations were not notably different for male or female patterns of use (Appendix O). Mule deer breeding season is characterized by increased activity levels by male deer and elevated mixed-sex contact rates (Relyea and Demarais 1994; Silbernagel et al. 2011). As a result, previous research has hypothesized that mixed-sex contacts during the rut are key in influencing in the spread of CWD and are a possible mechanism of elevated CWD prevalence in male deer (Potapov et al. 2013a; Storm et al. 2013b; Koen et al. 2017). However, we found limited support for the relationship between spatial risk of CWD and contact locations during the rut. In our study, collar deployments and subsequent drop-offs partially excluded mule deer breeding season. Thus, our sampling during this time period may not have allowed for accurate measures of contact dynamics. We recommend that future iterations of this work fully encompass breeding season to better understand the relationship between mating behaviours in the transmission of CWD.

In general, the above patterns suggest that seasonal shifts in types of areas that characterize contact locations may be due largely to season-specific habitat selection and use. Although our comparisons with use were only qualitative, we were able to discern that the trends in habitat variables at contact locations differed from used points within the same area of

overlap, depending on the variable in question. The distributions and median values of percent woody cover, edge density and distance to roads were the most consistently different from those of use, particularly for between-group contact locations. We hypothesize that where seasonal contact rates are likely to be different from the overall expected use by individual deer may be due to strong preference for habitats that have patchy availability (i.e., woody cover), attractive forage (i.e., roads), and fulfill multiple requirements (i.e., edge density). We predict that a more robust examination of deer use would confirm that within-group contacts occur in areas of high individual use, while between-group contacts display distinct patterns that reflect the propensity for habitat to facilitate direct contacts. Thus, in modeling studies where CWD risk is based primarily on habitat selection (Dugal et al. 2013; Russell et al. 2015), the use of highly selected areas as a proxy for elevated contacts is justifiable. Although, caution should be taken when considering habitat types that could produce a nonlinear relationship between frequency of contact and contact probability.

In spatially relating the probability of average risk of a harvested deer being CWD positive within WMU 234 to where sex-specific, seasonal contact were highest, we found most support for contacts among within and between-group male dyads in winter and between female groups in summer influencing disease occurrence. That male contacts in winter influence disease on the landscape in this area is not surprising because male mule deer in Alberta had higher prevalence (8.3%) than female mule deer (2.5%) and all other cervid species (Smolko et al. 2021), which also has been true in other jurisdictions at the beginning of a CWD epidemic (Miller and Conner 2005; Osnas et al. 2009; Rees et al. 2012). Our risk metrics represent predictions weighted by broad assumptions of population level sex ratios where females (70%) are weighted more heavily than males (30%; Freeman et al. 2014). Thus, any biases of sex-

specific prevalence numbers would have favoured the influence of contacts between females, which is not the case. To date, there are no detected differences in physiologically mediated susceptibility to CWD between sexes (Grear et al. 2006; Mawdsley 2020; Escobar et al. 2020); therefore, behavioural differences are likely the primary contributing factor to male infections. Winter aggregations have often been proposed as a mechanism for increased prevalence because of greater overlap between groups and elevated rates of potentially infectious contacts (Habib et al. 2011; Silbernagel et al. 2011; Garlick et al. 2014, Chapter 2). We also found that winter habitats that are far from roads, with low edge density, high ruggedness, and close to wells facilitate within-group contacts among male dyads. Other studies suggest infections among males result from mixed-sex contacts during the rut or among bachelor groups during summer (Grear et al. 2006; Storm et al. 2013b). Indeed, Potapov et al. (2013) found that the 2:1 ratio in male to female prevalence did not exist when their models did not include strong sexual segregation. Conversely, our findings suggest that most contacts between males take place on winter range and not during summer when sexual segregation occurs. However, we cannot rule out that the evidence for winter contacts among males could also be the result of a cumulative number of winter contacts in other groups because RCPs of between-group male dyads were highly correlated with contact probabilities across other group and dyad types in winter.

There was also evidence that contact locations among between-group female dyads in the summer were also positively associated with spatial predictions of CWD risk. Our findings are consistent with the hypothesis (H_5) that contacts with deer outside of established female social groups influenced disease risk by facilitating pathogen transmission that was otherwise largely within self-interacting groups. In socially structured populations, between-group contacts can facilitate population-wide transmission by spreading disease to new, uninfected groups (Keeling

and Eames 2005; Sah et al. 2018). For example, disease simulations derived from contact networks of GPS collared badgers (*Meles meles*) demonstrated that populations with greater degrees of social structure (i.e. fewer between-group connections) resulted in smaller epidemics and lower peak prevalence of infection when compared to populations with more fluid social connections (Rozins et al. 2018). Alternatively, rapid spread of CWD within female groups of mule deer and white-tailed deer have been attributed to matrilineal social structures (Hawkins and Klimstra 1970; Mathews and Porter 1993), which is supported by studies demonstrating that individuals highly related to infected deer are more likely to be CWD-positive (Grear et al. 2010; Cullingham et al. 2011b). In Wyoming, where CWD has been endemic since the 1970's, female prevalence estimates were greater than in males among populations of white-tailed deer (Edmunds et al. 2016), indicating that later stages of epidemics are more dependent on transmission dynamics of female deer.

Our results lend support to intervention strategies currently proposed by government agencies to target the removal of males broadly in a population and female social groups on a landscape where CWD is emerging (Western Association of Fish and Wildlife Agencies 2018). We demonstrate where the probability of male contacts is high in winter, it is associated with high probability of disease risk; therefore, reducing densities of males that also have the highest prevalence is likely to reduce disease transmission especially if removed before winter when males appear to be most aggregated. Because the probability of between-group contacts among females is also associated with where CWD-infected animals occur, targeting infected female groups may also reduce transmission as indicated by the long-term management of mule deer in Colorado (Miller et al. 2020a), and white-tailed deer in Illinois (Manjerovic et al. 2014) where sustained government culling has maintained stable CWD prevalence numbers, as opposed to the

annual increase in prevalence observed in neighbouring Wisconsin where culling programs were concluded. Further, we propose that assumptions of CWD risk being associated with highly selected deer habitat are a useful approximation when devising surveillance strategies in areas without recorded cases of CWD positive animals.

TABLE 3. 1. Five non-mutually exclusive hypotheses outlining the mechanisms in which direct contact between mule deer influence transmission of chronic wasting disease and the relative contact probabilities (RCP) associated with each hypothesis. We model RCPs as a function of spatial risk of a deer being CWD-positive predicted using hunter surveillance data (Smolko et al. 2021) in Wildlife Management Unit 234 in central eastern Alberta, Canada (2019).

		Hypothesis	**Related RCPs**
Winter contacts	H_1	Large, mixed-sex groups in the winter increases transmission due to new contacts and greater local density.	Fem_{Winter}^{Within} | $Male_{Winter}^{Within}$ | Mix_{Winter}^{Within} $Fem_{Winter}^{Between}$ | $Male_{Winter}^{Between}$ | $Mix_{Winter}^{Between}$
Male contacts	H_2	Larger home ranges and dispersal behaviour increases transmission	$Male_{Winter}^{Within}$ | $Male_{Summer}^{Within}$ | $Male_{Winter}^{Between}$ $Male_{Summer}^{Between}$
Female contacts	H_3	Frequent contacts between females forming matrilineal groups.	Fem_{Winter}^{Within} | Fem_{Summer}^{Within} | $Fem_{Winter}^{Between}$ $Fem_{Summer}^{Between}$
Rut contacts	H_4	Elevated contacts between sexes during the rut increases transmission	Mix_{Rut}^{All} | Fem_{Summer}^{Within} | $Male_{Summer}^{Within}$
Between-group contacts	H_5	Contacts with deer outside of established social groups increases transmission.	$Fem_{Winter}^{Between}$ | $Male_{Winter}^{Between}$ | $Mix_{Winter}^{Between}$ $Fem_{Summer}^{Between}$ | $Male_{Summer}^{Between}$ | $Mix_{Summer}^{Between}$

TABLE 3. 2. Description of landscape covariates used in spatial modeling of relative contact probability of collared mule deer in 2019-2020 in Wildlife Management Unit 234 in central eastern Alberta, Canada.

Covariate	**Symbol**	**Units**	**Description**
Woody Cover	Cov	%	Percent of woody cover within a circular buffer. Woody cover included deciduous, deciduous/conifer mix and tall shrubland (Elaeagnus sp., upland mix) landcover categories (Merrill et al. 2013; Appendix F). Buffer size varies in winter (250m), summer (1000m) and rut (250m; Appendix P).
Edge Density	Edge	km/km^2	Linear density of edge within a circular buffer. Edge defined as the boundary between open habitat and woody cover delineated from landcover data produced by Merrill et al. (2013; Appendix F). Buffer size for linear density varied in winter (250m), summer and rut (500m; Appendix P).
Cropland Cover	Crop	%	Percent of agricultural cover within a circular buffer. Agricultural cover consisted of cultivated/cropland landcover categories (Merrill et al. 2013; Appendix F). Buffer size varies in winter (1000m), summer and rut (500m; Appendix P).
Distance to Streams	Stream	km	Euclidean distance to streams fit with a decay function[1](Gritter et al. 2021- Altalis, 2018)
Distance to Roads	Road	km	Euclidean distance to roads fit with a decay function[1] (Gritter et al. 2021 – Altalis, 2020)
Distance to Wells	Well	km	Euclidean distance to wells fit with a decay function[1] (Gritter et al. 2021 – AER, 2020)
Terrain Ruggedness	Rugg		Terrain ruggedness index (Riley et al. 1999), derived from digital elevation model (NRC, 2019)

[1] $e^{(-\alpha * distance)}$, $\alpha = 0.01$

TABLE 3. 3. Number of contact locations among 68 (n = 19 males, 49 females) mule deer collared on the Cresthill Grazing Lease in central easter Alberta (2019- 2020) summarized by season, group type and dyad type (F, female-female; M, male-male; Mis, mixed sex). Contacts were derived from proximity loggers and contact location from the GPS locations of the beginning the contact (see Fig 3.2).

Season	**Group**	**Dyad**	**n**	**Recorded Contacts**			**Total**
				Mean ± SE		**Range**	
Winter	Within	F	44	533	± 122	11 - 3310	23451
		M	11	483	± 134	26 - 1386	5318
		Mix	12	193	± 63.5	22 - 674	2316
	Between	F	34	29.4	± 12.1	1 - 335	1000
		M	6	19	± 9.8	1 - 59	114
		Mix	37	9.0	± 5.7	1 - 212	333
Summer	Within	F	10	1818	± 548	96 - 4582	18189
		M	5	380	± 270	9 - 1447	1902
	Between	F	37	76.2	± 31.2	1 - 865	2821
		M	5	51.6	± 23	1 - 122	258
		Mix	25	10.9	± 6.4	1 - 162	273
Rut		Mix	18	84	± 45.5	1 - 374	672

TABLE 3. 4. Model coefficients of logistic regressions relating landscape covariates to contact locations compared to randomly generate points within areas of space use overlap, number of model parameters (k), and model weights calculated from AIC model selection (w). We display top models for each season, group types and dyad types (female-female F; male-male M; mixed-sex Mix). Contacts derived from collared mule deer within Wildlife Management Unit 234 in central eastern Alberta, Canada, 2019 – 2020.

Group	Dyad	Road	Rugg	Edge	Crop	Cov	Cov^2	Stream	Well	k	w
					Winter						
Within	F	-0.1	0.3	-0.1	-0.9	-0.8	0.8	-0.4	0.1	8	1.0
	M	-0.1	0.2	-0.1					0.1	4	0.5
	Mix	-0.1	0.6	-0.1	-3.4	1.9	-1.2	-0.1		6	0.5
Between	F	-0.3	0.7		-0.8	-1.3	1.5	-0.3	0.1	7	0.7
	M	-0.4	2.0	-0.8	-5.2*					4	0.7
	Mix	0.3	0.6	-0.3	-26.0	-0.3	1.2*	-1.6		7	0.6
					Summer						
Within	F	-0.2	0.6	0.3	-0.5	-3.1	2.7	-0.2	-0.0	8	1.0
	M	-0.3			1.0	-1.6	1.3*	-1.7		5	0.5
Between	F	0.1	0.5	0.4	0.4	-3.2	2.6	-0.1	0.1	8	1.0
	M	0.4			4.0	5.0	-3.1	-0.3	-0.2	6	0.9
	Mix			0.2		7.4	-7.2	-0.4		4	0.8
					Rut						
All	Mix	-0.3	0.3	0.0	-9.1	2.4	-2.1	-0.2	-0.3	8	1.0

* Beta estimates with 95% confidence intervals overlapping zero

TABLE 3. 5. Differences in the mean relative contact probability values (RCP) scaled between 0 and 1 at known contact locations (n) compared using a t-test to those at randomly generated locations (n) within Wildlife Management Unit 234 in central eastern Alberta, Canada.

Season	**Group**	**Dyad**	**n**	**Mean RCP Value (± SD)**		p-value
				Contact	**Random**	
Winter	Within	F	23451	0.6 ± 0.05	0.6 ± 0.10	<0.001
		M	5318	0.2 ± 0.04	0.2 ± 0.05	<0.001
		Mix	2316	0.5 ± 0.04	0.3 ± 0.14	<0.001
	Between	F	1000	0.4 ± 0.05	0.4 ± 0.06	<0.001
		M	114	0.3 ± 0.06	0.2 ± 0.07	<0.001
		Mix	333	0.9 ± 0.02	0.7 ± 0.26	<0.001
Summer	Within	F	18197	0.4 ± 0.06	0.3 ± 0.06	<0.001
		M	1902	0.9 ± 0.04	0.9 ± 0.13	<0.001
	Between	F	2821	0.3 ± 0.06	0.3 ± 0.07	<0.001
		M	258	0.6 ± 0.07	0.5 ± 0.14	0.07
		Mix	273	0.7 ± 0.09	0.6 ± 0.16	<0.001
Rut		Mix	677	0.9 ± 0.03	0.6 ± 0.24	<0.001

TABLE 3. 6. Beta estimates ($\boldsymbol{\beta}$) and 95% confidence intervals (CI) for top univariate models relating predictions of spatial CWD risk with values of relative contact probability within 5km buffered points (n=5000) between collared mule deer in variable seasons, group, and dyad types in central eastern Alberta, Canada, 2019–2020.

Hypothesis		**Representative RCP**			$\boldsymbol{\beta}$	**95% CI**
		Season	**Group**	**Dyad**		
H_1	Winter	Winter	Within	Male	0.05	0.04, 0.06
H_2	Male	Winter	Within	Male	0.05	0.04, 0.06
H_3	Female	Summer	Between	Female	0.01	0.01, 0.01
H_4	Rut	Rut		Mix	-0.001	-0.001, -0.0004
H_5	Between	Winter	Between	Male	0.003	0.002, 0.003

TABLE 3. 7. Beta estimates ($\boldsymbol{\beta}$) and 95% confidence intervals (CI) for covariates included in top general linear model using representative RCP predictors for each hypothesis relating relative contact probability (RCP) between collared mule deer in variable seasons, group, and dyad types in central eastern Alberta, Canada, 2019–2020.

	RCP Covariates			
Season	**Group**	**Dyad**	$\boldsymbol{\beta}$	**95% CI**
Winter	Between	Male	0.03	0.03, 0.05
	Within	Male	0.01	0.01, 0.01
Summer	Between	Female	0.002	0.001, 0.003

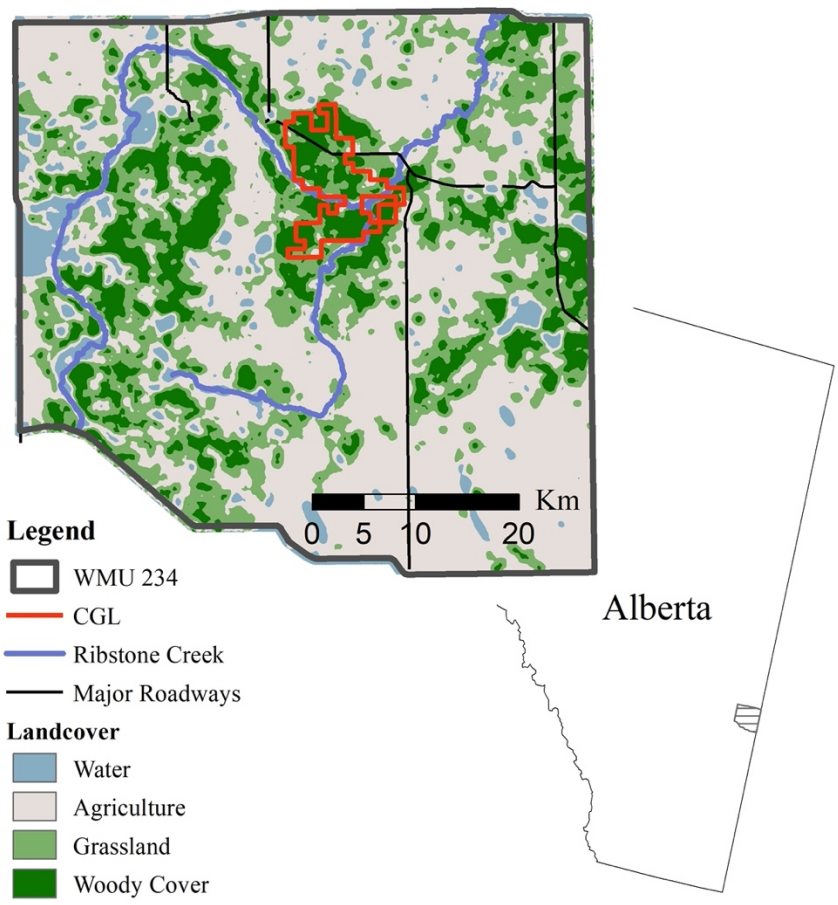

FIGURE 3. 1. Study area within Wildlife Management Unit 234 in central eastern Alberta, Canada. Deer telemetry focused around Cresthill Grazing Lease.

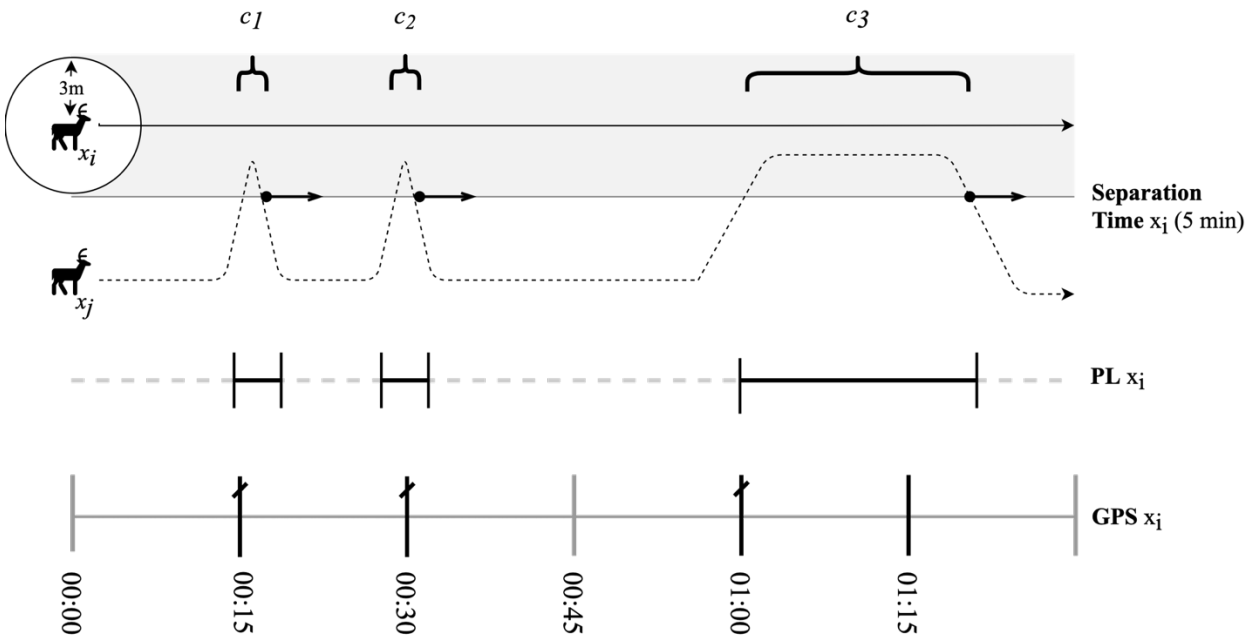

FIGURE 3. 2. Diagram of collar functioning in relation to separation time, defined as the time elapsed that allows a proximity event to be recorded as a new contact. Dotted line leading from deer xj represents its path as it overlaps with deer xi. The shaded grey area represents the threshold at which collars will begin recording contact events (cij). Bolded arrow represents separation time. Dashed line (PL xi) denotes times recorded by PL depending on whether a contact has been detected. The demarcated line (GPS xi) denotes the altered 15-minute GPS schedule where bolded sections are fixes recorded depending on whether a contact has been detected. Crossed lines represent points used in the relative contact probability analysis. If separation time is surpassed, the end time of contact event will be recorded at the time collared exited the contact threshold (3m).

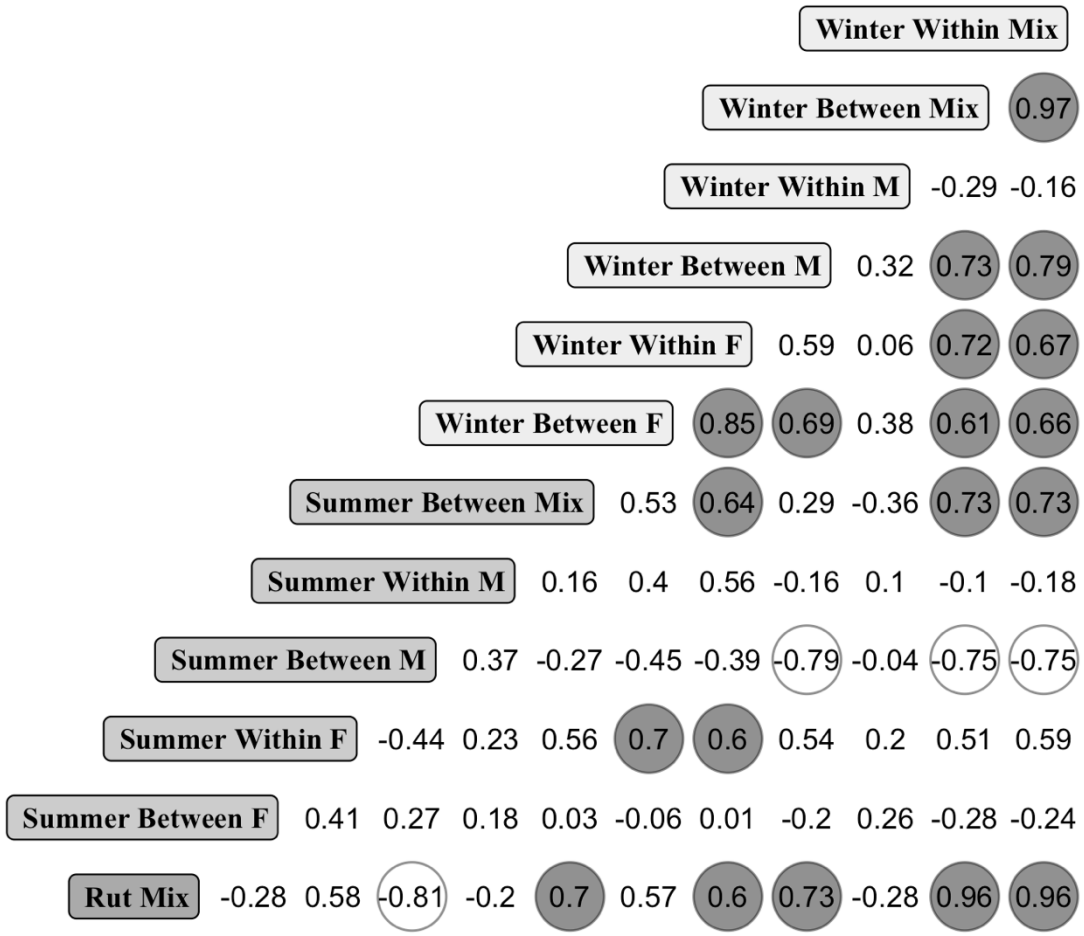

FIGURE 3. 3. Pearson's correlation values between values of relative contact probability of collared mule deer at a location in winter, summer, and rut for mule deer within and between groups and by dyad types (female-female, F; male-male, M; mixed-sex, Mix) in central eastern Alberta, Canada, 2019-2020, Dark grey circles represent correlations values that are significantly above 0.6 and hollow circles represent those below -0.6.

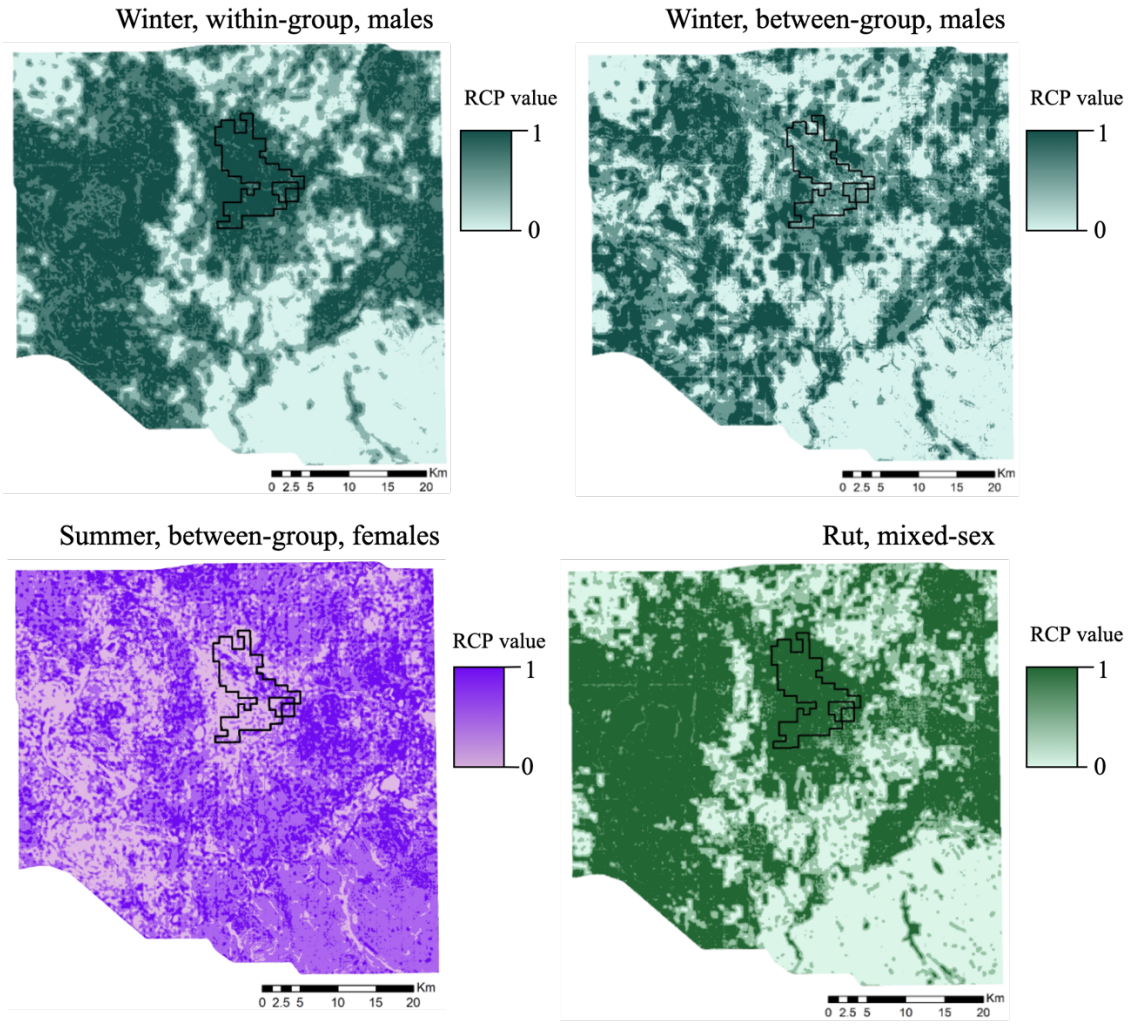

FIGURE 3. 4. Predictive maps depicting normalized values of relative contact probability across Wildlife Management Unit 234 for season, group types and dyad types that best represent proposed hypotheses relating spatial risk of a harvested mule deer (2019) being CWD positive with direct contact between mule deer collared in the Cresthill Grazing Lease (black outline) in central eastern Alberta, Canada (2019-2020).

CHAPTER 4 – CONCLUSION

Chronic wasting disease (CWD) has been a predominate focus of wildlife management of many wildlife agencies over recent years because the disease has continued to spread and additional foci have emerged throughout North America and Europe (Mysterud and Edmunds 2019; Miller and Vaske 2022). The lack of a vaccine or other cure has hindered effective control of the disease leaving harvest management as the primary tool available to managers (Wasserberg et al. 2009; Potapov et al. 2016). Thus, identifying host classes and environments that are disproportionately contributing to CWD spread is necessary for targeting management efforts. Delineating primary routes of disease transmission is complicated by the latency in appearance of symptoms and the multiple avenues of exposure from both direct and indirect transmission (Bollinger et al. 2004). Epidemiological models play an essential role in assessing the importance of different transmission pathways as well as evaluating management approaches. For example, Potapov et al. (2013) compared model outcomes between plausible mechanisms of transmission to explain what could produce the trends in CWD prevalence being twice as high in males as female and found multiple, plausible pathways but that the direction of direct transmission between the sex, sexual segregation, and environmental exposure played a key role. Similarly, other studies have used empirically derived contact rates to modeled potential modes of transmission that reflect patterns in prevalence data (Joly et al. 2006; Habib et al. 2011, Xu in prep). Thus, reliable measures of direct contacts and the factors influencing variability between host classes and environments is crucial in providing an invaluable tool in CWD management.

In this thesis, I investigated the social and environmental factors affecting direct contacts between conspecific mule deer and related my findings to their implications on the dynamics of CWD transmission. I used new technology based on proximity loggers, which provided contact

rates that were considerably higher than those reported for contacts based on GPS collars because of the different contact definitions between the two metrics (Schauber et al. 2007). My findings confirm trends in contact rates derived from GPS collars and PL are similar, implying that PL derived contacts could provide more comprehensive estimates of wildlife interactions. In Chapter 2, I found significant seasonal trends in the contact rates of within and between-group dyads as well as sex-specific dyads. Although social groups of mule deer are subject to fission-fusion dynamics (Bowyer 1985; Lingle 2003), we found that distinguishing between group types yielded distinct trends that imply the mechanisms affecting inter and intra-group contacts are different, thus support modeling approaches where host classes are treated as distinct units. As expected, within-group contact rates were several orders of magnitude greater than between-group and this was consistent between seasons. Between-group rates were greater in winter compared to summer, where contact rates of female dyads were higher when compared to male and mixed-sex dyad types. I determined that social factors are more influential for contact rates among within-group dyads, whereas habitat features have a greater influence on between-group contact rates.

Where Chapter 2 quantified rates of direct contact and the factors influencing those rates, Chapter 3 examined where contacts were most likely to occur such that this might add to our understanding of the patterns of disease on the landscape (Conner and Miller 2004; O'Hara Ruiz et al. 2013; Smolko et al. 2021). I found that habitats influencing contacts in winter were very similar among within and between-group, and sex-specific dyads. This was not unexpected because deer habitat in winter is most restricted, and their use of the limited, suitable habitat puts them in close proximity. Although my comparisons with individual deer use were only qualitative, contact locations in summer were more reflective of sex-specific patterns of habitat

selection, particularly among female dyads. The exceptions seemed to be in winter, where woody cover was high and when edge density was low, between-group contact probabilities were higher than use and in summer, between-group contacts were closer to roads than indicated by use. Thus, using habitat selection models of host species to identify areas of risk for CWD as is done by management agencies when preparing to detect and monitor CWD (Dugal et al. 2013; Russell et al. 2015), is a reasonable approach, but some caution is necessary because mechanisms influence frequency of contact (i.e. rates) are not strictly spatial. Further, we did not examine the relationship between rates and spatial probabilities of contact, but it is possible that the two are not linearly related. However, general consistency in the factors that influence the probability of host contact and disease risk on the landscape suggests habitat factors that influence host behavior contribute to host exposure and transmission.

Alberta is one of three provinces where CWD is known in wild populations in Canada. The continued spread of disease could cause deer populations to decline dramatically, resulting in severe social, ecologic, and economic consequences. Further modeling efforts in Alberta could lead Canada in devising and implementing strategies to limit CWD spread. The results of my study provide valuable inputs for spatial epidemiological models that can weight estimates of sex-specific, seasonal direct contact rates in space when using either individual-based, movement models of disease spread (Belsare et al. 2021, Gritter 2022) or epidemiological models that use host space use overlap to incorporate disease exposure (Xu et al. in press). Although incorporating heterogeneity in environmental exposure will be a key next step, my work contributes to providing more realistic model outcomes to inform management strategies that target the individuals and environments most likely to transmit CWD.

LITERATURE CITED

Alberta Energy Regulator. 2020. ST37: List of Wells in Alberta. Alberta Energy Regulator.

Alberta Government. 2022. Chronic Wasting Disease – Updates. https://www.alberta.ca/chronic-wasting-disease-updates.aspx. Accessed February 2022.

Almberg ES, Cross PC, Johnson CJ, Heisey DM, Richards BJ. 2011. Modeling Routes of Chronic Wasting Disease Transmission: Environmental Prion Persistence Promotes Deer Population Decline and Extinction. Public Library of Science. *PLoS ONE* 6:e19896.

Almberg ES, Manlove KR, Cassirer EF, Ramsey J, Carson K, Gude J, Plowright RK. 2022. Modelling management strategies for chronic disease in wildlife: Predictions for the control of respiratory disease in bighorn sheep. John Wiley & Sons, Ltd. *Journal of Applied Ecology* 59:693–703.

Altalis. 2018a. Hydrography. Altalis.

———. 2018b. 25m Raster DEM. Altalis.

———. 2020. Access. Altalis.

Altizer S, Nunn C, Thrall P, Gittleman J, Antonovics J, Cunningham A, Dobson A, Ezenwa V, Jones K, Pedersen A, et al. 2003. Social organization and parasite risk in mammals: Integrating theory and empirical studies. *ANNUAL REVIEW OF ECOLOGY EVOLUTION AND SYSTEMATICS* 34:517–547.

Altizer S, Ostfeld RS, Johnson PTJ, Kutz S, Harvell CD. 2013. Climate Change and Infectious Diseases: From Evidence to a Predictive Framework. *Science* 341:514–519.

Anderson E, Long R, Atwood M, Kie J, Thomas T, Zager P, Bowyer R. 2012. Winter resource selection by female mule deer Odocoileus hemionus: functional response to spatio-temporal changes in habitat. *WILDLIFE BIOLOGY* 18:153–163.

Anderson RM, May RM. 1979. Population biology of infectious diseases: Part I. *Nature* 280:361–367.

Arnot C, Laate E, Unterschultz J, Adamowicz W. 2009. Chronic Wasting Disease (CWD) Potential Economic Impact on Cervid Farming in Alberta. Taylor & Francis. *null* 72:1014–1017.

Arthur R, Gurley E, Salje H, Bloomfield L, Jones J. 2017. Contact structure, mobility, environmental impact and behaviour: The importance of social forces to infectious disease dynamics and disease ecology. *Philosophical Transactions of the Royal Society B: Biological Sciences* 372:20160454.

Bansal S, Grenfell BT, Meyers LA. 2007. When individual behaviour matters: homogeneous and network models in epidemiology. *J R Soc Interface* 4:879–891.

Becker DJ, Streicker DG, Altizer S. 2018. Using host species traits to understand the consequences of resource provisioning for host–parasite interactions. *Journal of Animal Ecology* 87:511–525.

van Beest FM, Vander Wal E, Stronen AV, Brook RK. 2013. Factors driving variation in movement rate and seasonality of sympatric ungulates. *Journal of Mammalogy* 94:691–701.

Begon M, Bennett M, Bowers RG, French NP, Hazel SM, Turner J. 2002a. A clarification of transmission terms in host-microparasite models: numbers, densities and areas. *Epidemiology and infection* 129:147–53.

Bellis E, Graves H. 1971. DEER MORTALITY ON A PENNSYLVANIA INTERSTATE HIGHWAY. *JOURNAL OF WILDLIFE MANAGEMENT* 35:232-.

Belsare A V, Millspaugh JJ, Mason JR, Sumners J, Viljugrein H, Mysterud A. 2021. Getting in Front of Chronic Wasting Disease: Model-Informed Proactive Approach for Managing an Emerging Wildlife Disease. *FRONTIERS IN VETERINARY SCIENCE* 7.

Benjamini Y, Hochberg Y. 1995. Controlling the False Discovery Rate: A Practical and Powerful Approach to Multiple Testing. [Royal Statistical Society, Wiley]. *Journal of the Royal Statistical Society Series B (Methodological)* 57:289–300.

Best EC, Dwyer RG, Seddon JM, Goldizen AW. 2014. Associations are more strongly correlated with space use than kinship in female eastern grey kangaroos. *Animal Behaviour* 89:1–10.

Biggerstaff MT, Lashley MA, Chitwood MC, Moorman CE, DePerno CS. 2017. Sexual segregation of forage patch use: Support for the social-factors and predation hypotheses. *Behavioural Processes* 136:36–42.

Blanchong J, Scribner K, Kravchenko A, Winterstein S. 2007. TB-infected deer are more closely related than non-infected deer. *BIOLOGY LETTERS* 3:103–105.

Blower SM, McLean AR. 1991. Mixing ecology and epidemiology. Royal Society. *Proceedings of the Royal Society of London Series B: Biological Sciences* 245:187–192.

Bollinger T, Caley P, Merrill E, Messier F, Miller M, Samuel M, Vanopdenbosch E. 2004. Chronic Wasting Disease in Canadian Wildlife: An Expert Opinion on the Epidemiology and Risks to Wild Deer.

Bowyer R, McCullough D, Belovsky G. 2001. Causes and consequences of sociality in mule deer. In: W. Ballard and A. Rogers, editors. pp. 371–402.

Bowyer RT. 1985. Correlates of group living in southern mule deer. Ph.D., University of Michigan, Ann Arbor, 100 pp.

https://login.ezproxy.library.ualberta.ca/login?url=https://www.proquest.com/dissertations-theses/correlates-group-living-southern-mule-deer/docview/303379784/se-2?accountid=14474. Accessed.

Bowyer TR, Kie JG. 2004. Effects of Foraging Activity on Sexual Segregation in Mule Deer. *Journal of Mammalogy* 85:498–504.

Bradley CA, Altizer S. 2007. Urbanization and the ecology of wildlife diseases. *Trends in Ecology & Evolution* 22:95–102.

Caley P, Ramsey D. 2001. Estimating Disease Transmission in Wildlife, with Emphasis on Leptospirosis and Bovine Tuberculosis in Possums, and Effects of Fertility Control. [British Ecological Society, Wiley]. *Journal of Applied Ecology* 38:1362–1370.

Carrollo EM, Johnson HE, Fischer JW, Hammond M, Dorsey PD, Anderson C, Vercauteren KC, Walter WD. 2017. Influence of Precipitation and Crop Germination on Resource Selection by Mule Deer (Odocoileus hemionus) in Southwest Colorado. *Scientific Reports* 7:15234.

Carstensen M, O'Brien DJ, Schmitt SM. 2011. Public acceptance as a determinant of management strategies for bovine tuberculosis in free-ranging US wildlife. Elsevier. *Veterinary microbiology* 151:200–204.

Carter KD, Seddon JM, Frère CH, Carter JK, Goldizen AW. 2013. Fission–fusion dynamics in wild giraffes may be driven by kinship, spatial overlap and individual social preferences. *Animal Behaviour* 85:385–394.

Chiyo P, Archie E, Hollister-Smith J, Lee P, Poole J, Moss C, Alberts S. 2011. Association patterns of African elephants in all-male groups: the role of age and genetic relatedness. *ANIMAL BEHAVIOUR* 81:1093–1099.

Coe PK, Clark DA, Nielson RM, Gregory SC, Cupples JB, Hedrick MJ, Johnson BK, Jackson DH. 2018. Multiscale models of habitat use by mule deer in winter. John Wiley & Sons, Ltd. *The Journal of Wildlife Management* 82:1285–1299.

Colorado Parks and Wildlife. 2022. About CWD and Adaptive Management. https://cpw.state.co.us/learn/Pages/About-CWD-in-Colorado.aspx#:~:text=As%20of%20February%202020%2C%20CWD,in%20many%20affected%20Colorado%20herds. Accessed February 2022.

Colson KE, Brinkman TJ, Person DK, Hundertmark KJ. 2012. Fine-scale social and spatial genetic structure in Sitka black-tailed deer. *Conservation Genetics* 14:439–449.

Conner M, Miller M. 2004. Movement patterns and spatial epidemiology of a prion disease in mule deer population units. *ECOLOGICAL APPLICATIONS* 14:1870–1881.

Connolly GE. 1981. Trends in populations and harvests. *Mule and black-tailed deer of North America University of Nebraska Press, Lincoln, Nebraska, USA*:225–243.

Craft ME. 2015. Infectious disease transmission and contact networks in wildlife and livestock. *Philosophical Transactions of the Royal Society B: Biological Sciences* 370:20140107.

Craft ME, Caillaud D. 2011. Network Models: An Underutilized Tool in Wildlife Epidemiology? Hindawi Publishing Corporation. *Interdisciplinary Perspectives on Infectious Diseases* 2011:676949.

Craft ME, Volz E, Packer C, Meyers LA. 2011. Disease transmission in territorial populations: the small-world network of Serengeti lions. *J R Soc Interface* 8:776–786.

Cross P, Lloyd-Smith J, Johnson P, Getz W. 2005. Duelling timescales of host movement and disease recovery determine invasion of disease in structured populations. *ECOLOGY LETTERS* 8:587–595.

Cross PC, Creech TG, Ebinger MR, Heisey DM, Irvine KM, Creel S. 2012. Wildlife contact analysis: emerging methods, questions, and challenges. *Behavioral Ecology and Sociobiology* 66:1437–1447.

Cross PC, Creech TG, Ebinger MR, Manlove K, Irvine K, Henningsen J, Rogerson J, Scurlock BM, Creel S. 2013. Female elk contacts are neither frequency nor density dependent. *Ecology* 94:2076–2086.

Cullingham C, Merrill E, Pybus M, Bollinger T, Wilson G, Coltman D. 2011a. Broad and fine-scale genetic analysis of white-tailed deer populations: estimating the relative risk of chronic wasting disease spread. *EVOLUTIONARY APPLICATIONS* 4:116–131.

Cullingham CI, Nakada SM, Merrill EH, Bollinger TK, Pybus MJ, Coltman DW. 2011b. Multiscale population genetic analysis of mule deer (Odocoileus hemionus hemionus) in western Canada sheds new light on the spread of chronic wasting disease. *Can J Zool* 89:134–147.

Currie-Fraser E, Shah P, True S. 2010. Data analysis using GeneMapper® v4.1: Comparing the Newest Generation of GeneMapper Software to Legacy Genescan® and Genotyper® Software. Association of Biomolecular Resource Facilities. *J Biomol Tech* 21:S31–S31.

Daszak P, Berger L, Cunningham AA, Hyatt AD, Green DE, Speare R. 1999. Emerging infectious diseases and amphibian population declines. Centers for Disease Control and Prevention. *Emerg Infect Dis* 5:735–748.

Daszak P, Cunningham AA, Hyatt AD. 2001. Anthropogenic environmental change and the emergence of infectious diseases in wildlife. *Acta Tropica* 78:103–116.

Daszak P, Epstein JH, Kilpatrick AM, Aguirre AA, Karesh WB, Cunningham AA. 2007. Collaborative Research Approaches to the Role of Wildlife in Zoonotic Disease

Emergence. In: *Wildlife and Emerging Zoonotic Diseases: The Biology, Circumstances and Consequences of Cross-Species Transmission*, J. E. Childs, J. S. Mackenzie, and J. A. Richt, editors. Springer Berlin Heidelberg, Berlin, Heidelberg. pp. 463–475. https://doi.org/10.1007/978-3-540-70962-6_18. Accessed.

De Castro F, Bolker B. 2005. Mechanisms of disease-induced extinction. John Wiley & Sons, Ltd. *Ecology Letters* 8:117–126.

D'eon R, Serrouya R, Smith G, Kochanny C. 2002. GPS radiotelemetry error and bias in mountainous terrain. *Wildlife Society Bulletin* 30:430–439.

D'Eon RG, Serrouya R. 2005. Mule deer seasonal movements and multiscale resource selection using global positioning system radiotelemetry. American Society of Mammalogists. *Journal of Mammalogy* 86:736–744.

Devivo MT, Edmunds DR, Kauffman MJ, Schumaker BA, Binfet J, Kreeger TJ, Richards BJ, Schätzl HM, Cornish TE. 2017. Endemic chronic wasting disease causes mule deer population decline in Wyoming. Public Library of Science (PLoS). *PLOS ONE* 12:e0186512.

Drolet CA. 1976. Distribution and movements of white-tailed deer in southern New Brunswick in relation to environmental factors. *Canadian Field Naturalist* 902:123–136.

Dudley JP, Hang'Ombe BM, Leendertz FH, Dorward LJ, de Castro J, Subalusky AL, Clauss M. 2016. Carnivory in the common hippopotamus Hippopotamus amphibius: implications for the ecology and epidemiology of anthrax in African landscapes. John Wiley & Sons, Ltd. *Mammal Review* 46:191–203.

Dugal CJ, van Beest FM, Vander Wal E, Brook RK. 2013. Targeting hunter distribution based on host resource selection and kill sites to manage disease risk. John Wiley & Sons, Ltd. *Ecology and Evolution* 3:4265–4277.

Dunn OJ. 1964. Multiple Comparisons Using Rank Sums. Taylor & Francis. *Technometrics* 6:241–252.

Edmunds DR, Kauffman MJ, Schumaker BA, Lindzey FG, Cook WE, Kreeger TJ, Grogan RG, Cornish TE. 2016. Chronic Wasting Disease Drives Population Decline of White-Tailed Deer. Public Library of Science (PLoS). *PLOS ONE* 11:e0161127.

Ehrmann S, Ruyts S, Scherer-Lorenzen M, Bauhus J, Brunet J, Cousins S, Deconchat M, Decocq G, De Frenne P, De Smedt P, et al. 2018. Habitat properties are key drivers of Borrelia burgdorferi (s.l.) prevalence in Ixodes ricinus populations of deciduous forest fragments. *PARASITES & VECTORS* 11.

Epstein PR. 2001. Climate change and emerging infectious diseases. *Microbes and Infection* 3:747–754.

Escobar LE, Pritzkow S, Winter SN, Grear DA, Kirchgessner MS, Dominguez-Villegas E, Machado G, Townsend Peterson A, Soto C. 2020. The ecology of chronic wasting disease in wildlife. Blackwell Publishing Ltd. *Biological Reviews* 95:393–408.

Evans TS, Kirchgessner MS, Eyler B, Ryan CW, Walter WD. 2016. Habitat influences distribution of chronic wasting disease in white-tailed deer. *Jour Wild Mgmt* 80:284–291.

Farnsworth ML, Wolfe LL, Hobbs NT, Burnham KP, Williams ES, Theobald DM, Conner MM, Miller MW. 2005. HUMAN LAND USE INFLUENCES CHRONIC WASTING DISEASE PREVALENCE IN MULE DEER. *Ecological Applications* 15:119–126.

Ferrari MJ, Perkins SE, Pomeroy LW, Bjrnstad ON. 2011. Pathogens, social networks, and the paradox of transmission scaling. *Interdisciplinary Perspectives on Infectious Diseases* 2011.

Ferrari N, Rosà R, Lanfranchi P, Ruckstuhl KE. 2010. Effect of sexual segregation on host–parasite interaction: Model simulation for abomasal parasite dynamics in alpine ibex (Capra ibex). *International Journal for Parasitology* 40:1285–1293.

Forand KJ, Marchinton RL. 1989. Patterns of Social Grooming in Adult White-tailed Deer. University of Notre Dame. *The American Midland Naturalist* 122:357–364.

Fountain-Jones NM, Kraberger S, Gagne RB, Trumbo DR, Salerno PE, Chris Funk W, Crooks K, Biek R, Alldredge M, Logan K, et al. 2021. Host relatedness and landscape connectivity shape pathogen spread in the puma, a large secretive carnivore. *Communications Biology* 4:12.

Frair J, Nielsen S, Merrill E, Lele S, Boyce M, Munro R, Stenhouse G, Beyer H. 2004. Removing GPS collar bias in habitat selection studies. *JOURNAL OF APPLIED ECOLOGY* 41:201–212.

Franz M, Kramer-Schadt S, Greenwood A, Courtiol A. 2018. Sickness-induced lethargy can increase host contact rates and pathogen spread in water-limited landscapes. *FUNCTIONAL ECOLOGY* 32:2194–2204.

Freeman ED, Larsen RT, Peterson ME, Anderson Jr CR, Hersey KR, Mcmillan BR. 2014. Effects of male-biased harvest on mule deer: Implications for rates of pregnancy, synchrony, and timing of parturition. John Wiley & Sons, Ltd. *Wildlife Society Bulletin* 38:806–811.

Garlick M, Powell J, Hooten M, MacFarlane L. 2014. Homogenization, sex, and differential motility predict spread of chronic wasting disease in mule deer in southern Utah. *JOURNAL OF MATHEMATICAL BIOLOGY* 69:369–399.

Garvin MC, Basbaum JP, Ducore RM, Bell KE. 2003. PATTERNS OF HAEMOPROTEUS BECKERI PARASITISM IN THE GRAY CATBIRD (DUMATELLA CAROLINENSIS) DURING THE BREEDING SEASON. *Journal of Wildlife Diseases* 39:582–587.

Gilbert SL, Hundertmark KJ, Person DK, Lindberg MS, Boyce MS. 2017. Behavioral plasticity in a variable environment: snow depth and habitat interactions drive deer movement in winter. *Journal of Mammalogy* 98:246–259.

Gilbertson MLJ, White LA, Craft ME. 2021. Trade-offs with telemetry-derived contact networks for infectious disease studies in wildlife. *Methods in Ecology and Evolution* 12:76–87.

Grear DA, Samuel MD, Langenberg JA, Keane D. 2006. Demographic Patterns and Harvest Vulnerability of Chronic Wasting Disease Infected White-Tailed Deer in Wisconsin. John Wiley & Sons, Ltd. *The Journal of Wildlife Management* 70:546–553.

Grear DA, Samuel MD, Scribner KT, Weckworth BV, Langenberg JA. 2010. Influence of genetic relatedness and spatial proximity on chronic wasting disease infection among female white-tailed deer: Social transmission of CWD. *Journal of Applied Ecology* 47:532–540.

Griffith B. 1988. Group Predator Defense by Mule Deer in Oregon. [American Society of Mammalogists, Oxford University Press]. *Journal of Mammalogy* 69:627–629.

Gritter KM. 2022. Individual-based movement model of mule deer (*Odocoileus hemionus*) contacts and application to artificial attractants. MSc Thesis, University of Alberta.

Grogan LF, Berger L, Rose K, Grillo V, Cashins SD, Skerratt LF. 2014. Surveillance for Emerging Biodiversity Diseases of Wildlife. Public Library of Science. *PLOS Pathogens* 10:e1004015.

Gudelj I, White KAJ. 2004. Spatial heterogeneity, social structure and disease dynamics of animal populations. *Theoretical Population Biology* 66:139–149.

Gulsby WD, Kilgo JC, Vukovich M, Martin JA. 2017. Landscape Heterogeneity Reduces Coyote Predation on White-Tailed Deer Fawns. [Wiley, Wildlife Society]. *The Journal of Wildlife Management* 81:601–609.

Habib TJ, Merrill EH, Pybus MJ, Coltman DW. 2011. Modelling landscape effects on density–contact rate relationships of deer in eastern Alberta: implications for chronic wasting disease. Elsevier. *Ecological Modelling* 222:2722–2732.

Haley NJ, Hoover EA. 2014. Chronic Wasting Disease of Cervids: Current Knowledge and Future Perspectives. *Annual Review of Animal Biosciences* 3:305–325.

Hamede RK, McCallum H, Jones M. 2013. Biting injuries and transmission of Tasmanian devil facial tumour disease. *Journal of Animal Ecology* 82:182–190.

Han BA, O'Regan SM, Paul Schmidt J, Drake JM. 2020. Integrating data mining and transmission theory in the ecology of infectious diseases. *ECOLOGY LETTERS* 23:1178–1188.

Härkönen T, Harding K, Rasmussen TD, Teilmann J, Dietz R. 2007. Age- and Sex-Specific Mortality Patterns in an Emerging Wildlife Epidemic: The Phocine Distemper in European Harbour Seals. Public Library of Science. *PLOS ONE* 2:e887.

Harrell FE. 2017. Regression modeling strategies. Springer. *Bios* 330:14.

Hawkins R, Klimstra W. 1970. A preliminary study of social organization of white-tailed deer. *Journal of Wildlife Management* 34:407-.

Hedman HD, Varga C, Brown WM, Shelton P, Roca AL, Novakofski JE, Mateus-Pinilla NE. 2020. Spatial analysis of chronic wasting disease in free-ranging white-tailed deer (*Odocoileus virginianus*) in Illinois, 2008–2019. *Transbound Emerg Dis*:tbed.13901.

Hefley TJ, Hooten MB, Russell RE, Walsh DP, Powell JA. 2017. When mechanism matters: Bayesian forecasting using models of ecological diffusion.

Heisey D, Osnas E, Cross P, Joly D, Langenberg J, Miller M. 2010. Linking process to pattern: estimating spatiotemporal dynamics of a wildlife epidemic from cross-sectional data. *ECOLOGICAL MONOGRAPHS* 80:221–240.

Herrera J, Nunn CL. 2019. Behavioural ecology and infectious disease: implications for conservation of biodiversity. *Phil Trans R Soc B* 374:20180054.

Hoque MN, Faisal GM, Chowdhury FR, Haque A, Islam T. 2022. The urgency of wider adoption of one health approach for the prevention of a future pandemic. *Health* 8:20–33.

Horncastle VJ, Fenner Yarborough R, Dickson BG, Rosenstock SS. 2013. Summer habitat use by adult female mule deer in a restoration-treated ponderosa pine forest. John Wiley & Sons, Ltd. *Wildlife Society Bulletin* 37:707–713.

Jackson LE, Hilborn ED, Thomas JC. 2006. Towards landscape design guidelines for reducing Lyme disease risk. *International Journal of Epidemiology* 35:315–322.

Janousek WM, Graves TA, Berman EE, Chong GW, Cole EK, Dewey SR, Johnston AN, Cross PC. 2021. Human activities and weather drive contact rates of wintering elk. *J Appl Ecol* 58:667–676.

Jennelle CS, Henaux V, Wasserberg G, Thiagarajan B, Rolley RE, Samuel MD. 2014. Transmission of Chronic Wasting Disease in Wisconsin White-Tailed Deer: Implications for Disease Spread and Management. Public Library of Science. *PLOS ONE* 9:e91043.

Ji W, White PCL, Clout MN. 2005. Contact rates between possums revealed by proximity data loggers. John Wiley & Sons, Ltd. *Journal of Applied Ecology* 42:595–604.

Joly DO, Samuel MD, Langenberg JA, Blanchong JA, Batha CA, Rolley RE, Keane DP, Ribic CA. 2006a. SPATIAL EPIDEMIOLOGY OF CHRONIC WASTING DISEASE IN WISCONSIN WHITE-TAILED DEER. Wildlife Disease Association. *Journal of Wildlife Diseases* 42:578–588.

Kappeler PM, Cremer S, Nunn CL. 2015. Sociality and health: impacts of sociality on disease susceptibility and transmission in animal and human societies Introduction. *PHILOSOPHICAL TRANSACTIONS OF THE ROYAL SOCIETY B-BIOLOGICAL SCIENCES* 370.

Keeling MJ, Eames KTD. 2005. Networks and epidemic models. Royal Society. *Journal of The Royal Society Interface* 2:295–307.

Kelly AC, Mateus-Pinilla NE, Douglas M, Douglas M, Brown W, Ruiz MO, Killefer J, Shelton P, Beissel T, Novakofski J. 2010. Utilizing disease surveillance to examine gene flow and dispersal in white-tailed deer: Gene flow from disease surveillance. *Journal of Applied Ecology* 47:1189–1198.

Ketz AC. 2019. Chronic wasting disease and implications for cervid populations. *CAB Reviews* 14. http://www.cabi.org/cabreviews/review/20193322221. Accessed July 2021.

Kie JG, Bowyer RT, Nicholson MC, Boroski BB, Loft ER. 2002. LANDSCAPE HETEROGENEITY AT DIFFERING SCALES: EFFECTS ON SPATIAL DISTRIBUTION OF MULE DEER. *Ecology* 83:530–544.

Kilpatrick AM, Briggs CJ, Daszak P. 2010. The ecology and impact of chytridiomycosis: an emerging disease of amphibians. *Trends in Ecology & Evolution* 25:109–118.

Kirkeby C, Halasa T, Gussmann M, Toft N, Græsbøll K. 2017. Methods for estimating disease transmission rates: Evaluating the precision of Poisson regression and two novel methods. *Scientific Reports* 7:9496.

Kjaer L, Schauber E, Nielsen C. 2008. Spatial and Temporal Analysis of Contact Rates in Female White-Tailed Deer. *JOURNAL OF WILDLIFE MANAGEMENT* 72:1819–1825.

Koen EL, Tosa MI, Nielsen CK, Schauber EM. 2017. Does landscape connectivity shape local and global social network structure in white-tailed deer? Public Library of Science. *PLoS One* 12:e0173570–e0173570.

Krauss S, Stallknecht DE, Negovetich NJ, Niles LJ, Webby RJ, Webster RG. 2010. Coincident ruddy turnstone migration and horseshoe crab spawning creates an ecological “hot spot” for influenza viruses. The Royal Society. *Proc Biol Sci* 277:3373–3379.

Krull CR, McMillan LF, Fewster RM, van der Ree R, Pech R, Dennis T, Stanley MC. 2018. Testing the feasibility of wireless sensor networks and the use of radio signal strength indicator to track the movements of wild animals. *Wildl Res* 45:659–667.

Langwig KE, Voyles J, Wilber MQ, Frick WF, Murray KA, Bolker BM, Collins JP, Cheng TL, Fisher MC, Hoyt JR, et al. 2015. Context-dependent conservation responses to emerging wildlife diseases. John Wiley & Sons, Ltd. *Frontiers in Ecology and the Environment* 13:195–202.

Latifovic R. 2019. 2015 Land Cover of Canada. Government of Canada; Natural Resources Canada; Canada Centre for Remote Sensing.

Lavelle MJ, Fischer JW, Phillips G, Hildreth A, Campbell TA, HEWITT DG, HYGNSTROM SE, VERCAUTEREN KC. 2014. Assessing Risk of Disease Transmission. [American Institute of Biological Sciences, Oxford University Press]. *BioScience* 64:524–530.

Lendrum P, Anderson C, Long R, Kie J, Bowyer R. 2012. Habitat selection by mule deer during migration: Effects of landscape structure and natural-gas development. *Ecosphere* 3.

Lingle S. 2001. Anti-predator strategies and grouping patterns in white-tailed deer and mule deer. *ETHOLOGY* 107:295–314.

Lingle S. 2003. Group composition and cohesion in sympatric white-tailed deer and mule deer. NRC Research Press. *Can J Zool* 81:1119–1130.

Lingle SE, Pellis SM, Wilson WF. 2005. Interspecific variation in antipredator behaviour leads to differential vulnerability of mule deer and white tailed deer fawns early in life. *Journal of Animal Ecology* 74:1140–1149.

Lloyd-Smith J, Cross P, Briggs C, Daugherty M, Getz W, Latto J, Sanchez M, Smith A, Swei A. 2005. Should we expect population thresholds for wildlife disease? *TRENDS IN ECOLOGY & EVOLUTION* 20:511–519.

Loft ER, Menke JW, Kie JG. 1991. Habitat Shifts by Mule Deer: The Influence of Cattle Grazing. [Wiley, Wildlife Society]. *The Journal of Wildlife Management* 55:16–26.

Long JA, Webb SL, Harju SM, Gee KL. 2021. Analyzing Contacts and Behavior from High Frequency Tracking Data Using the wildlifeDI R Package. John Wiley & Sons, Ltd. *Geographical Analysis* n/a. https://doi.org/10.1111/gean.12303. Accessed March 2022.

Long RA, Kie JG, Bowyer RT, Hurley MA. 2009. Resource Selection and Movements by Female Mule Deer Odocoileus hemionus: Effects of Reproductive Stage. *Wildlife Biology* 15:288–298.

Mackie RJ. 1970. Range Ecology and Relations of Mule Deer, Elk, and Cattle in the Missouri River Breaks, Montana. [Wiley, Wildlife Society]. *Wildlife Monographs*:3–79.

Magle SB, Samuel MD, Van Deelen TR, Robinson SJ, Mathews NE. 2013. Evaluating Spatial Overlap and Relatedness of White-tailed Deer in a Chronic Wasting Disease Management Zone. *PLoS ONE* 8:e56568.

Manjerovic MB, Green ML, Mateus-Pinilla N, Novakofski J. 2014. The importance of localized culling in stabilizing chronic wasting disease prevalence in white-tailed deer populations. *Preventive Veterinary Medicine* 113:139–145.

Manlove KR, Cassirer EF, Plowright RK, Cross PC, Hudson PJ. 2017. Contact and contagion: Probability of transmission given contact varies with demographic state in bighorn sheep. *J Anim Ecol* 86:908–920.

Maraud S, Roturier S. 2021. Chronic Wasting Disease (CWD) in Sami Reindeer Herding: The Socio-Political Dimension of an Epizootic in an Indigenous Context. *Animals* 11. https://www.mdpi.com/2076-2615/11/2/297. Accessed.

Marfievici R, Murphy AL, Picco GP, Ossi F, Cagnacci F. 2013. Are Those Trees Messing with My Wireless Sensor Network? In: *Proceedings of the 11th ACM Conference on Embedded Networked Sensor Systems*. Association for Computing Machinery, New York, NY, USA. https://doi.org/10.1145/2517351.2517425. Accessed.

Mathews NE, Porter WF. 1993. Effect of Social Structure on Genetic Structure of Free-Ranging White-Tailed Deer in the Adirondack Mountains. *Journal of Mammalogy* 74:33–43.

Mathiason CK, Hays SA, Powers J, Hayes-Klug J, Langenberg J, Dahmes SJ, Osborn DA, Miller KV, Warren RJ, Mason GL, et al. 2009. Infectious Prions in Pre-Clinical Deer and Transmission of Chronic Wasting Disease Solely by Environmental Exposure. *PLoS ONE* 4:e5916.

May R, Anderson R. 1979. May RM, Anderson RM. Population biology of infectious diseases: part II. Nature 280: 455-461. *Nature* 280:455–61.

McCallum H. 2009. Transmission dynamics of Tasmanian devil facial tumor disease may lead to disease-induced extinction. Brooklyn Botanical Garden, Brooklyn, NY : *Ecology* 90.

McClure MF, Bissonette JA, Conover MR. 2005. Migratory strategies, fawn recruitment, and winter habitat use by urban and rural mule deer (Odocoileus hemionus). *European Journal of Wildlife Research* 51:170–177.

McDonald JL, Smith GC, McDonald RA, Delahay RJ, Hodgson D. 2014. Mortality trajectory analysis reveals the drivers of sex-specific epidemiology in natural wildlife–disease interactions. Royal Society. *Proceedings of the Royal Society B: Biological Sciences* 281:20140526.

McGinnis S, Kerans BL. 2013. Land use and host community characteristics as predictors of disease risk. *Landscape Ecol* 28:29–44.

McGovern PG, Dinsmore SJ, Blanchong JA. 2020. Survival of white-tailed deer fawns in central Iowa. Public Library of Science. *PLOS ONE* 15:e0229242.

McRoberts RE, Mech LD, Peterson RO. 1995. The Cumulative Effect of Consecutive Winters' Snow Depth on Moose and Deer Populations: A Defence. [Wiley, British Ecological Society]. *Journal of Animal Ecology* 64:131–135.

Mejia-Salazar M, Goldizen A, Menz C, Dwyer R, Blomberg S, Weidner C, Cullingham C, Bollinger T. 2017. Mule deer spatial association patterns and potential implications for transmission of an epizootic disease. *PLOS ONE* 12.

Merrill EH, Pybus MJ, Nobert BR, Habib TJ, Brownrigg E, Jones P, Garrett C, Bertrand A, Wachowski J, Stevens J, et al. 2013. Alberta Chronic Wasting Disease: North Border Deer Study. :1–76.

Meurens F, Dunoyer C, Fourichon C, Gerdts V, Haddad N, Kortekaas J, Lewandowska M, Monchatre-Leroy E, Summerfield A, Wichgers Schreur PJ, et al. 2021. Animal board invited review: Risks of zoonotic disease emergence at the interface of wildlife and livestock systems. *Animal* 15:100241.

Miller CA, Vaske JJ. 2022. How state agencies are managing chronic wasting disease. Routledge. *null*:1–10.

Miller MW, Conner MM. 2005. EPIDEMIOLOGY OF CHRONIC WASTING DISEASE IN FREE-RANGING MULE DEER: SPATIAL, TEMPORAL, AND DEMOGRAPHIC INFLUENCES ON OBSERVED PREVALENCE PATTERNS. *Journal of Wildlife Diseases* 41:275–290.

Miller MW, Runge JP, Andrew Holland A, Eckert MD. 2020a. Hunting pressure modulates prion infection risk in mule deer herds. *Journal of Wildlife Diseases* 56:781–790.

Miller MW, Wild MA. 2004. Epidemiology of Chronic Wasting Disease in Captive White-Tailed and Mule Deer. Wildlife Disease Association. *Journal of Wildlife Diseases* 40:320–327.

Miller MW, Williams ES, Hobbs NT, Wolfe LL. 2004. Environmental sources of prion transmission in mule deer. *Emerging Infectious Diseases* 10:1003–1006.

Miller MW, Williams ES, McCarty CW, Spraker TR, Kreeger TJ, Larsen CT, Thorne ET. 2000. Epizootiology of Chronic Wasting Disease in Free-Ranging Cervids in Colorado and Wyoming. *Journal of Wildlife Diseases* 36:676–690.

Miller WL, Miller-Butterworth CM, Diefenbach DR, Walter WD. 2020c. Assessment of spatial genetic structure to identify populations at risk for infection of an emerging epizootic disease. *ECOLOGY AND EVOLUTION* 10:3977–3990.

Miller-Butterworth CM, Vonhof MJ, Rosenstern J, Turner GG, Russell AL. 2014. Genetic Structure of Little Brown Bats (Myotis lucifugus) Corresponds with Spread of White-Nose Syndrome among Hibernacula. *Journal of Heredity* 105:354–364.

Millspaugh J, Gitzen R, Kernohan B, Larson J, Clay C. 2004. Comparability of three analytical techniques to assess joint space use. *WILDLIFE SOCIETY BULLETIN* 32:148–157.

Morano S, Stewart KM, Dilts T, Ellsworth A, Bleich VC. 2019. Resource selection of mule deer in a shrub-steppe ecosystem: influence of woodland distribution and animal behavior. John Wiley & Sons, Ltd. *Ecosphere* 10:e02811.

Muggeo VMR. 2017. Interval estimation for the breakpoint in segmented regression: a smoothed score-based approach. *Australian & New Zealand Journal of Statistics* 59:311–322.

Mysterud A, Edmunds DR. 2019a. A review of chronic wasting disease in North America with implications for Europe. Springer Science and Business Media LLC. *European Journal of Wildlife Research* 65. https://dx.doi.org/10.1007/s10344-019-1260-z. Accessed.

Mysterud A, Østbye E. 1999. Cover as a habitat element for temperate ungulates: effects on habitat selection and demography. JSTOR. *Wildlife society bulletin*:385–394.

Nixon CM, Hansen LP, Brewer PA, Chelsvig JE. 1991. Ecology of White-Tailed Deer in an Intensively Farmed Region of Illinois. [Wiley, Wildlife Society]. *Wildlife Monographs*:3–77.

Nixon CM, Mankin PC, Etter DR, Hansen LP, Brewer A, Chelsvig JE, Esker TL, Sullivan JB, The S, Midland A, et al. 2007. White-Tailed Deer Dispersal Behavior in an Agricultural Environment. 157:212–220.

Nobert BR. 2012. Landscape Ecology of Mule Deer (Odocoileus hemionus) and White-tailed Deer (O. virginianus) with Implications for Chronic Wasting Disease. PhD Thesis, University of Alberta.

Nobert BR, Merrill EH, Pybus MJ, Bollinger TK, Hwang YT. 2016. Landscape connectivity predicts chronic wasting disease risk in Canada. Wiley. *Journal of Applied Ecology* 53:1450–1459.

Noble CW, Bono JM, Pigage HK, Hale DW, Pigage JC. 2016. Fine-Scale Genetic Structure in Female Mule Deer (*Odocoileus hemionus*). *Western North American Naturalist* 76:417–426.

Northrup JM, Anderson Jr CR, Gerber BD, Wittemyer G. 2021. Behavioral and Demographic Responses of Mule Deer to Energy Development on Winter Range. John Wiley & Sons, Ltd. *Wildlife Monographs* 208:1–37.

Northrup JM, Anderson Jr CR, Wittemyer G. 2016. Environmental dynamics and anthropogenic development alter philopatry and space-use in a North American cervid. Wiley Online Library. *Diversity and Distributions* 22:547–557.

O'Brien PP, Webber QMR, Vander Wal E. 2018. Consistent individual differences and population plasticity in network-derived sociality: An experimental manipulation of density in a gregarious ungulate. Public Library of Science. *PLOS ONE* 13:e0193425.

O'Hara Ruiz M, Kelly AC, Brown M W, Novakofski JE, Mateus-Pinilla NE. 2013. Influence of landscape factors and management decisions on spatial and temporal patterns of the transmission of chronic wasting disease in white-tailed deer. Università degli studi Federico II, Dipartimento di patologia e sanità animale. *Geospatial health* 8:215–227.

Oja R, Velström K, Moks E, Jokelainen P, Lassen B. 2017. How does supplementary feeding affect endoparasite infection in wild boar? *Parasitology Research* 116:2131–2137.

Oraby T, Vasilyeva O, Krewski D, Lutscher F. 2014. Modeling seasonal behavior changes and disease transmission with application to chronic wasting disease. *Journal of Theoretical Biology* 340:50–59.

Osnas EE, Heisey DM, Rolley RE, Samuel MD. 2009. Spatial and temporal patterns of chronic wasting disease: fine-scale mapping of a wildlife epidemic in Wisconsin. *Ecological Applications* 19:1311–1322.

Ossi F, Focardi S, Tolhurst BA, Picco GP, Murphy AL, Molteni D, Giannini N, Gaillard J-M, Cagnacci F. 2022. Quantifying the errors in animal contacts recorded by proximity loggers. John Wiley & Sons, Ltd. *The Journal of Wildlife Management* 86:e22151.

Ostfeld R, Glass G, Keesing F. 2005a. Spatial epidemiology: an emerging (or re-emerging) discipline. *Trends in Ecology & Evolution* 20:328–336.

Özmen Ö, Nutaro JJ, Pullum LL, Ramanathan A. 2016. Analyzing the impact of modeling choices and assumptions in compartmental epidemiological models. SAGE Publications Ltd STM. *SIMULATION* 92:459–472.

Ozoga JJ. 1972. Aggressive Behavior of White-Tailed Deer at Winter Cuttings. [Wiley, Wildlife Society]. *The Journal of Wildlife Management* 36:861–868.

Page K, Swihart R, Kazacos K. 2001. Changes in transmission of Baylisacaris procyonis to intermediate hosts as a function of spatial scale. *Oikos* 93:213–220.

Parlee B, Ahkimnachie K, Cunningham H, Jordan M, Goddard E. 2021. "It's important to know about this" - risk communication and the impacts of chronic wasting disease on indigenous food systems in Western Canada. *Environmental Science & Policy* 123:190–201.

Patterson JEH, Ruckstuhl KathreenE. 2013. Parasite infection and host group size: a meta-analytical review. Cambridge University Press. *Parasitology* 140:803–813.

Paull SH, Song S, McClure KM, Sackett LC, Kilpatrick AM, Johnson PTJ. 2012. From superspreaders to disease hotspots: Linking transmission across hosts and space. *Frontiers in Ecology and the Environment* 10:75–82.

Pepin KM, Golnar A, Podgorski T. 2021. Social structure defines spatial transmission of African swine fever in wild boar. *JOURNAL OF THE ROYAL SOCIETY INTERFACE* 18.

Pew J, Muir PH, Wang J, Frasier TR. 2015. related: an R package for analysing pairwise relatedness from codominant molecular markers. John Wiley & Sons, Ltd. *Molecular Ecology Resources* 15:557–561.

Pierce BM, Bowyer RT, Bleich VC. 2004. Habitat Selection by Mule Deer: Forage Benefits or Risk of Predation? [Wiley, Wildlife Society]. *The Journal of Wildlife Management* 68:533–541.

Plummer IH, Johnson CJ, Chesney AR, Pedersen JA, Samuel MD. 2018. Mineral licks as environmental reservoirs of chronic wasting disease prions. Public Library of Science. *PLOS ONE* 13:e0196745.

Podgórski T, Apollonio M, Keuling O. 2017. Contact rates in wild boar populations: Implications for disease transmission. *The Journal of Wildlife Management* 82.

Podgórski T, Borowik T, Łyjak M, Woźniakowski G. 2020. Spatial epidemiology of African swine fever: Host, landscape and anthropogenic drivers of disease occurrence in wild boar. *Preventive Veterinary Medicine* 177:104691.

Podgórski T, Pepin KM, Radko A, Podbielska A, Łyjak M, Woźniakowski G, Borowik T. 2021. How do genetic relatedness and spatial proximity shape African swine fever infections in wild boar? John Wiley & Sons, Ltd. *Transboundary and Emerging Diseases* n/a. https://doi.org/10.1111/tbed.14418. Accessed February 2022.

Potapov A, Merrill E, Lewis MA. 2012. Wildlife disease elimination and density dependence. *Proc R Soc B* 279:3139–3145.

Potapov A, Merrill E, Pybus M, Coltman D, Lewis MA. 2013a. Chronic wasting disease: Possible transmission mechanisms in deer. Elsevier B.V. *Ecological Modelling* 250:244–257.

Pybus M. 2012. *CWD Program Review 2012*. Alberta Sustainable Resources Development, Fish and Wildlife Division, 38 pp. https://open.alberta.ca/dataset/f8adbf7d-14ce-4ba8-bc23-98f11e0f94f0/resource/f54d0e01-f843-49db-b385-fde89a942b00/download/2012-cwd-programreview-may-2012.pdf. Accessed.

Queller DC, Goodnight KF. 1989. Estimating Relatedness Using Genetic Markers. [Society for the Study of Evolution, Wiley]. *Evolution* 43:258–275.

Real LA, Biek R. 2007. Spatial dynamics and genetics of infectious diseases on heterogeneous landscapes. *J R Soc Interface* 4:935–948.

Rees EE, Merrill EH, Bollinger TK, Hwang Y Ten, Pybus MJ, Coltman DW. 2012. Targeting the detection of chronic wasting disease using the hunter harvest during early phases of an outbreak in Saskatchewan, Canada. Elsevier B.V. *Preventive Veterinary Medicine* 104:149–159.

Relyea R, Demarais S. 1994. ACTIVITY OF DESERT MULE DEER DURING THE BREEDING-SEASON. *JOURNAL OF MAMMALOGY* 75:940–949.

Riley SJ, DeGloria SD, Elliot R. 1999. Index that quantifies topographic heterogeneity. *intermountain Journal of sciences* 5:23–27.

Robert K, Garant D, Pelletier F. 2012. Keep in touch: Does spatial overlap correlate with contact rate frequency? Wiley. *The Journal of Wildlife Management* 76:1670–1675.

Robinette WL. 1966. Mule Deer Home Range and Dispersal in Utah. [Wiley, Wildlife Society]. *The Journal of Wildlife Management* 30:335–349.

Rozins C, Silk MJ, Croft DP, Delahay RJ, Hodgson DJ, McDonald RA, Weber N, Boots M. 2018. Social structure contains epidemics and regulates individual roles in disease transmission in a group-living mammal. John Wiley & Sons, Ltd. *Ecology and Evolution* 8:12044–12055.

RStudio Team. 2019. *RStudio: Integrated Development Environment for R*. RStudio, Inc., Boston, MA. http://www.rstudio.com/. Accessed.

Ruckstuhl KE, Neuhaus P. 2000. Sexual Segregation in Ungulates: A New Approach. Brill. *Behaviour* 137:361–377.

Russell RE, Gude JA, Anderson NJ, Ramsey JM. 2015. Identifying priority chronic wasting disease surveillance areas for mule deer in Montana. John Wiley & Sons, Ltd. *The Journal of Wildlife Management* 79:989–997.

Rutz C, Morrissey MB, Burns ZT, Burt J, Otis B, St Clair JJH, James R. 2015. Calibrating animal-borne proximity loggers. John Wiley & Sons, Ltd. *Methods in Ecology and Evolution* 6:656–667.

Sah P, Mann J, Bansal S. 2018. Disease implications of animal social network structure: A synthesis across social systems. John Wiley & Sons, Ltd. *Journal of Animal Ecology* 87:546–558.

Sanchez JN, Hudgens BR. 2015. Interactions between density, home range behaviors, and contact rates in the Channel Island fox (Urocyon littoralis). John Wiley & Sons, Ltd. *Ecology and Evolution* 5:2466–2477.

Sawyer H, Nielson RM, Lindzey F, McDonald LL. 2006. Winter habitat selection of mule deer before and during development of a natural gas field. *Journal of Wildlife Management* 70:396–403.

Schauber EM, Nielsen CK, Kjær LJ, Anderson CW, Storm DJ. 2015. Social affiliation and contact patterns among white-tailed deer in disparate landscapes: implications for disease transmission. *JMAMMAL* 96:16–28.

Schauber EM, Storm DJ, Nielsen CK. 2007. Effects of Joint Space Use and Group Membership on Contact Rates Among White-Tailed Deer. *Journal of Wildlife Management* 71:155–163.

Schmidt KT, Seivwright LJ, Hoi H, Staines BW. 1998. The effect of depletion and predictability of distinct food patches on the timing of aggression in red deer stags. John Wiley & Sons, Ltd. *Ecography* 21:415–422.

Seidel KD. 1992. *Statistical Properties and Applications of a New Measure of Joint Space Use for Wildlife*. University of Washington. https://books.google.ca/books?id=WxjntgAACAAJ. Accessed.

Shorthouse JD. 2010. Ecoregions of Canada's prairie grasslands. In: .

Silbernagel E. 2010. Factors affecting movement patterns of mule deer (Odocoileus hemionus). Master Thesis, University of Saskatchewan, 112 pp.

Silbernagel ER, Skelton NK, Waldner CL, Bollinger TK. 2011. Interaction among deer in a chronic wasting disease endemic zone. *The Journal of Wildlife Management* 75:1453–1461.

Silk MJ, Hodgson DJ, Rozins C, Croft DP, Delahay RJ, Boots M, McDonald RA. 2019. Integrating social behaviour, demography and disease dynamics in network models: applications to disease management in declining wildlife populations. *Phil Trans R Soc B* 374:20180211.

Smith KF, Acevedo-Whitehouse K, Pedersen AB. 2009a. The role of infectious diseases in biological conservation. *Animal Conservation* 12:1–12.

Smith MJ, Telfer S, Kallio ER, Burthe S, Cook AR, Lambin X, Begon M. 2009b. Host-pathogen time series data in wildlife support a transmission function between density and frequency dependence. *Proceedings of the National Academy of Sciences* 106:7905–7909.

Smith SM, Krausman PR, Painter G. 2015. Winter habitat use by mule deer in Idaho and Montana. Society for Northwestern Vertebrate Biology. *Northwestern Naturalist* 96:50–70.

Smolko P, Seidel D, Pybus M, Hubbs A, Ball M, Merrill E. 2021a. Spatio-temporal changes in chronic wasting disease risk in wild deer during 14 years of surveillance in Alberta, Canada. *Preventive Veterinary Medicine* 197:105512.

Sorensen A. 2014. Habitat selection by sympatric ungulates in an agricultural landscape : implications for disease transmission and human-wildlife conflict. *Masters Thesis University of Saskatchewan*.

Storm DJ, Samuel MD, Rolley RE, Shelton P, Keuler NS, Richards BJ, Deelen TRV. 2013a. Deer density and disease prevalence influence transmission of chronic wasting disease in white-tailed deer. *Ecosphere* 4:art10.

Tardy O, Masse A, Pelletier F, Fortin D. 2018a. Interplay between contact risk, conspecific density, and landscape connectivity: An individual-based modeling framework. *ECOLOGICAL MODELLING* 373:25–38.

Thompson AK, Samuel MD, Deelen TRV. 2008. Alternative Feeding Strategies and Potential Disease Transmission in Wisconsin White-Tailed Deer. *Journal of Wildlife Management* 72:416–421.

Tosa MI, Schauber EM, Nielsen CK. 2015. Familiarity breed contempt: Combining proximity loggers and GPS reveals female white-tailed deer (Odocoileus virginianus) avoiding close contact with neighbors. *Journal of Wildlife Diseases* 51:79.

Triguero-Ocaña R, Vicente J, Acevedo P. 2019. Performance of proximity loggers under controlled field conditions: an assessment from a wildlife ecological and epidemiological perspective. *Animal Biotelemetry* 7:24.

Uchii K, Telschow A, Minamoto T, Yamanaka H, Honjo MN, Matsui K, Kawabata Z. 2011. Transmission dynamics of an emerging infectious disease in wildlife through host reproductive cycles. *The ISME Journal* 5:244–251.

Uehlinger FD, Johnston AC, Bollinger TK, Waldner CL. 2016. Systematic review of management strategies to control chronic wasting disease in wild deer populations in North America. *BMC Vet Res* 12:173.

Vander Wal E, Yip H, McLoughlin P. 2012. Sex-based differences in density-dependent sociality: an experiment with a gregarious ungulate. *ECOLOGY* 93:206–212.

VanderWaal KL, Ezenwa VO. 2016a. Heterogeneity in pathogen transmission: mechanisms and methodology. *Funct Ecol* 30:1606–1622.

Vikøren T, Våge J, Madslien KI, Røed KH, Rolandsen CM, Tran L, Hopp P, Veiberg V, Heum M, Moldal T, et al. 2019. First Detection of Chronic Wasting Disease in a Wild Red Deer (Cervus elaphus) in Europe. Wildlife Disease Association. *Journal of Wildlife Diseases* 55:970.

Walter WD, Baasch DM, Hygnstrom SE, Trindle BD, Tyre AJ, Millspaugh JJ, Frost CJ, Boner JR, VerCauteren KC. 2011. Space use of sympatric deer in a riparian ecosystem in an area where chronic wasting disease is endemic. Nordic Board for Wildlife Research. *wbio* 17:191–209.

Walter WD, Evans TS, Stainbrook D, Wallingford BD, Rosenberry CS, Diefenbach DR. 2018. Heterogeneity of a landscape influences size of home range in a North American cervid. *Scientific Reports* 8:14667.

Waring G, Griffis J, Vaughn M. 1991. White-tailed deer roadside behavior, wildlife warning reflectors, and highway mortality. Elsevier. *Applied Animal Behaviour Science* 29:215–223.

Wasserberg G, Osnas EE, Rolley RE, Samuel MD. 2009. Host culling as an adaptive management tool for chronic wasting disease in white-tailed deer: a modelling study. *Journal of Applied Ecology* 46:457–466.

Webb SL, Dzialak MR, Kosciuch KL, Winstead JB. 2013. Winter Resource Selection by Mule Deer on the Wyoming–Colorado Border Prior to Wind Energy Development. Society for Range Management. *rama* 66:419–427.

Western Association of Fish and Wildlife Agencies. 2018. Recommendations for adaptive management of chronic wasting disease in the west. Western Association of Fish and Wildlife Agencies, Edmonton, AB, Canada and Fort Collins, Colorado, USA.

Whitehead H. 2008. *Analyzing Animal Societies: Quantitative Methods for Vertebrate Social Analysis*. University of Chicago Press. https://doi.org/10.7208/9780226895246. Accessed.

Wilber MQ, Knapp RA, Toothman MH, Briggs CJ. 2017. Resistance, tolerance and environmental transmission dynamics determine host extinction risk in a load-dependent amphibian disease. *Ecology letters* 20 9:1169–1181.

Winter SN, Kirchgessner MS, Frimpong EA, Escobar LE. 2021. A Landscape Epidemiological Approach for Predicting Chronic Wasting Disease: A Case Study in Virginia, US. *Frontiers in Veterinary Science* 8.

Wiszniewski J, Lusseau D, Möller LM. 2010. Female bisexual kinship ties maintain social cohesion in a dolphin network. *Animal Behaviour* 80:895–904.

Wood AK, Hamlin KL, Mackie RJ (Richard J, Montana Wildlife Division. 1989. *Ecology of sympatric populations of mule deer and white-tailed deer in a prairie environment*. Wildlife Division, Montana Dept. of Fish, Wildlife & Parks, [S.l.] : https://www.biodiversitylibrary.org/item/137531. Accessed.

Wood SN. 2004. Stable and efficient multiple smoothing parameter estimation for generalized additive models. *Journal of the American Statistical Association* 99:673–686.

Yoder J. 2002. Deer-Inflicted Crop Damage and Crop Choice in Wisconsin. Routledge. *null* 7:179–196.

Zimmer N, Boxall P, Adamowicz W. 2011. The Impact of Chronic Wasting Disease and its Management on Hunter Perceptions, Opinions, and Behaviors in Alberta, Canada. *Journal of toxicology and environmental health Part A* 74:1621–35.

APPENDIX A. DEER COLLAR SUMMARY

TABLE A.1. Summary of mule deer collaring efforts and results of anti-mortem testing using biopsied rectal or retropharyngeal (tonsil) lymphoid tissues taken during captures throughout the study period (2018-2020) on the Cresthill Grazing Lease (CGL) in Wildlife Management Unit 234 central eastern, Alberta, Canada. Post-mortem testing was also conducted whenever viable obex or retropharyngeal tissues were available during mortality site investigations of collared deer.

Capture			Deer	Collar		Sex	Pregnan	CWD Testing		Status	Cause
Date	Year	Site	ID	ID	Type		cy	Anti-	Post		
23-1-18	2018	CGL	181005	80860	LP	M		Rectal	Pos	Drop	
23-1-18	2018	CGL	181005	80861	LP	M		Rectal	INF	Un	Error
23-1-18	2018	CGL	181005	80862	LP	M		Rectal	Neg	Drop	
23-1-18	2018	CGL	181005	80863	LP	M		Rectal	INF	Drop	
23-1-18	2018	CGL	181006	80864	LP	M		Rectal	INF	Drop	
23-1-18	2018	CGL	181006	80865	LP	M		Rectal	INF	Drop	
23-1-18	2018	CGL	181006	80866	LP	M		Rectal	Neg	Mort	Vehicle
23-1-18	2018	CGL	181006	80867	LP	M		Rectal	INF	Drop	
23-1-18	2018	CGL	182003	80843	LP	F	P	Rectal	INF	Drop	
24-1-18	2018	CGL	182004	80844	LP	F	P	Rectal	INF	Un	Error
24-1-18	2018	CGL	182004	80845	LP	F	P	Rectal	INF	Mort	Pred
24-1-18	2018	CGL	182004	80846	LP	F	P	Rectal	INF	Drop	
24-1-18	2018	CGL	182004	80847	LP	F	P	Rectal	Neg	Drop	
23-1-18	2018	CGL	182004	80848	LP	F	P	Rectal	INF	Drop	
24-1-18	2018	CGL	182004	80849	LP	F	P	Rectal	INF	Drop	
23-1-18	2018	CGL	182004	80850	LP	F	P	Rectal	Neg	Drop	
23-1-18	2018	CGL	182004	80851	LP	F	P	Rectal	INF	Drop	
23-1-18	2018	CGL	182004	80852	LP	F	P	Rectal	Neg	Un	Error
24-1-18	2018	CGL	182004	80853	LP	F	NP			Mort	Hunter
24-1-18	2018	CGL	182005	80854	LP	F	P			Drop	
24-1-18	2018	CGL	182005	80855	LP	F	P	Rectal	Neg	Drop	
24-1-18	2018	CGL	182005	80856	LP	F	P	Rectal	INF	Drop	
24-1-18	2018	CGL	182005	80857	LP	F	P		INF	Drop	
23-1-18	2018	CGL	182005	80858	LP	F	P	Rectal	Neg	Drop	
24-1-18	2018	CGL	182005	80859	LP	F	P	Rectal	INF	Mort	Pred

28-1-19	2019	CGL	191000	82626	LP-15	M		Tonsil	Neg		Drop	
25-1-19	2019	CGL	191000	82627	LP-15	M		Tonsil	Pos	Neg	Mort	Pred
28-1-19	2019	CGL	191000	82657	LP-15	M					Drop	
29-1-19	2019	CGL	191000	82631	LP-15	M					Un	Error
26-1-19	2019	CGL	191001	82658	LP-15	M		Tonsil	Neg		Drop	
25-1-19	2019	CGL	191002	82650	LP-15	M		Tonsil	Pos	Pos	Mort	Pred
28-1-19	2019	CGL	191003	82656	LP-15	M					Drop	
29-1-19	2019	CGL	191003	82629	LP-15	M					Drop	
29-1-19	2019	CGL	191003	82633	LP-15	M					Drop	
29-1-19	2019	CGL	192000	80845	LP-15	F	NP				Drop	
26-1-19	2019	CGL	192000	80859	LP-15	F	P	Tonsil	Neg		Drop	
28-1-19	2019	CGL	192000	82625	LP-15	F	P	Tonsil	Neg		Mort	Vehicle
28-1-19	2019	CGL	192000	82628	LP-15	F	P	Tonsil	Neg		Drop	
29-1-19	2019	CGL	192000	82630	LP-15	F	P				Drop	
28-1-19	2019	CGL	192001	82632	LP-15	F	P	Tonsil	Neg	Neg	Mort	Pred
26-1-19	2019	CGL	192001	82634	LP-15	F	P	Tonsil	Neg		Drop	
26-1-19	2019	CGL	192001	82635	LP-15	F	P	Tonsil	Neg		Drop	
29-1-19	2019	CGL	192001	82636	LP-15	F	INF				Drop	
29-1-19	2019	CGL	192001	82637	LP-15	F	P				Drop	
29-1-19	2019	CGL	192001	82653	LP-15	F	P				Drop	
26-1-19	2019	CGL	192001	82641	LP-15	F	P	Tonsil	Neg	Pos	Mort	Hunter
29-1-19	2019	CGL	192002	82642	LP-15	F	P				Drop	
26-1-19	2019	CGL	192002	82643	LP-15	F	P	Tonsil	Neg	Pos	Mort	Pred
29-1-19	2019	CGL	192002	82644	LP-15	F	P				Drop	
25-1-19	2019	CGL	192002	82645	LP-15	F	P	Tonsil	Neg		Drop	
29-1-19	2019	CGL	192002	82646	LP-15	F	INF				Drop	
25-1-19	2019	CGL	192002	82647	LP-15	F	P	Tonsil	Neg		Drop	
28-1-19	2019	CGL	192002	82648	LP-15	F	P				Drop	
29-1-19	2019	CGL	192002	82651	LP-15	F	P				Drop	
29-1-19	2019	CGL	192003	82652	LP-15	F	NP				Drop	
26-1-19	2019	CGL	192003		LP-15	F	P	Tonsil	Neg	Neg	Mort	Capture
29-1-19	2019	CGL	192003	82654	LP-15	F	P				Drop	
28-1-19	2019	CGL	182005	82649	LP-15	F	P			Neg	Drop	Hunter

Appendix A Continued

25-1-20	2020	CGL	201001	80867	LP-15+	M		Rectal	INF		Un	Battery
25-1-20	2020	CGL	201002	82629	LP-15+	M		Rectal	Neg		Drop	
25-1-20	2020	CGL	201003	80862	LP-15+	M		Rectal	INF		Drop	
25-1-20	2020	CGL	201004	80864	LP-15+	M		Rectal	Pos		Drop	
25-1-20	2020	CGL	201005	80865	LP-15+	M		Rectal	INF		Un	Battery
26-1-20	2020	CGL	201007	80860	LP-15+	M		Rectal	INF		Drop	
29-1-20	2020	CGL	201008	82656	LP-15+	M		Rectal	Pos		Un	Battery
26-1-20	2020	CGL	201009	82626	LP-15+	M				Neg	Mort	Pred
29-1-20	2020	CGL	201010	82633	LP-15+	M					Drop	
26-1-20	2020	CGL	201011	82658	LP-15+	M		Rectal	Neg		Drop	
29-1-20	2020	CGL	201012	82655	LP-15+	M					Drop	
29-1-20	2020	CGL	201013	82650	LP-15+	M					Drop	
29-1-20	2020	CGL	201041	82626	LP-15+	M					Drop	
25-1-20	2020	CGL	202014	82639	LP-15+	F	P	Rectal	INF		Drop	
25-1-20	2020	CGL	202015	82654	LP-15+	F	P	Rectal	Pos		Drop	
25-1-20	2020	CGL	202016	80855	LP-15+	F	P			Pos	Mort	Pred
25-1-20	2020	CGL	202017	80858	LP-15+	F	P	Rectal	INF	Pos	Mort	Pred
25-1-20	2020	CGL	202018	82630	LP-15+	F	P	Rectal	INF		Drop	
25-1-20	2020	CGL	202020	80846	LP-15+	F	P				Drop	
25-1-20	2020	CGL	202021	81538	LP-15+	F	P			Pos	Mort	Pred
26-1-20	2020	CGL	202022	82628	LP-15+	F	P	Rectal	Neg		Drop	
26-1-20	2020	CGL	202023	81539	LP-15+	F	P				Drop	
26-1-20	2020	CGL	202024	80859	LP-15+	F	P			Pos	Mort	Pred
26-1-20	2020	CGL	202025	82642	LP-15+	F	P	Rectal	Neg		Drop	
26-1-20	2020	CGL	202026	82645	LP-15+	F	P	Rectal	Pos		Drop	
26-1-20	2020	CGL	202027	80853	LP-15+	F	P				Drop	
26-1-20	2020	CGL	202029	81537	LP-15+	F	P	Rectal	INF		Drop	
26-1-20	2020	CGL	202030	80851	LP-15+	F	P	Rectal	INF	Neg	Mort	Pred
28-1-20	2020	CGL	202031	82651	LP-15+	F	P	Rectal	Neg		Drop	
26-1-20	2020	CGL	202032	80856	LP-15+	F	P	Rectal	Neg		Drop	
26-1-20	2020	CGL	202033	80849	LP-15+	F	P	Rectal	INF		Mort	Pred
29-1-20	2020	CGL	202034	82652	LP-15+	F	P				Drop	

Appendix A Continued

29-1-20	2020	CGL	202035	82638	LP-15+	F	P				Drop	
28-1-20	2020	CGL	202036	86162	LP-15+	F	P	Rectal	INF		Drop	
28-1-20	2020	CGL	202037	80848	LP-15+	F	P				Drop	
29-1-20	2020	CGL	202038	80843	LP-15+	F	P				Un	Battery
28-1-20	2020	CGL	202039	80845	LP-15+	F	P				Drop	
28-1-20	2020	CGL	202040	82644	LP-15+	F	P	Rectal	Neg		Mort	Pred
28-1-20	2020	CGL	202042		LP-15+	F	--			Pos	Mort	Capture
25-1-20	2020	CGL	182004	82640	LP-15+	F	P				Drop	
26-1-20	2020	CGL	191000	82627	LP-15+	M		Rectal	Pos	Pos	Mort	Pred
28-1-20	2020	CGL	192001	82634	LP-15+	F	P				Drop	

APPENDIX B. PROXIMITY LOGGER TESTING

METHODS

To confirm the calibration of the RSSI threshold that would correspond to a registered contact event at 3 meters we conducted 10 trials assessing proximity logger functionality. We determined that a RSSI threshold of -97 dBm would best represent our desired contact distance through results from previous preliminary testing of Lotek collars and consultation with engineers from Lotek. In each trail, a single collar was mounted 1.3m from the ground while an observer carried two additional collars towards the stationary collar. The observer activated the mobile collars from 8 meters away and approached the stationary collar, moving in increments of 0.5 meter each minute. We programmed the separation time for all collars as 0, so if the signal between the receiver and mobile collars dropped below the RSSI threshold, a separate contact event would be initiated when the threshold was surpassed again. The trials were repeated for RSSI threshold of 2 trials at -96 dBm (n=2) and -95 dBm (n=1).

RESULTS

At a RSSI threshold of -97 dBm, the mean distance at which contacts between collars were initiated was 2.91±0.48 m (n=32). The -97 dBm RSSI threshold aligned consistently with our desired contact threshold distance of 3 m. Because our trials were conducted in highly controlled environments without variation in position and habitat type, we decreased the RSSI threshold to -100 dBm for collar deployment.

APPENDIX C. DELINEATION OF BIOLOGICAL SEASONS

The variation between dyad specific, seasonal start ranged from 0-29 days between years (10.8 ± 4.9), with the largest variation occurring between male-male summer start dates. Within seasons, variation in start dates ranged from 0-5 (2.3 ± 0.52) and 10-30 (14.75± 5.56) in 2018 and 2019, respectively. To determine population level start dates we measured the average date across all dyad types for each year and season. In 2018, we define winter (Jan 31 – Apr 25), summer (Apr 26 – Nov 17) and rut (Nov 17 – Dec 7). In 2019, we define winter (Feb 04 – May 10), summer (May 10 – Nov 11) and rut (Nov 12– Nov 22). Our analysis is constrained based on available collar data. Therefore, winter start dates are delineated one week after collar deployment to account for variation in behaviours after capture (Table D.1). Similarly, we delineate the end of rut when collars drop-offs are activated.

We used the same date (15 December) outlined in Silbernagel et al. (2011) to delineate the beginning of the winter (early gestation) season, as collars were not deployed on mule deer during our study throughout that time. In the summer (fawning/prerut), the GAMM analysis delineated a summer start date (3 May) that was 13 days earlier than that outlined in Silbernagel et al. (2011; 16 May). For the rut, the GAMM delineated start dates (15 November) that was 15 days ealier than for deer in Saskatchewan (1 November). The final dates used throughout the my thesis are averaged between both sources (Table D.2)

TABLE C.1. Seasonal start dates delineated using generalized additive mixed model analysis relating Julian day with mean nearest neighbour distance variable dyad types of collared deer in central eastern Alberta, Canada (2018-2019). Winter start dates reflect a week after the initial day of collaring.

Year	**Dyad**	**Seasonal start dates**		
		Winter	**Summer**	**Rut**
2018	Female	31 Jan	24 Apr	19 Nov
	Male	31 Jan	29 Apr	18 Nov
	Mix	31 Jan	26 Apr	17 Nov
2019	Female	04 Feb	03 May	
	Male	04 Feb	28 May	07 Nov
	Mix	04 Feb	30 Apr	17 Nov
Average		02 Feb	03 May	15 Nov

TABLE C.2. Modified version of seasonal start dates outlined in et al. (2011) using deer biology and field observations in southwestern, Saskatchewan, Canada (April 2007–March 2009) compared with modified dates delineated using generalized additive mixed model analysis relating Julian day with mean pairwise distance between variable mule deer dyad central eastern Alberta, Canada (2018-2019).

Source	**Season**	**Start and ends dates**
Silbernagel	Early/Late Gestation	16 Dec - 15 May
	Fawning/Prerut	16 May - 31 Oct
	Rut	01 Nov - 15 Dec
Dobbin	Winter	16 Dec - 09 May
	Summer	10 May - 12 Nov
	Rut	13 Nov - 15 Dec

APPENDIX D. DYADIC GROUP TYPE DESIGNATION

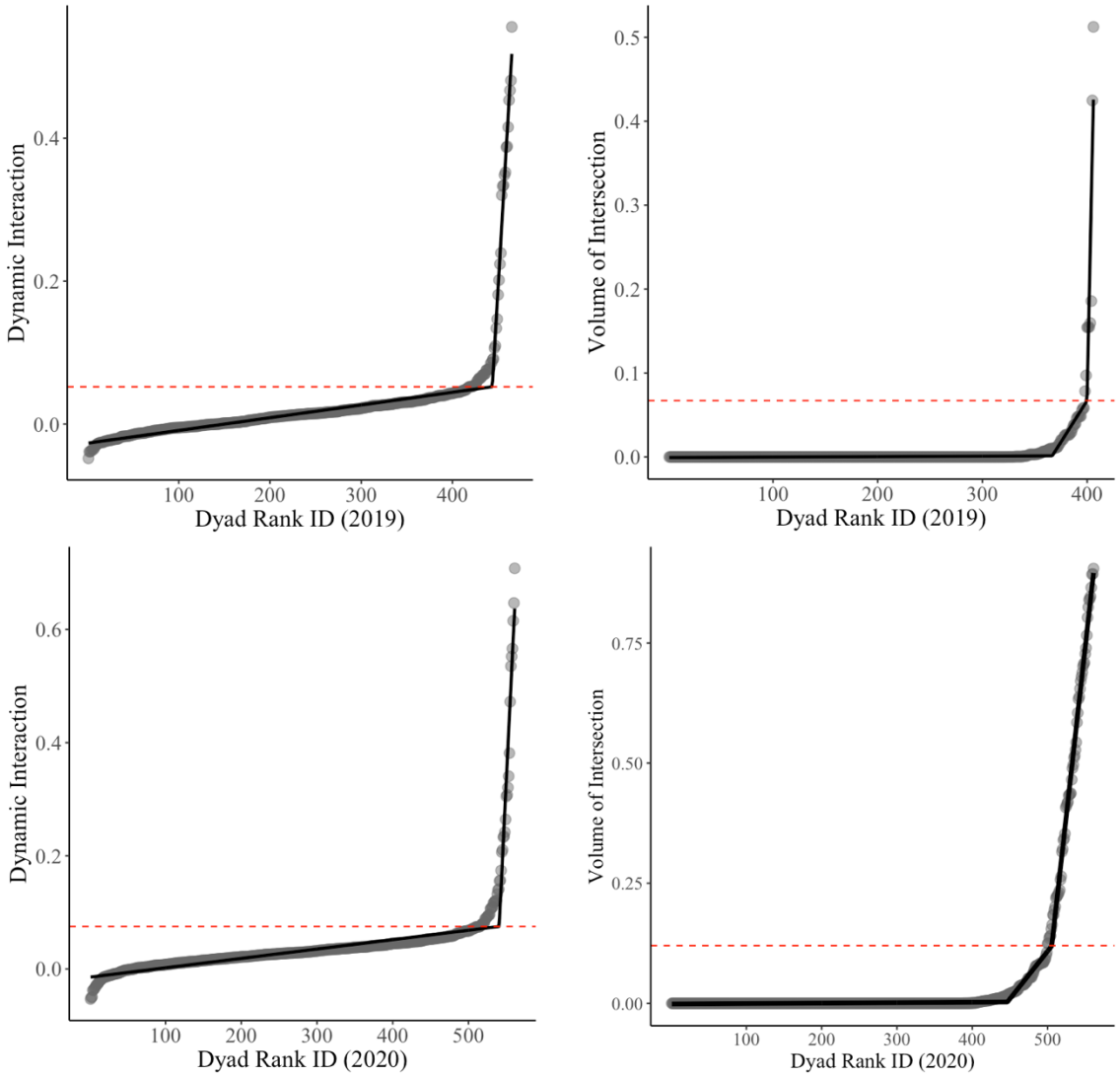

FIGURE D.1. Dyad IDs (grey circles) ranked by values of dynamic interaction index (left) and volume of intersection (right) from mule deer collared during winter (16 December – 9 May) in 2019 (top) and 2020 (bottom) in central eastern Alberta, Canada. Both metrics were fit with piecewise regression (black line) where threshold for group delineation were determined using breakpoints as a threshold (red dashed line).

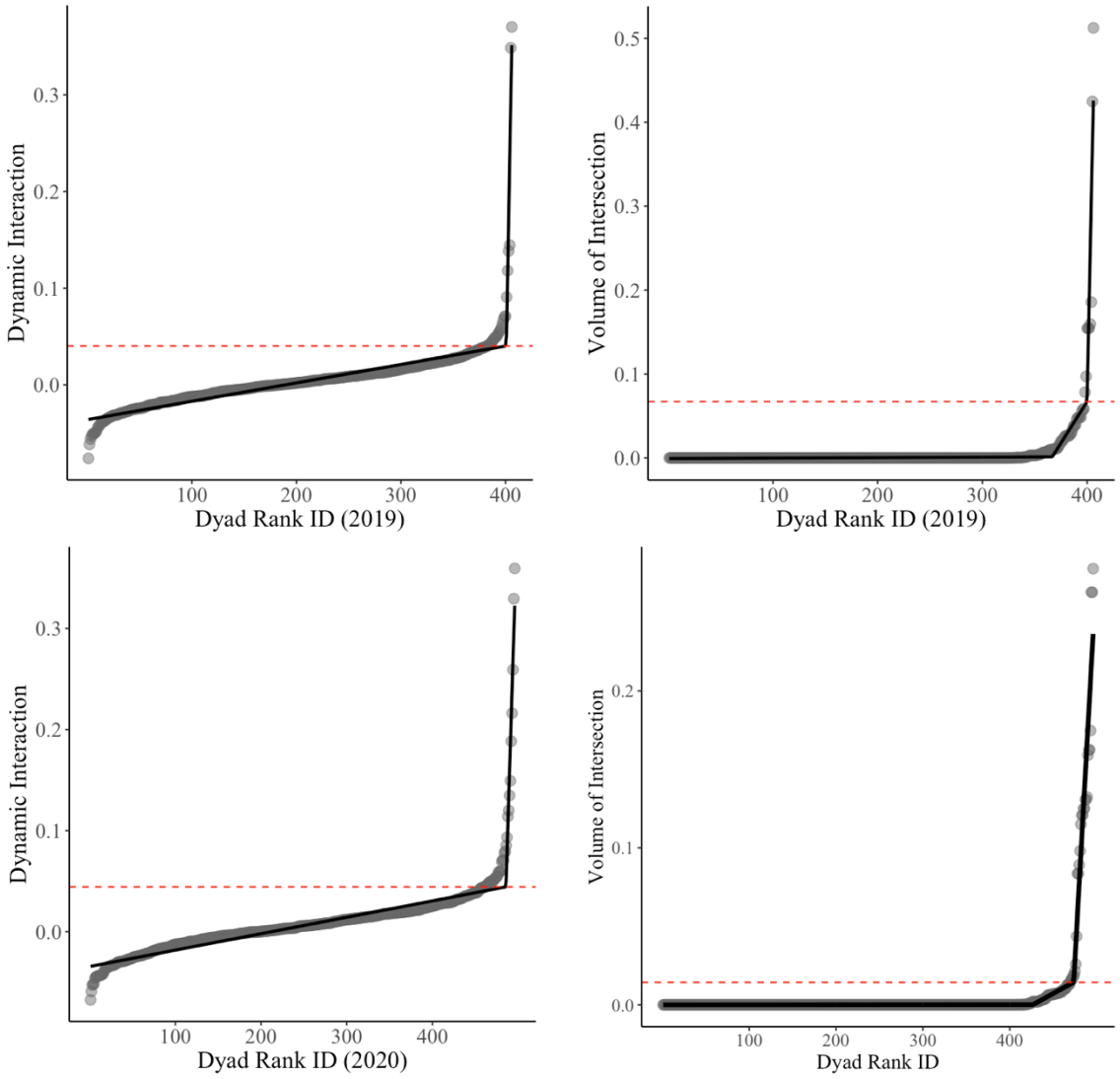

FIGURE D.2. Dyad IDs (grey circles) ranked by values of dynamic interaction index (left) and volume of intersection (right) from mule deer collared during summer (10 May – 12 November) in 2019 (top) and 2020 (bottom) in central eastern Alberta, Canada. Both metrics were fit with piecewise regression (black line) where threshold for group delineation were determined using breakpoints as a threshold (red dashed line).

APPENDIX E. GPS ERROR TESTING

METHODS - Error testing was conducted in fall 2019 (28 October -31 October) and in summer 2020 (30 August – 2 September) to represent periods before and after leaf out of deciduous trees. We used the same three Lotek Litetrack GPS-Proximity collars across both time periods. Three trials were conducted at three geographically separate plots within the CGL. Each plot had open (grassland or low shrubland), mixed (tall shrubland: upland mix, or *Elaeagnus sp.*), and closed (deciduous tree) habitat types. Collars were deployed on full water jugs and mounted on stands to simulate GPS interference due to the deer body and height off the ground. Trials were ongoing for 24 hours and collars were programmed with 15-minute GPS schedules. To calculate positional error, we calculated Euclidean distance between the GPS location and a verified "true" location. The true location was derived from waypoint averaging from two GPS units at the start and end of each trial. We compared GPS error between habitat and season using a non-parametric Scheirer–Ray–Hare test with a post-hoc multiple comparisons Dunn test.

RESULTS - There were 68-96 locations recorded per collar for each seasonal, habitat specific trial. We determined that GPS error varied by habitat type within seasons. There were significant differences in GPS positioning error among habitat types (H= 116, p<0.001; Fig B.1). A Dunn's multiple comparison test demonstrated that all three habitats were significantly different from one another. In summer, mean error was highest in closed habitat (11.0 ± 2.3), followed by mixed (5.8 ± 0.4) then open (4.7 ± 0.3). Similarly, in the winter, mean error was greatest in closed (7.0 ± 0.5), decreased in mixed habitat (4.5 ± 0.2) and lowest in open (4.4 ± 0.2). There was a significant difference in positional error between seasons (H= 20.4, p<0.001) but no significant interaction between season and habitat type, given α = 0.05 (H=5.2, p = 0.07).

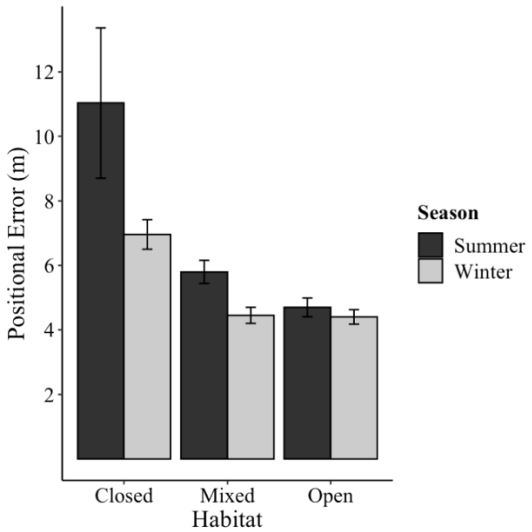

FIGURE E.1. Mean positioning error associated with Lotek Litetrack GPS proximity collars (n=3) from testing conducted in winter and summer across three habitat types in central eastern Alberta, Canada (2019-2020). Error bars represent standard error.

APPENDIX F. CREATION OF LANDSCAPE FEATURE LAYERS

To create the percent woody cover, percent agricultural cover and edge density rasters, we used an amalgamation of landcover data produced by Merrill et al. (2013) and the 2015 landcover of Canada (Latifovic 2019). We primarily used values from Merrill et al. (2013) whenever data was available across WMU 234. Landcover was mapped at 25-meter spatial resolution based on data collected in 2006 using a multi-temporal remote sensing approach, combining Landsat 5 TM satellite imagery and field observations. In areas with no or compromised Landsat imagery (southeast corner of WMU234) we supplemented landcover data with the publicly available 2015 landcover of Canada (Latifovic 2019). The Canada-wide data was mapped at 30-meter spatial resolution using Operational Land Imager (OLI) Landsat sensor data from 2015. We used nearest neighbor assignment resampling to resize 25-meter cells to 30 meters. To produce woody cover rasters, we defined woody cover (Table H.1.) from both sources and created a binary raster in which cells where delineated between woody cover (1) and no woody cover (0). We then determined the percent woody cover within varying buffer sizes (100, 250, 500, 1000m). We repeated the same process to produce the percent agricultural cover raster but created a binary raster that delineated between croplands (1) and non-agricultural landcover types (0). To determine edge density, we used the same binary woody cover raster and created polylines around all clusters of woody cover cells, thereby delineating edge habitat as the boundary between open and covered habitat types . We determined line density of edge habitat within varying buffer sizes (250, 500, 1000m).

TABLE F.1. Landcover classifications used to delineate binary rasters for percent woody cover, percent agricultural cover and edge density covariates for Wildlife Management Unit 234. Landcover data from Merrill et al. (2013) derived using a multi-temporal remote sensing approach in 2006 (25x25m) and from Latifovic (2019) derived using landndsat sensor data from 2015 (30x30 m).

Source	**Landcover Classifications**	
	Woody Cover	**Agriculture**
Merrill et al. 2013	• Tall shrubland (*Elaeagnus sp*.) • Tall shrubland (upland mix) • Deciduous • Deciduous/Conifer mix	• Cultivated/cropland • Forage/Moist grassland
Latifovic 2019	• Temperate or sub-polar needleleaf forest • Mixed forest • Temperate or sub-polar broadleaf forest • Temperate or sub-polar shrubland	• Cropland

Standardizing layers - We standardized all continuous covariates except for percent woody cover and percent agricultural cover. Each raster was standardized by subtracting the raster mean from each value then dividing by the standard deviation of all values. Cells with no data were removed from calculations of the mean and standard deviation.

TABLE F.1. Mean and standard deviation values used to standardize landscape covariates.

Covariate	Mean	Standard Deviation	Units
Terrain Ruggedness	3.6	7.3	
Distance to Stream Decay	0.06	0.2	Km
Distance to River Decay	0.005	0.05	Km
Distance to Road Decay	0.2	0.3	Km
Distance to Wells Decay	0.05	0.1	Km
Edge Density			
250	3.6	6.9	
500	2.3	4.1	
1000	3.6	5.3	

APPENDIX G. PEARSON'S CORRELATIONS FOR CONTACT RATE HURDLE MODELS

Prior to modelling contact rates as a function of dyad effects and landscape covariates we conducted a Pearson's correlation analysis to assess the relationship between all covariates. We did not include covariates in the same model if $r \geq |0.6|$ and r-values were significant, given $\alpha = 0.05$.

Between-group. In winter, we determined that distance to wells was positively correlated ($r = 0.63$, $p < 0.01$; Fig N.1.) with percent agriculture and with distance to roads ($r = 0.60$, $p < 0.01$). In summer, again, distance to wells was positively correlated with distance to roads ($r = 0.62$, $p < 0.01$.

Within-group. In winter, distance to roads was positively correlated ($r = 0.93$, $p < 0.01$; Fig N.2.) with percent agriculture and with distance to wells ($r = 0.84$, $p < 0.01$). There was also a positive correlation ($r = 0.65$, $p < 0.01$) between edge density and terrain ruggedness. In summer, there was a positive correlation between distance to roads and distance to wells ($r = 0.85$, $p < 0.01$) and distance to streams ($r = 0.65$, $p < 0.01$) as well as between streams and wells ($r = 0.65$, $p < 0.01$). Further, terrain ruggedness and edge density were positively correlated ($r = 0.81$, $p < 0.01$) in summer.

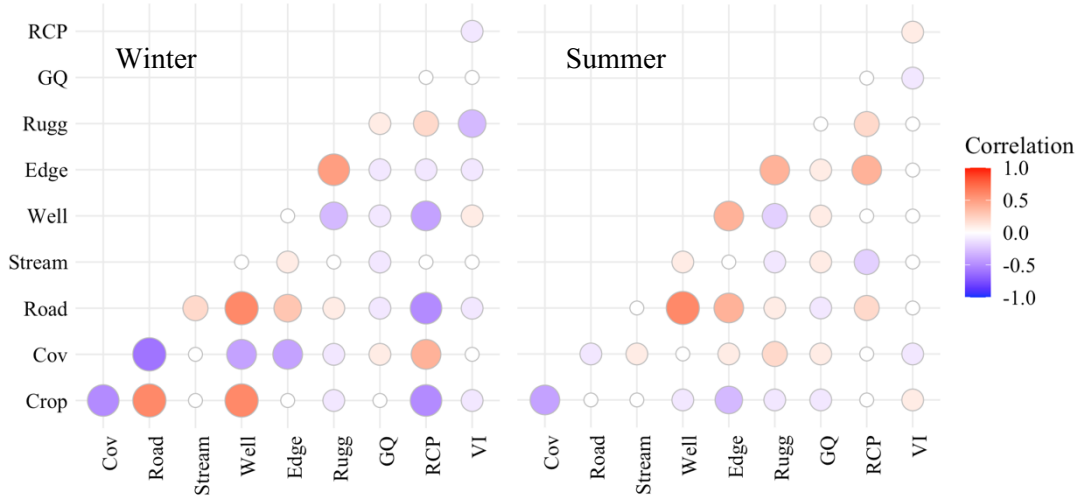

FIGURE G.1. Pearson's correlation values comparing values of covariates used in gamma general linear models with log link relating between-group, seasonal contact rates to genetic relatedness, volume of intersection and median values of landscape factors and relative contact probabilities extracted from areas of overlap between utilization distributions. Contact rates derived using proximity logger data from collared mule deer in central eastern Alberta, Canada (2019-2020).

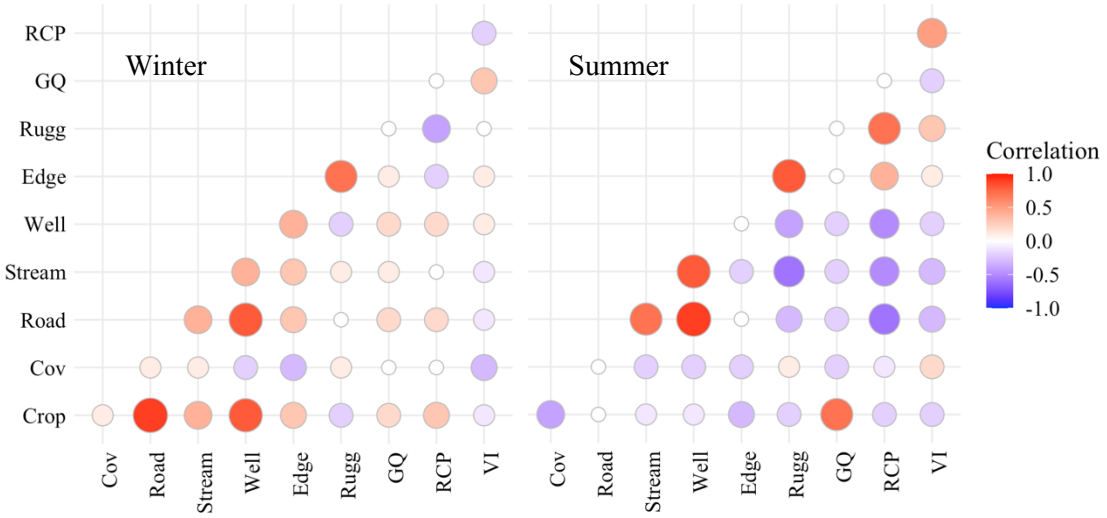

FIGURE G.2. Pearson's correlation values comparing values of covariates used in gamma general linear models with log link relating w-group, seasonal contact rates to genetic relatedness, volume of intersection and median values of landscape factors and relative contact probabilities extracted from areas of overlap between utilization distributions. Contact rates derived using proximity logger data from collared mule deer in central eastern Alberta, Canada (2019-2020).

APPENDIX H. COMPARISONS OF PAIRWISE GENETIC RELATEDNESS ESTIMATES (GQ)

TABLE H.1. Results of Mann-Whitney U test comparing QG estimates of genetic relatedness between within and between-group types. Relatedness estimates (QG) were derived using sampled collected from mule deer collared in central eastern Alberta, Canada (2019-2020).

Variable	W	p value	df
Group	17606	0.1	1

TABLE H.2. Results of Mann-Whitney U test between seasonal (winter, summer) means of QG estimates of genetic relatedness between and between-group dyads. Relatedness estimates (QG) were derived using sampled collected from mule deer collared in central eastern Alberta, Canada (2019-2020).

Group	W	p value	df
Between	758	0.9	1
Within	25271	0.9	1

TABLE H.3. Results of Kruskal-Wallis rank sum test between dyad specific (female-female, male-male, mixed-sex) mean daily contact rates within seasons and group types. Relatedness estimates (QG) were derived using sampled collected from mule deer collared in central eastern Alberta, Canada (2019-2020).

Group	Season	X^2	p value	df
Between	Winter	0.2	0.6	2
	Summer	0.04	0.9	2
Within	Winter	0.3	0.8	2
	Summer	0.2	0.6	1

APPENDIX I. COMPARISONS OF VOLUME OF INTERSECTION VALUES

TABLE I.1. Results of Mann-Whitney U test between volume of intersection (VI) values between within and between-group types. Seasonal utilization distributions, used to calculate VI values, calculated using telemetry data from mule deer collared in central eastern Alberta, Canada (2019-2020).

Variable	W	p value	df
Group	1727	<0.001	1

TABLE I.2. Results of Mann-Whitney U test between volume of intersection (VI) values derived from seasonal (winter, summer) utilizations for within and between-group dyads. Seasonal utilization distributions, used to calculate VI values, calculated using telemetry data from mule deer collared in central eastern Alberta, Canada (2019-2020).

Group	X^2	p value	df
Between	17800	< 0.001	1
Within	182	< 0.001	1

TABLE I.2. Results of Kruskal-Wallis rank sum test comparing volume of intersection (VI) values between dyads (female-female, male-male, mixed-sex) for each season and group type. Seasonal utilization distributions, used to calculate VI values, calculated using telemetry data from mule deer collared in central eastern Alberta, Canada (2019-2020).

Group	Season	X^2	p value	df
Between	Winter	8.0	0.02	2
	Summer	1.7	0.4	2
Within	Winter	3.1	0.2	2
	Summer	0.2	0.7	1

TABLE I.3. Pairwise comparison of volume of intersection (VI) values for between-group dyads in winter across dyad type (female-female F, male-male M, mixed-sex Mix) using Dunn (1964) Kruskal-Wallis multiple comparison p-values adjusted with the Benjamini-Hochberg method. Seasonal utilization distributions, used to calculate VI values, calculated using telemetry data from mule deer collared in central eastern Alberta, Canada (2019-2020).

		p value	
Comparison	Z	Unadjusted	Adjusted
F - M	2.2	0.03	0.04
F - Mix	2.5	0.01	0.04
M - Mix	0.8	0.4	0.4

APPENDIX J. CORRELATION BETWEEN VOLUME OF INTERSECTION AND PAIRWISE GENETIC RELATEDNESS

TABLE J.1. Relationships between values of genetic relatedness (QG; Queller and Goodnight 1989) and volume of intersection for mule deer collared in central eastern Alberta, Canada (2019-2020) by season and group type (female-female F; male-male M; mixed-sex Mix). We report Pearson's correlation coefficient (r).

Group	Season	Dyad	n	r	p value
Between	Winter	F	82	-0.1	0.6
		M	23	0.1	0.8
		Mix	134	0.1	0.5
	Summer	F	84	0.1	0.4
		M	42	0.1	0.4
		Mix	130	-0.2	0.1
Within	Winter	F	46	0.2	0.3
		M	11	-0.1	0.8
		Mix	13	0.4	0.2
	Summer	F	20	-0.3	0.8
		M	7	-0.1	0.5
		Mix	0	--	--

APPENDIX K. COMPARISON OF GPS AND PROXIMITY LOGGER DERIVED MEAN DAILY CONTACT RATES

TABLE K.1. Comparison of mean daily contact rates calculated using concurrent GPS and proximity logger data for within and between-group dyads across seasons using Kendall's rank correlation test (tau). Contacts derived from collared mule deer, using either concurrent GPS locations within 25 meters or recorded by proximity loggers when deer came within 3 meters with data from the same individuals. Mule deer were collared in central eastern Alberta, Canada (2019-2020).

Group	Season	n	tau	p-value
Between	Winter	44	0.5	< 0.001
	Summer	34	0.7	< 0.001
Within	Winter	49	0.7	< 0.001
	Summer	10	0.6	0.01

APPENDIX L. COMPARISONS OF MEAN DAILY CONTACT RATES

TABLE L.1. Results of Mann-Whitney U test comparing mean daily contact rates between within and between-group types. Contacts recorded using proximity logger data from mule deer collared in central eastern Alberta, Canada (2019-2020).

Variable	W	p value	df
Group	669	< 0.001	1

TABLE L.2. Results of Mann-Whitney U test between seasonal (winter, summer) mean daily contact rates for within and between-group dyads. Contacts recorded using proximity logger data from mule deer collared in central eastern Alberta, Canada (2019-2020).

Group	W	p value	df
Between	22035	< 0.001	1
Within	689	0.4	1

TABLE L.3. Results of Kruskal-Wallis rank sum test between dyad specific (female-female, male-male, mixed-sex) mean daily contact rates within seasons and group types. Contacts recorded using proximity logger data from mule deer collared in central eastern Alberta, Canada (2019-2020).

Group	Season	X^2	p value	df
Between	Winter	10.2	0.006	2
	Summer	12.0	0.003	2
Within	Winter	3.1	0.2	2
	Summer	4.2	0.04	1

TABLE L.4. Pairwise comparison of between-group mean daily contact rates in winter across dyad types (female-female F, male-male M, mixed-sex Mix) using Dunn (1964) Kruskal-Wallis multiple comparison p-values adjusted with the Benjamini-Hochberg method. Contacts recorded using proximity logger data from mule deer collared in central eastern Alberta, Canada (2019-

Comparison	Z	P value	
		Unadjusted	Adjusted
F - M	-0.9	0.4	0.4
F - Mix	2.5	0.01	0.04
M - Mix	2.5	0.01	0.02

TABLE L.5. Pairwise comparison of between-group mean daily contact rates in summer across dyad types (female-female F, male-male M, mixed-sex Mix) using Dunn (1964) Kruskal-Wallis multiple comparison p-values adjusted with the Benjamini-Hochberg method. Contacts recorded using proximity logger data from mule deer collared in central eastern Alberta, Canada (2019-2020).

Comparison	**Z**	**P value**	
		Unadjusted	**Adjusted**
F - M	3.1	0.002	0.005
F - Mix	2.7	0.007	0.01
M - Mix	-1.2	0.2	0.2

APPENDIX M. RELATIONSHIP BETWEEN CONTACT RATES AND VOLUME OF INTERSECTION

TABLE M.1. Model selection for competing structures describing relationship between mean daily contact rates as a function of volume of intersection for within-group dyads in winter. Contact rates and utilization distributions to calculate volume of intersection were derived using data recorded from mule deer collared in central eastern Alberta, Canada (2019-2020).

Model	Intercept	VI	df	LL	AICc	Δ	*w*
Gamma(log)	-3.20	6.88	3.00	-148.79	303.95	0.00	1.00
gaussian(inverse)	0.73	-0.76	3.00	-207.52	421.40	117.45	0.00
gaussian(identity)	-12.47	28.93	3.00	-211.75	429.86	125.91	0.00

TABLE M.2. Model selection for competing structures describing relationship between mean daily contact rates as a function of volume of intersection for between-group dyads in winter. Contact rates and utilization distributions to calculate volume of intersection were derived using data recorded from mule deer collared in central eastern Alberta, Canada (2019-2020).

Model	Intercept	VI	df	LL	AICc	Δ	*w*
Gamma(log)	-5.53	9.90	3	1048.19	-2090.27	0.00	1.00
gaussian(identity)	-0.04	0.90	3	101.75	-197.40	1892.87	0.00
gaussian(inverse)	16.59	-23.02	3	94.19	-182.28	1907.99	0.00

TABLE M.3. Model selection for competing structures describing relationship between mean daily contact rates as a function of volume of intersection for within-group dyads in summer. Contact rates and utilization distributions to calculate volume of intersection were derived using data recorded from mule deer collared in central eastern Alberta, Canada (2019-2020).

Model	Intercept	VI	df	LL	AICc	Δ	*w*
Gamma(log)	-0.19	3.34	3	-60.53	128.20	0.00	1.00
gaussian(identity)	-5.99	23.56	3	-76.77	160.69	32.49	0.00
gaussian(inverse)	-40713.53	20184.3	3	-89.84	186.82	58.62	0.00

TABLE M.4. Model selection for competing structures describing relationship between mean daily contact rates as a function of volume of intersection for between-group dyads in summer. Contact rates and utilization distributions to calculate volume of intersection were derived using data recorded from mule deer collared in central eastern Alberta, Canada (2019-2020).

Model	Intercept	VI	df	LL	AICc	Δ	*w*
Gamma(log)	-4.25	8.30	3.00	1231.63	-2457.15	0.00	1.00
gaussian(identity)	0.01	0.34	3.00	231.40	-456.70	2000.45	0.00
gaussian(inverse)	39.56	-63.23	3.00	226.82	-447.55	2009.61	0.00

APPENDIX N. CONACT RATE HURDLE MODEL AICc OUTPUT TABLES

TABLE N.1. Complete results of model selection for binomial logistic regressions comparing dyads with recorded contact rates in winter (1) to those with no recorded contacts (0) as a function of volume of intersection, genetic relatedness, dyad type, and landscape covariates measured from areas of overlap between utilization distributions. Contact rates were derived using data recorded mule deer collared in central eastern Alberta, Canada (2019-2020).

Intercept	VI	QG	fem	male	VI*cov	cov	stream	crop	edge	road	rugg	df	LL	AICc	Δ	*w*
-1.12	46.80				-48.51	-0.17						4	-116.5	241.1	0.0	0.6
-1.13	46.73		0.01		-48.43	-0.17						5	-116.5	243.2	2.1	0.2
-1.13	46.74	-0.04	0.02		-48.44	-0.16						6	-116.5	245.3	4.2	0.1
-0.40	10.56					-1.22						3	-121.1	248.3	7.2	0.0
-0.40	10.56					-1.22						3	-121.1	248.3	7.2	0.0
-1.20	10.16											2	-122.3	248.6	7.5	0.0
-1.20	10.16											2	-122.3	248.6	7.5	0.0
-0.66	10.15					-0.95		-35.16		0.65	-2.17	6	-118.4	249.2	8.1	0.0
-0.48	10.22					-1.27					-1.16	4	-120.7	249.6	8.5	0.0
-1.30	9.86										-0.99	3	-122.0	250.2	9.1	0.0
-0.40	10.56	0.02				-1.23						4	-121.1	250.3	9.3	0.0
-0.08	10.17					-1.88		-22.88			-1.85	5	-120.1	250.4	9.3	0.0
-0.74	10.16					-0.97		-34.78	0.03	0.65	-2.25	7	-118.4	251.3	10.2	0.0
-0.45	10.48	0.02	0.10			-1.19						5	-121.0	252.3	11.3	0.0
-0.66			0.53									2	-146.1	296.2	55.1	0.0
-0.48												1	-147.7	297.5	56.4	0.0
-0.51				0.41								2	-147.4	298.8	57.7	0.0
-0.49		-0.33										2	-147.7	299.4	58.3	0.0

TABLE N.2.Complete results of model selection for binomial logistic regressions comparing dyads. With recorded contact rates in summer (1) to those with no recorded contacts (0) as a function of volume of intersection, genetic relatedness, dyad type, and landscape covariates measured from areas of overlap between utilization distributions. Contact rates were derived using data recorded mule deer collared in central eastern Alberta, Canada (2019-2020).

Intercept	VI	QG	fem	male	cov	cov^2	stream	crop	edge	rugg	well	df	LL	AICc	Δ	*w*
-9.0	9.5		0.8		-1.7		-23.9				0.9	6	-113.5	239.4	0.0	0.4
-9.3	9.7	1.2	0.8		-1.9		-25.1				0.9	7	-112.8	240.2	0.7	0.3
-8.0	9.0				-1.8		-22.1				1.0	5	-116.2	242.8	3.3	0.1
-8.4	9.2	1.4			-1.9		-23.3				1.0	6	-115.2	242.9	3.4	0.1
-0.5	9.8		0.7		-1.7						0.7	5	-116.4	243.0	3.6	0.1
-7.7	9.3				-1.1		-22.0		-0.3		1.1	6	-115.7	243.8	4.4	0.0
-0.4	9.9	1.0	0.7		-1.8						0.7	6	-115.8	244.1	4.6	0.0
-0.5	9.6		0.7	-0.3	-1.8						0.7	6	-116.3	244.9	5.5	0.0
-0.2	9.4				-1.8						0.9	4	-118.7	245.5	6.1	0.0
-0.2	9.4				-1.8						0.9	4	-118.7	245.5	6.1	0.0
-8.0	9.2				-1.2		-21.8		-0.2	-0.8	1.1	7	-115.7	245.8	6.4	0.0
-8.0	9.2				-1.1		-21.9	0.6	-0.2	-0.8	1.1	8	-115.6	247.9	8.4	0.0
-1.2	9.2										0.8	3	-121.7	249.6	10.1	0.0
-8.0	9.2				-1.1	0.0	-21.9	0.6	-0.2	-0.8	1.1	9	-115.6	250.1	10.6	0.0
-0.3	8.9				-1.7							3	-123.1	252.4	12.9	0.0
-1.4			0.9									2	-125.5	255.1	15.6	0.0
-1.2	8.9											2	-126.0	256.1	16.7	0.0
-1.0				-0.8								2	-127.8	259.6	20.2	0.0
-1.1												1	-129.3	260.6	21.2	0.0
-1.0		1.0										2	-128.8	261.6	22.1	0.0

TABLE N.3.Complete results of model selection for gamma distributed general linear models with a log link relating mean daily contact rates in winter for between-group dyads with volume of intersection, genetic relatedness, dyad type, and landscape covariates measured from areas of overlap between utilization distributions. Contacts recorded from mule deer collared in central eastern Alberta, Canada (2019-2020).

Intercept	**VI**	**GQ**	**fem**	**male**	**VI*cov**	**cov**	**cov^2**	**stream**	**crop**	**edge**	**road**	**rugg**	**df**	**LL**	**AICc**	**Δ**	***w***
-3.4	7.4			1.0		-1.0		1.9				-2.4	7	194.0	-372.6	0.0	0.4
-3.2	7.2			1.0		-1.2		1.8	-23.1			-2.6	8	195.1	-372.2	0.4	0.3
-4.0	7.6			0.9				1.9				-2.4	6	191.7	-370.3	2.4	0.1
-4.1	7.5	-0.8		0.9				1.7				-2.2	7	192.8	-370.2	2.4	0.1
-3.1	7.3			1.0		-1.7	0.4	1.9	-23.6			-2.6	9	195.1	-369.8	2.9	0.1
-3.3	7.2	-0.6		1.0		-1.3	0.1	1.7	-20.0			-2.4	10	195.7	-368.4	4.2	0.0
-4.0	6.9			0.9		-1.0						-2.8	6	189.3	-365.6	7.0	0.0
-3.9	7.1	-0.9						1.5				-1.8	6	186.3	-359.5	13.1	0.0
-2.2	7.2					-4.5	3.2	1.7	-31.2			-1.9	8	187.6	-357.4	15.2	0.0
-2.4	7.1	-0.7				-4.1	2.9	1.6	-26.9			-1.8	9	188.4	-356.5	16.2	0.0
-2.8	9.8				-4.2	-3.1	2.4	1.7	-28.0			-1.6	9	188.4	-356.4	16.3	0.0
-4.4	6.8											-2.4	4	182.1	-355.7	16.9	0.0
-3.8	6.5					-0.9			-33.1			-2.6	6	184.3	-355.5	17.2	0.0
-2.1	7.1					-4.6	3.1	1.8	-27.4		-0.1	-1.9	9	187.7	-355.0	17.7	0.0
-4.4	6.8								-21.2			-2.4	5	182.8	-354.9	17.8	0.0
-2.5	7.1	-0.6	-0.1			-3.8	2.5	1.5	-24.3			-2.1	10	188.6	-354.2	18.4	0.0
-4.1	6.7									-0.1		-2.2	5	182.3	-353.8	18.8	0.0
-2.1	7.1					-4.9	3.4	1.8	-28.1	0.0	-0.1	-2.0	10	187.7	-352.4	20.2	0.0
-4.2	7.8												3	178.6	-350.9	21.8	0.0
-3.8	7.6					-0.5							4	179.1	-349.7	22.9	0.0
-4.1	7.8								-17.3				4	179.0	-349.6	23.0	0.0
-2.4		-2.8											3	119.8	-233.3	139.3	0.0
-2.2													2	115.6	-227.0	145.6	0.0

TABLE N.4.Complete results of model selection for gamma distributed general linear models with a log link relating mean daily contact rates in summer for between-group dyads with volume of intersection, genetic relatedness, dyad type, and landscape covariates measured from areas of overlap between utilization distributions. Contacts recorded from mule deer collared in central eastern Alberta, Canada (2019-2020).

Interc	**VI**	**QG**	**fem**	**male**	**cov**	**cov^2**	**strea**	**edge**	**road**	**rugg**	**df**	**LL**	**AICc**	**Δ**	***w***
-35.3	8.4	2.4			-15.2	14.3	-94.7		1.2	-10.4	9	96.8	-171.8	0.0	0.6
-35.4	7.9	2.4		-0.9	-14.5	13.8	-94.8		1.0	-10.2	10	97.9	-171.1	0.7	0.4
-41.7	6.2				-11.0	10.4	-108.5		1.7	-13.8	8	90.0	-161.0	10.8	0.0
-32.7	9.5	2.1	0.0		-0.9		-78.6		0.5	-11.6	9	91.3	-160.8	11.0	0.0
-43.1					-10.7	10.9	-111.9		1.5	-14.6	7	88.4	-160.6	11.2	0.0
-41.0	6.3		-0.5		-12.4	11.5	-107.7		1.6	-14.9	9	91.0	-160.2	11.6	0.0
-45.3	5.1				-17.2	15.2	-118.9	0.6	1.9	-15.8	9	90.7	-159.6	12.2	0.0
-38.3							-92.3		0.8	-14.9	5	84.9	-158.6	13.2	0.0
-38.2	6.9				-0.6		-92.7		1.1	-14.4	7	86.7	-157.2	14.6	0.0
-38.2	6.9				-0.6		-92.7		1.1	-14.4	7	86.7	-157.2	14.6	0.0
-38.7	5.9			-1.1	-0.5		-94.6		1.0	-13.8	8	87.9	-156.8	15.0	0.0
-45.1	5.1				-16.7	14.8	-117.9	0.5	1.9	-15.8	10	90.7	-156.7	15.1	0.0
-34.6							-81.1			-16.0	4	82.7	-156.6	15.2	0.0
-37.7					0.2		-90.1		0.8	-15.2	6	84.9	-156.2	15.6	0.0
-5.8	3.5									-16.7	4	79.6	-150.5	21.3	0.0
-2.1		2.1									3	76.2	-146.0	25.8	0.0
-1.8				-2.4							3	72.9	-139.4	32.4	0.0
-29.3							-76.5				3	71.9	-137.4	34.4	0.0
-29.7	3.1						-77.5				4	72.3	-135.8	36.1	0.0
-1.9											2	69.7	-135.2	36.6	0.0
-1.9	2.2										3	69.9	-133.3	38.5	0.0
-1.8			-0.2								3	69.9	-133.3	38.5	0.0

TABLE N.5.Complete results of model selection for gamma distributed general linear models with a log link relating mean daily contact rates in winter for within-group dyads with volume of intersection, genetic relatedness, dyad type, and covariates extracted from areas of overlap between utilization distributions including median relative contact probabilities and landscape covariates. Contacts recorded from mule deer collared in collared in central eastern Alberta, Canada (2019-2020).

Intercept	**VI**	**QG**	**fem**	**male**	**cov**	**cov^2**	**strea**	**road**	**rugg**	**df**	**LL**	**AICc**	**Δ**	***w***
-32.7	5.0		0.5				-86.2			5	-149.3	309.7	0.0	0.2
-33.5	5.2		0.4		1.1		-86.3			6	-148.5	310.6	0.8	0.1
-29.6	5.2				1.4		-76.1			5	-150.0	311.1	1.3	0.1
-27.6	4.9						-73.3			4	-151.4	311.5	1.8	0.1
-34.6	5.2				1.6		-89.5	0.4		6	-149.3	312.1	2.3	0.1
-32.8	5.0	0.1	0.5				-86.6			6	-149.3	312.1	2.4	0.1
-38.5	5.3				1.6		-101.0	0.6	1.8	7	-148.3	312.7	2.9	0.0
-33.5	5.1		0.6	0.2	1.0		-86.5			7	-148.4	312.9	3.1	0.0
-30.6	5.3			-0.2	1.3		-78.7			6	-149.7	313.0	3.3	0.0
-27.6	4.9	0.1					-73.5			5	-151.4	313.9	4.1	0.0
-1.3	4.9									3	-154.0	314.3	4.6	0.0
-1.6	5.0		0.4							4	-152.8	314.4	4.6	0.0
-2.2	5.1				1.2					4	-152.9	314.4	4.7	0.0
-2.3	5.2		0.3		1.0					5	-152.1	315.3	5.6	0.0
-2.3	5.2		0.3		1.0					5	-152.1	315.3	5.6	0.0
-1.7	4.9		0.5	0.3						5	-152.6	316.2	6.5	0.0
-1.3	4.9	0.1								4	-154.0	316.6	6.9	0.0
-2.2	5.2			-0.1	1.2					5	-152.8	316.6	6.9	0.0
-1.1	5.2		0.2		-3.5	3.8				6	-151.6	316.7	7.0	0.0
-2.2	5.2	-0.1			1.2					5	-152.8	316.7	7.0	0.0
-0.8	5.3	-0.1			-4.2	4.6				6	-151.9	317.4	7.7	0.0
-2.3	5.2	-0.1	0.3		1.0					6	-152.1	317.8	8.0	0.0
1.8										2	-170.1	344.4	34.7	0.0
1.8		0.9								3	-169.1	344.6	34.9	0.0
1.6			0.2							3	-169.9	346.2	36.4	0.0
1.8				0.1						3	-170.1	346.6	36.9	0.0

TABLE N.6.Complete results of model selection for gamma distributed general linear models with a log link relating mean daily contact rates in summer for within-group dyads with volume of intersection, genetic relatedness, dyad type, and landscape covariates measured from areas of overlap between utilization distributions. Contacts recorded from mule deer collared in central eastern Alberta, Canada (2019-2020).

Intercept	**VI**	**QG**	**fem**	**cov**	**crop**	**edge**	**road**	**stream**	**well**	**rugg**	**df**	**LL**	**AICc**	**Δ**	***w***
0.6			1.3								3	-61.3	130	0.00	0.2
1.7			1.1	-2.0							4	-60.2	130	0.70	0.1
2.8				-2.5							3	-61.6	130	0.7	0.1
1.7											2	-63.3	131	1.3	0.1
1.6		2.3									3	-62.0	131	1.4	0.1
2.0	-1.5										3	-62.6	132	2.7	0.1
2.9	-0.6			-2.5							4	-61.5	133	3.4	0.0
1.6					3.0						3	-63.0	133	3.4	0.0
1.6									-0.4		3	-63.0	133	3.5	0.0
2.1						-0.2					3	-63.1	133	3.6	0.0
1.5							-0.4				3	-63.1	133	3.7	0.0
1.8										0.9	3	-63.2	134	3.9	0.0
-2.7								-12.4			3	-63.3	134	3.9	0.0

APPENDIX O. COMPARISON OF USE AND CONTACT LOCATIONS

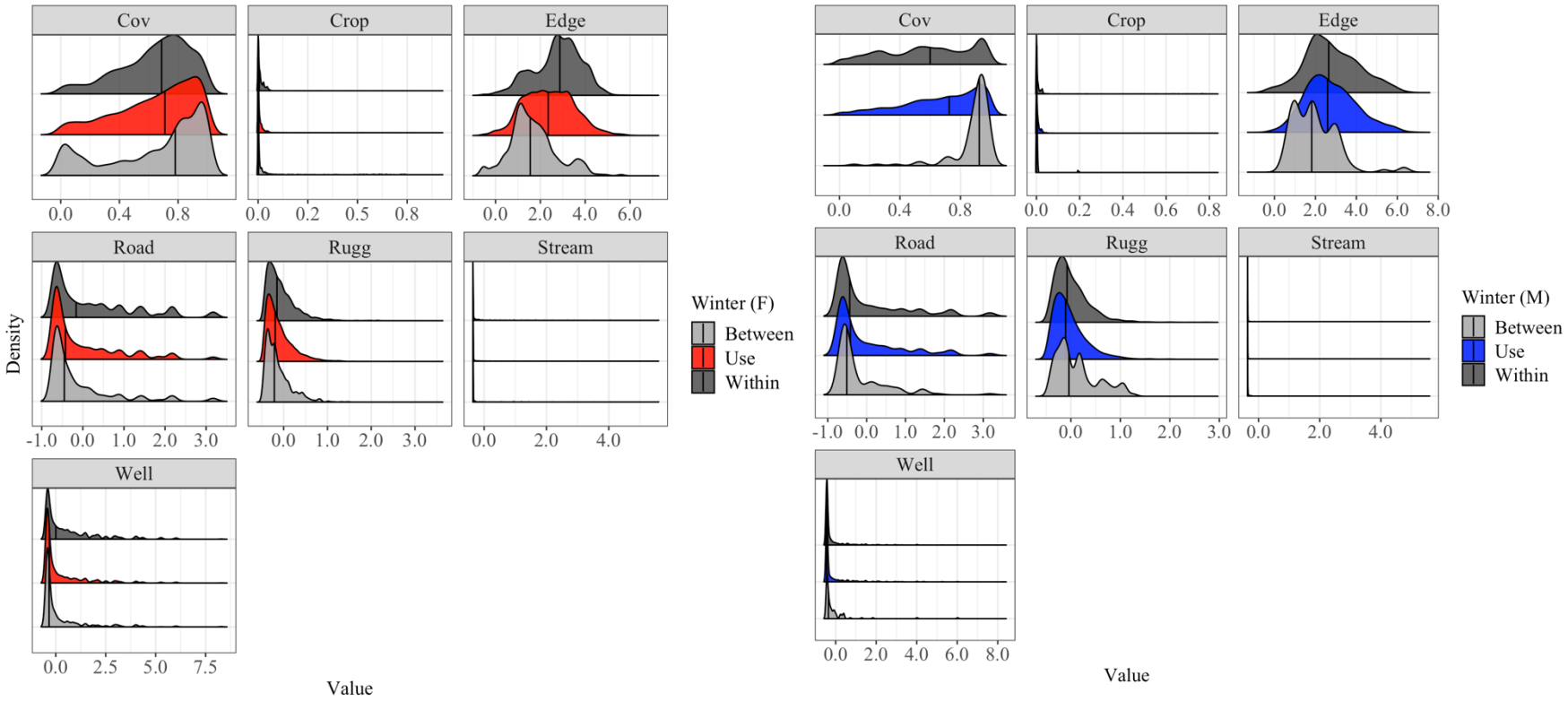

FIGURE. O.1. Comparison between density distributions of landscape covariates (Table 3.2.) between locations of individual female (red) and male (blue) use points and contact locations among within and between-group same-sex dyads in winter. Use is defined by GPS locations along 2-hour intervals within areas of overlap between the same deer that comprise sex-specific, seasonal dyads. Used and contact locations were recorded from collared mule deer captured within Wildlife Management Unit 234 in central eastern Alberta, Canada (2019-2020). Horizontal black lines represent medians.

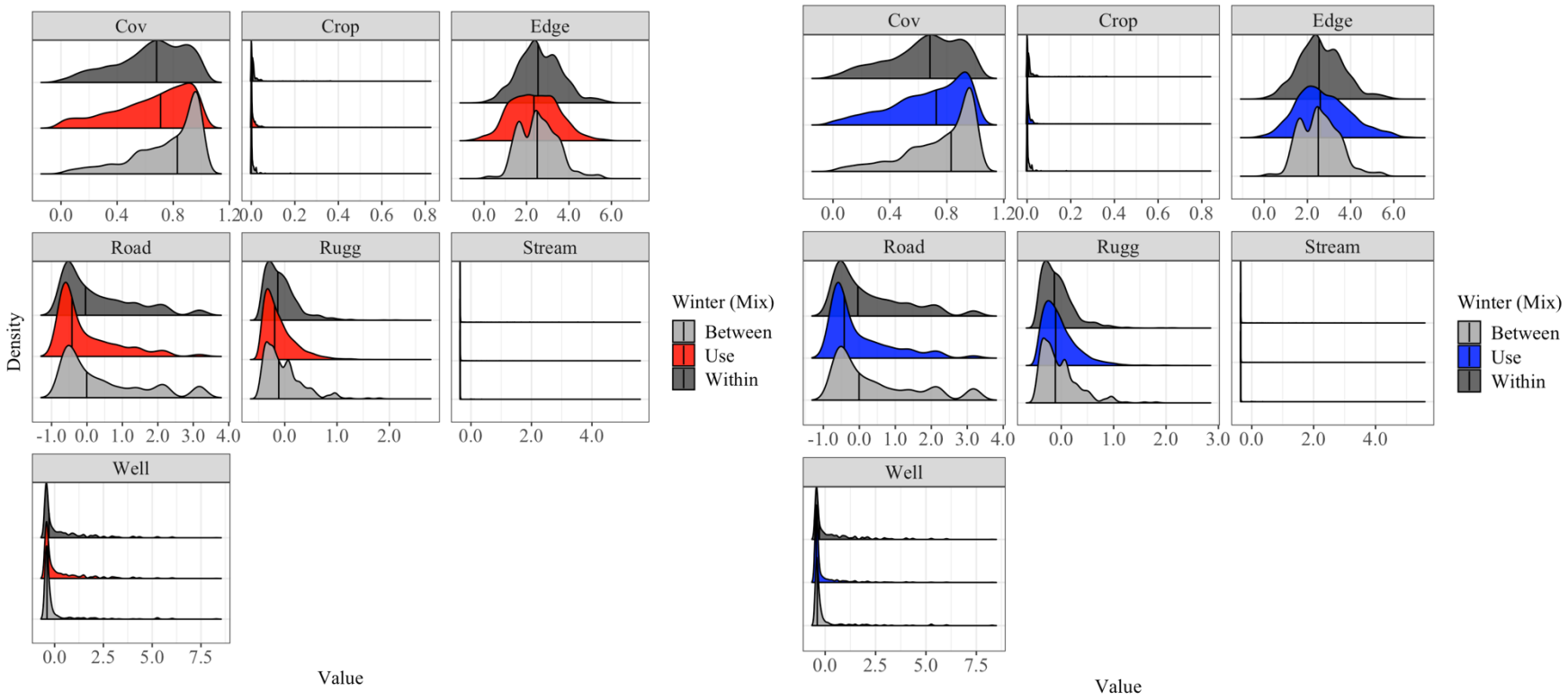

FIGURE. O.2. Comparison between density distributions of landscape covariates (Table 3.2.) between locations of individual female (red) and male (blue) use points and contact locations among within and between-group mixed-sex dyads in winter. Note that only the use distributions change between the right and left panels because mixed-sex dyads stay consistent among graphs. Use is defined by GPS locations along 2-hour intervals within areas of overlap between the same deer that comprise seasonal, mixed-sex dyads. Used and contact locations were recorded from collared mule deer captured within Wildlife Management Unit 234 in central eastern Alberta, Canada (2019-2020). Horizontal black lines represent medians.

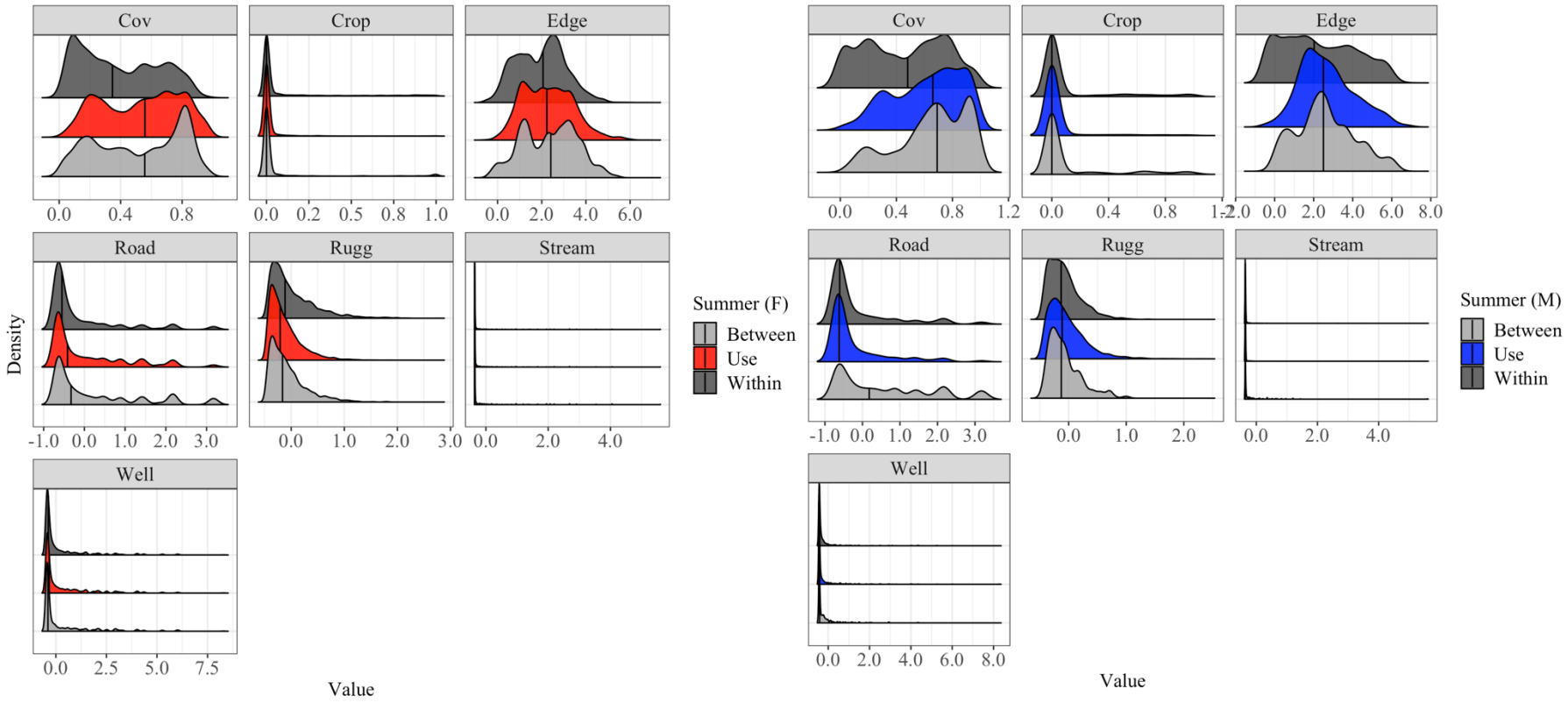

FIGURE. O.3. Comparison between density distributions of landscape covariates (Table 3.2.) between locations of individual female (red) and male (blue) use points and contact locations among within and between-group same-sex dyads in summer. Use is defined by GPS locations along 2-hour intervals within areas of overlap between the same deer that comprise sex-specific, seasonal dyads. Used and contact locations were recorded from collared mule deer captured within Wildlife Management Unit 234 in central eastern Alberta, Canada (2019-2020). Horizontal black lines represent medians.

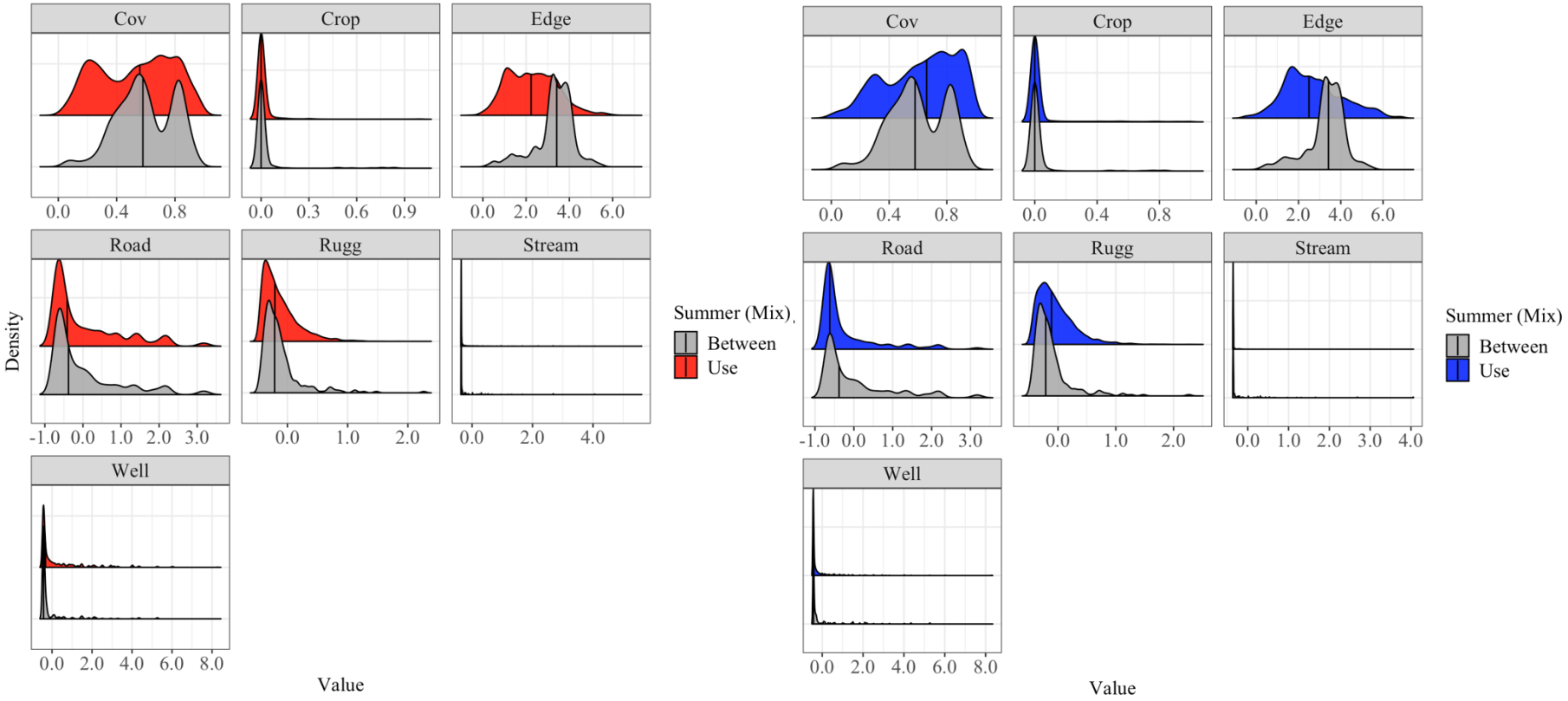

FIGURE. O.4. Comparison between density distributions of landscape covariates (Table 3.2.) between locations of individual female (red) and male (blue) use points and contact locations among between-group mixed-sex dyads in summer. Note that only the use distributions change between the right and left panels because mixed-sex dyads stay consistent among graphs. Use is defined by GPS locations along 2-hour intervals within areas of overlap between the same deer that comprise seasonal, mixed-sex dyads. Used and contact locations were recorded from collared mule deer captured within Wildlife Management Unit 234 in central eastern Alberta, Canada (2019-2020). Horizontal black lines represent medians.

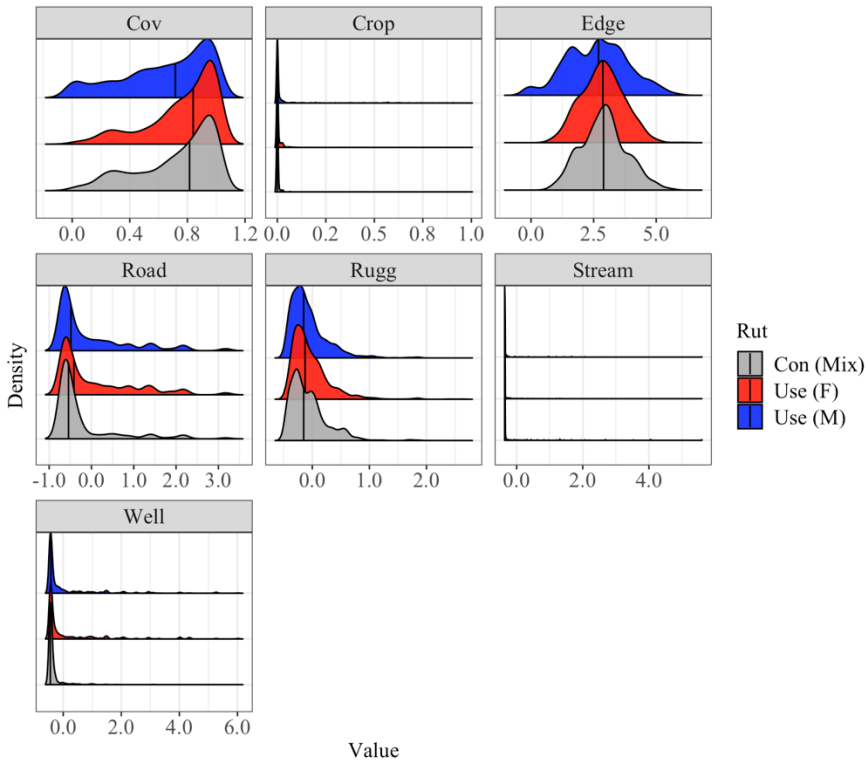

FIGURE. O.5. Comparison between density distributions of landscape covariates (Table 3.2.) between locations of individual female (red) and male (blue) use points and contact locations among mixed-sex dyads in rut. Use is defined by GPS locations along 2-hour intervals within areas of overlap between the same deer that comprise dyads during the rut. Used and contact locations were recorded from collared mule deer captured within Wildlife Management Unit 234 in central eastern Alberta, Canada (2019-2020). Horizontal black lines represent medians.

APPENDIX P. SEASONAL BUFFER SIZES FOR RELATIVE CONTACT PROBABILITY MODELS

Table P.1. Logistic regressions comparing contact locations (1) and random locations (0) as a function of standardized edge density values within variable buffer sizes in winter, summer, and rut seasons. Contacts recorded between collared mule deer central eastern Alberta, Canada, 2019–2020. Bolded rows represent top models.

Season	Intercept	Buffer size (m)			df	LL	Δ	w
		1000	250	500				
Winter	**-2.64**			**-0.03**	**2**	**243360.38**	**0.00**	**1.00**
	-2.78	0.03			2	243372.10	11.72	0.00
	-2.73		0.01		2	243380.75	20.37	0.00
Summer	**-2.94**		**0.12**		**2**	**174975.14**	**0.00**	**1.00**
	-2.53	-0.08			2	175351.31	376.18	0.00
	-2.70			0.00	2	175463.59	488.45	0.00
Rut	**-3.00**		**0.16**		**2**	**5127.63**	**0.00**	**1.00**
	-2.93			0.08	2	5145.54	17.91	0.00
	-2.83	0.05			2	5150.23	22.59	0.00

Table P.2. Logistic regressions comparing contact locations (1) and random locations (0) as a function of percent woody cover within variable buffer sizes in winter, summer, and rut seasons. Contacts recorded between collared mule deer central eastern Alberta, Canada, 2019–2020. Bolded rows represent top models.

Season	Intercept	Buffer size (m)			df	LL	Δ	w
		1000	250	500				
Winter	**-2.80**		**0.15**		**2**	**-121658.21**	**0.00**	**1.00**
	-2.81	0.16			2	-121673.87	31.33	0.00
	-2.77			0.10	2	-121681.81	47.21	0.00
Summer	**-2.52**	**-0.44**			**2**	**-87569.03**	**0.00**	**1.00**
	-2.57			-0.32	2	-87621.92	105.78	0.00
	-2.62		-0.20		2	-87676.34	214.62	0.00
Rut	**-2.88**		**0.24**		**2**	**-2572.05**	**0.00**	**0.53**
	-2.87			0.22	2	-2572.59	1.08	0.31
	-2.82	0.16			2	-2573.22	2.34	0.16

Table P.3. Logistic regressions comparing contact locations (1) and random locations (0) as a function of percent agricultural cover values within variable buffer sizes in winter, summer, and rut seasons. Contacts recorded between collared mule deer central eastern Alberta, Canada, 2019–2020. Bolded rows represent top models.

Season	**Intercept**	**Buffer size (m)**			**df**	**LL**	**Δ**	***w***
		1000	250	500				
Winter	**-2.69**	**-0.62**			**2**	**-121652.41**	**0.00**	**1.00**
	-2.70		-0.34		2	-121669.99	35.16	0.00
	-2.70			-0.37	2	-121671.31	37.80	0.00
Summer	**-2.73**			**0.25**	**2**	**-87705.64**	**0.00**	**1.00**
	-2.71		0.06		2	-87727.40	43.53	0.00
	-2.71	0.06			2	-87728.05	44.82	0.00
Rut	**-2.64**			**-9.34**	**2**	**-2541.03**	**0.00**	**1.00**
	-2.64		-21.77		2	-2547.32	12.58	0.00
	-2.65	-4.16			2	-2555.33	28.59	0.00

APPENDIX Q. CORRELATIONS BETWEEN LANDSCAPE COVARIATES IN RELATIVE CONTACT PROBABILITY MODELS

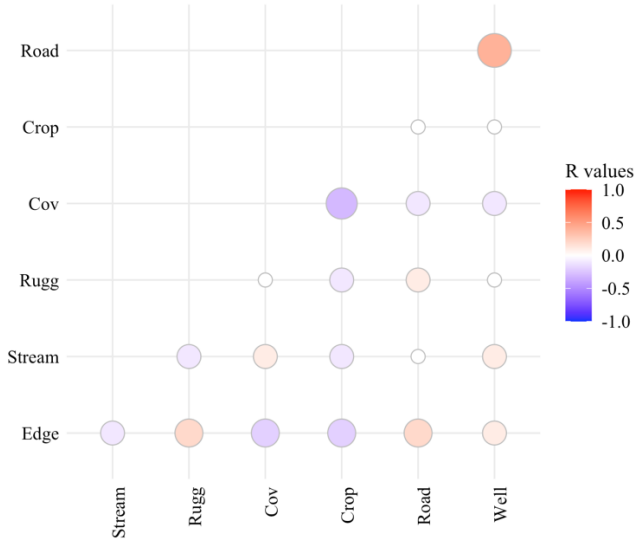

FIGURE Q.1. Pearson's correlation values comparing values of landscape covariates (Table 3.2) used in logistic regressions comparing contact locations (1) and random locations (0) within areas of overlap between seasonal utilization distributions in winter. Contact locations derived using proximity logger data from collared mule deer in central eastern Alberta, Canada (2019-2020). None of the r values exceed r = |0.60|.

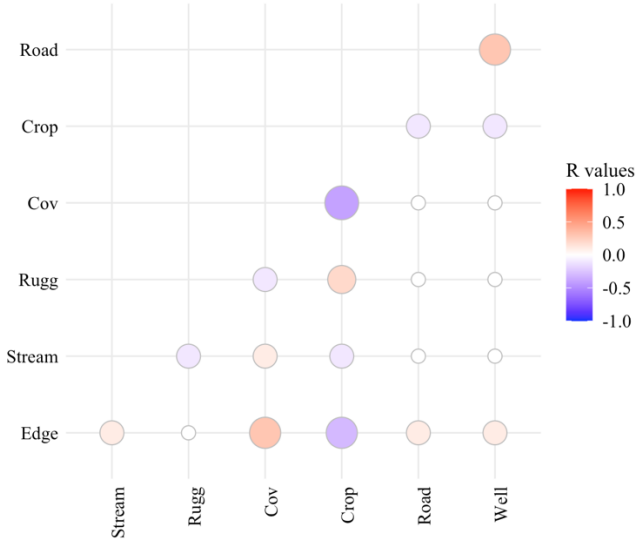

FIGURE Q.2. Pearson's correlation values comparing values of landscape covariates (Table 3.2) used in logistic regressions comparing contact locations (1) and random locations (0) within areas of overlap between seasonal utilization distributions in summer. Contact locations derived using proximity logger data from collared mule deer in central eastern Alberta, Canada (2019-2020). None of the r values exceed r = |0.60|.

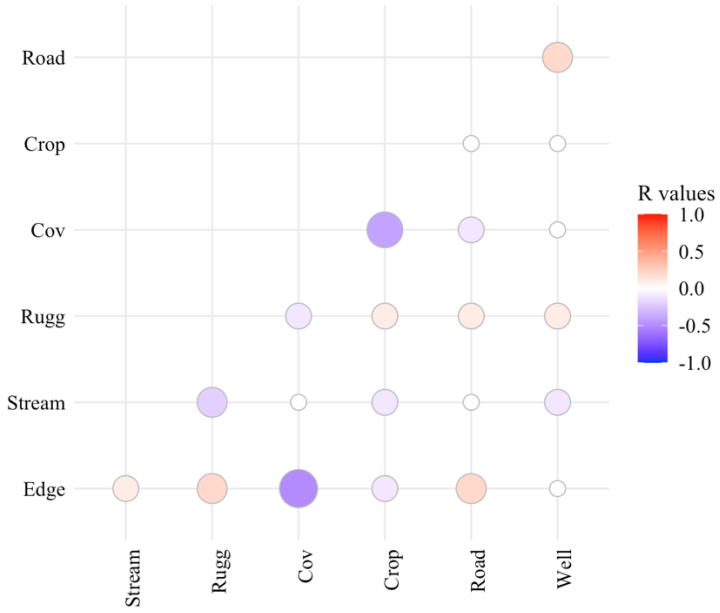

FIGURE Q.3. Pearson's correlation values comparing values of landscape covariates (Table 3.2) used in logistic regressions comparing contact locations (1) and random locations (0) within areas of overlap between seasonal utilization distributions in rut. Contact locations derived using proximity logger data from collared mule deer in central eastern Alberta, Canada (2019-2020). None of the r values exceed r = |0.60|.

APPENDIX R. RELATIVE CONTACT PROBABILITY MODEL AIC OUTPUT TABLES

TABLE R.1. Complete results of model selection for logistic regression relating habitat covariates at known contact locations from collared deer in 2019-2020 and randomly generated locations within areas of home range overlap. Contact locations were derived from collared deer in central eastern Alberta, Canada (2019-2020).

Models	Intercept	Crop	Cov	Cov^2	Roads	Rugg	Streams	Wells	Edge	df	LL	AIC	Δ	*w*
Winter *Within-Group Female*														
global	-2.47	-0.89	-0.81	0.84	-0.06	0.30	-0.38	0.07	-0.07	10	-86862	173743	0	1
mod3	-2.44	-0.87	-0.70	0.74	-0.03	0.29	-0.38		-0.08	9	-86943	173904	161	0
mod4	-2.45	-0.95			-0.04	0.26	-0.37		-0.10	7	-86984	173982	239	0
mod5	-2.45	-0.99				0.27	-0.37		-0.10	6	-87002	174016	273	0
mod10	-2.75	-0.64				0.25	-0.35	0.04		6	-87035	174082	339	0
mod6	-2.73	-0.66				0.25	-0.35			5	-87076	174162	419	0
mod7	-2.75					0.26	-0.34			4	-87094	174195	452	0
mod8	-2.77						-0.35			3	-87169	174343	600	0
mod9	-2.68					0.28				3	-87622	175251	1508	0
null	-2.71									2	-87722	175449	1706	0
Winter *Within-Group Male*														
mod5	-2.55				-0.08	0.25		0.06	-0.05	6	-19855	39723	0	0.49
mod4	-2.52		0.03	-0.1	-0.09	0.24		0.06	-0.05	8	-19854	39723	0.83	0.32
mod3	-2.51	-0.07		-0.08	-0.09	0.24		0.06	-0.05	9	-19854	39725	2.54	0.14
global	-2.5	-0.07		-0.08	-0.09	0.24	0.03	0.06	-0.05	10	-19853	39727	4.24	0.06
mod6	-2.59	-0.02				0.22			-0.04	5	-19874	39759	36.0	0
mod10	-2.71	0.18				0.19	0.01	0.04		6	-19879	39771	48.1	0
mod9	-2.71					0.18				3	-19883	39772	48.9	0
mod8	-2.63								-0.03	3	-19889	39783	60.4	0
mod7	-2.62	-0.06							-0.03	4	-19888	39785	62.2	0
null	-2.71									2	-19893	39790	67.1	0

Appendix R Continued

Model	Intercept	Crop	Cov	Cov^2	Roads	Rugg	Streams	Wells	Edge	df	LL	AIC	Δ	*w*
Winter *Within-Group Mixed*														
mod5	-2.90	-3.38	1.90	-1.15	-0.1	0.60	-0.10		-0.11	9	-8471	16960	0	0.5
global	-2.90	-3.42	1.92	-1.18	-0.09	0.60	-0.10	-0.03	-0.11	10	-8470	16960	0.03	0.5
mod3	-3.08	-3.17	1.30	-0.63	-0.08	0.58	-0.12	-0.03		9	-8480	16978	17.3	0
mod4	-3.09	-3.14	1.27	-0.6	-0.09	0.59	-0.12			8	-8481	16978	17.4	0
mod6	-3.08	-3.12	1.19	-0.51		0.56				6	-8495	17002	41.7	0
mod10	-2.57	-4.42				0.56	-0.09	-0.07		6	-8525	17062	102	0
mod7	-2.57	-4.31				0.56				4	-8534	17076	115	0
mod8	-2.61	-4.44								3	-8567	17140	179	0
mod9	-2.64					0.62				3	-8621	17249	288	0
null	-2.71									2	-8663	17331	370	0
Winter *Between-Group Female*														
mod5	-2.56	-0.84	-1.34	1.48	-0.31	0.70	-0.32	0.12		9	-3637	7293	0	0.69
global	-2.55	-0.85	-1.18	1.35	-0.3	0.69	-0.31	0.12	-0.03	10	-3637	7294	1.6	0.31
mod3	-2.73		-0.84	1.18	-0.31	0.72	-0.29	0.13	-0.02	9	-3643	7303	10.2	0
mod4	-2.71		-0.81	1.13	-0.29	0.69	-0.28		-0.02	8	-3653	7321	28.4	0
mod6	-2.88		-0.96	1.33	-0.31		-0.32			6	-3669	7351	57.8	0
mod10	-2.6	-0.94				0.84	-0.32	0.08		6	-3688	7389	96	0
mod7	-2.81		-1.45	1.78			-0.30			5	-3707	7425	132	0
mod8	-2.79						-0.33			3	-3728	7462	169	0
mod9	-2.97		0.41							3	-3731	7468	175	0
null	-2.71									2	-3741	7485	193	0

Appendix R Continued

Model	Intercept	Crop	Cov	Cov^2	Road	Rugg	Streams	Well	Edge	df	LL	AIC	Δ	*w*
Winter *Between-Group Male*														
mod5	-0.73	-5.21			-0.44	1.98			-0.79	6	-354	721	0	0.69
mod3	-0.73	-5.07			-0.48	2.00	0.04	0.19	-0.77	8	-354	723	2.39	0.21
global	-1.71	-3.21	0.12	0.8	-0.46	2.01	0.01	0.20	-0.67	10	-352	725	3.84	0.1
mod4	-0.92	-6.13			-0.58		-0.04	0.17	-0.7	7	-376	765	44.6	0
mod7	-1.06				-0.57				-0.69	4	-383	773	52.7	0
mod6	-1.08				-0.61			0.20	-0.66	5	-382	774	52.7	0
mod10	-3.12	-7.51				1.54	-1.48	0.24		6	-404	820	99.2	0
mod9	-2.73					1.56				3	-409	825	104	0
mod8	-2.71				-0.5					3	-417	839	118	0
null	-2.71									2	-426	857	136	0
Winter *Between-Group Mixed*														
mod5	-2.67	-25.7	-0.34	1.21	0.30	0.61	-1.55		-0.32	9	-1152	2322	0	0.55
global	-2.69	-25.9	-0.46	1.35	0.28	0.62	-1.59	0.07	-0.31	10	-1151	2322	0.4	0.45
mod4	-1.93	-32.0			0.28	0.48	-1.68		-0.41	7	-1165	2344	22.8	0
mod3	-1.93	-32.2			0.27	0.48	-1.70	0.03	-0.41	8	-1165	2346	24.5	0
mod6	-1.30	-31.5			0.25	0.48			-0.43	6	-1173	2357	35.7	0
mod7	-1.36	-31.7			0.25				-0.42	5	-1177	2365	43.1	0
mod8	-3.53		-0.54	1.86	0.32	0.70	-1.49	0.07	-0.17	9	-1181	2379	57.8	0
mod10	-2.66				0.29	0.49	-1.60		-0.24	6	-1213	2439	117	0
mod9	-2.66				0.29	0.49	-1.61	0.01	-0.24	7	-1213	2441	119	0
null	-2.71									2	-1246	2495	174	0

Appendix R Continued

Model	Intercept	Crop	Cov	Cov^2	Road	Rugg	Streams	Well	Edge	df	LL	AIC	Δ	*w*
Summer *Within-Group Females*														
global	-2.61	-0.45	-3.06	2.7	-0.19	0.57	-0.19	-0.04	0.29	10	-66390	132800	0	1
mod3	-2.53	-0.45	-3.24	2.86	-0.18	0.58		-0.05	0.29	9	-66500	133018	219	0
mod4	-2.7		-2.92	2.66	-0.18	0.57		-0.05	0.3	8	-66556	133128	328	0
mod5	-2.69		-2.95	2.67	-0.19	0.58			0.3	7	-66575	133163	363	0
mod6	-2.77		1.03	-1.37	-0.19	0.65				6	-67127	134267	1467	0
mod10	-2.67	-0.39				0.69	-0.2	-0.09		6	-67181	134374	1574	0
mod7	-2.68				-0.19	0.66				4	-67187	134383	1583	0
mod8	-2.68					0.7				3	-67429	134864	2064	0
mod9	-2.71				-0.21					3	-67785	135576	2776	0
null	-2.71									2	-68073	136149	3349	0
Summer *Within-Group Males*														
mod4	-2.92	0.96	-1.57	1.32	-0.3		-1.65			7	-6831	13676	0	0.53
mod3	-2.98	0.95	-1.2	0.96	-0.3	-0.12	-1.67		-0.02	9	-6829	13677	0.9	0.34
global	-2.98	0.95	-1.2	0.97	-0.3	-0.12	-1.66	0.02	-0.02	10	-6829	13678	2.72	0.14
mod6	-2.91	0.88	-1.85	1.67			-1.78			6	-6895	13803	127	0
mod5	-2.93	0.87	-1.42	1.25			-1.78		-0.03	7	-6895	13804	128	0
mod10	-3.31	1.13				-0.32	-1.74	-0.03		6	-6903	13818	142	0
mod7	-3.27	1.23					-1.68			4	-6911	13831	155	0
mod8	-2.78	1.08								3	-7069	14145	470	0
mod9	-2.72					-0.21				3	-7110	14227	552	0
null	-2.71									2	-7114	14233	557	0

Appendix R Continued

Model	Intercept	Crop	Cov	Cov^2	Roads	Rugg	Streams	Wells	Edge	df	LL	AIC	Δ	*w*
Summer *Between-Group Female*														
global	-2.62	0.39	-3.19	2.55	0.07	0.54	-0.11	0.05	0.35	10	-10363	20746	0	1
mod3	-2.58	0.4	-3.23	2.59	0.08	0.58		0.05	0.34	9	-10374	20765	19.6	0
mo4	-2.6	0.42	-2.98	2.35		0.58		0.07	0.33	8	-10382	20780	34.1	0
mod5	-2.47		-3.36	2.62		0.6		0.07	0.33	7	-10386	20786	40.6	0
mod6	-2.41		-3.38	2.59		0.59			0.32	6	-10395	20802	56.4	0
mod7	-2.44		-0.11	-0.44		0.59				5	-10485	20981	235	0
mod10	-2.7	0.5				0.5	-0.08	0.07		6	-10486	20983	237	0
mod8	-2.65					0.52				3	-10513	21032	287	0
mod9	-2.52		-0.15	-0.29						4	-10533	21073	328	0
null	-2.71									2	-10552	21109	363	0
Summer *Between-Group Male*														
mod5	-4.91	4.03	5.03	-3.14	0.37		-0.30	-0.21		8	-911	1838	0.00	0.85
global	-4.89	4.03	5.22	-3.33	0.37	0.16	-0.29	-0.21	-0.02	10	-911	1841	3.49	0.15
mod3	-4.81	4.03	4.96	-3.06	0.37	0.27		-0.21	-0.02	9	-915	1849	11.1	0
mod4	-4.56	3.79	6.00	-4.34		0.24		-0.12	-0.11	8	-936	1888	49.8	0
mod10	-2.91	2.48				0.11	-0.26	-0.08		6	-940	1893	54.8	0
mod8	-2.84	2.25								3	-945	1897	59.1	0
mod7	-2.82	2.23							-0.01	4	-945	1899	61.1	0
mod6	-2.79	2.27				0.24			-0.02	5	-945	1900	61.8	0
mod9	-2.56								-0.08	3	-964	1933	95.5	0
null	-2.71									2	-965	1934	96.4	0

Appendix R continued

Model	Intercept	Crop	Cov	Cov^2	Roads	Rugg	Streams	Wells	Edge	df	LL	AIC	Δ	*w*
Summer *Between-Group Mixed*														
mod5	-4.6		7.36	-7.17			-0.41		0.18	6	-975	1961	0	0.75
mod4	-4.64		7.25	-7.04	0.01	-0.16	-0.42		0.19	8	-974	1965	3.51	0.13
mod3	-4.69		7.47	-7.22	-0.01	-0.15	-0.43	0.09	0.18	9	-974	1965	4.24	0.09
global	-4.83	0.36	7.84	-7.49	-0.01	-0.15	-0.43	0.09	0.19	10	-974	1967	6.06	0.04
mod6	-3.67					-0.33	-0.46		0.42	5	-987	1984	22.8	0
mod9	-2.75						-0.38			3	-1011	2028	67.2	0
mod10	-2.72	-0.82				-0.03	-0.38	0.12		6	-1009	2029	68.3	0
mod7	-2.76					-0.04	-0.38			4	-1011	2030	69.2	0
mod8	-2.69					0.12				3	-1021	2048	87	0
null	-2.71									2	-1024	2050	89	0
Rut *All Mixed*														
global	-3.31	-9.11	2.4	-2.14	-0.29	0.26	-0.22	-0.34	0.02	10	-2499	5018	0	0.98
mod3	-3.2	-9.29	2.54	-2.22	-0.33	0.22	-0.21			8	-2505	5027	9.11	0.01
mod4	-3.24	-9.12	2.69	-2.36	-0.32		-0.22			7	-2507	5028	10.4	0.01
mod5	-2.7	-8.92			-0.31		-0.22			5	-2517	5043	25.7	0
mod10	-2.77	-8.91				0.27	-0.19	-0.43		6	-2525	5063	44.8	0
mod6	-2.77				-0.31		-0.21			4	-2544	5097	79	0
mod9	-2.75				-0.29					3	-2556	5117	99.6	0
mod8	-3.57		3.44	-2.7						4	-2559	5126	109	0
mod7	-2.72						-0.19			3	-2565	5136	118	0
null	-2.71									2	-2574	5151	133	0

APPENDIX S. UNIVARIATE RCP BIC OUTPUT TABLES

TABLE S.1. Results of model selection using Bayesian Information Criterion for univariate general linear models relating risk of CWD to relative contact probabilities of collared mule deer in central eastern Alberta, Canada.

RCP Covariate			Intercept	Beta	df	LL	BIC	Δ	*w*
Male Hypothesis									
Winter	Within	Male	0.39	0.051	3	8742	-17458	0	1
Winter	Between	Male	0.39	0.0026	3	8694	-17363	95	0
Winter	Between	Mix	0.38	-0.00028	3	8677	-17329	129	0
Winter	Within	Female	0.38	-0.0047	3	8674	-17323	135	0
Winter	Within	Male	0.38	-0.0015	3	8673	-17321	137	0
Null			0.38		2	8667	-17318	140	0
Winter	Between	Female	0.38	-0.0027	3	8671	-17316	142	0
Male Hypothesis									
Winter	Within	Male	0.39	0.051	3	8742	-17458	0	1
Winter	Between	Male	0.39	0.0026	3	8694	-17363	95	0
Summer	Within	Male	0.38	-0.0021	3	8683	-17341	118	0
Null			0.38		2	8667	-17318	140	0
Summer	Between	Male	0.39	-0.0013	3	8671	-17317	141	0
Female Hypothesis									
Summer	Between	Female	0.38	0.010	3	8692	-17357	0	1
Winter	Within	Female	0.38	-0.0047	3	8674	-17323	34	0
Null			0.38		2	8667	-17318	40	0
Winter	Between	Female	0.38	-0.0027	3	8671	-17316	41	0
Summer	Within	Female	0.38	-0.00016	3	8667	-17309	48	0
Between Hypothesis									
Winter	Between	Male	0.39	0.0026	3	8694	-17363	0	0.94
Summer	Between	Female	0.38	0.010	3	8692	-17357	5.6	0.06
Summer	Between	Mix	0.39	-0.0039	3	8687	-17349	15	0
Winter	Between	Mix	0.38	-0.00028	3	8677	-17329	34	0
Null			0.38		2	8667	-17318	45	0
Summer	Between	Male	0.39	-0.0013	3	8671	-17317	46	0
Winter	Between	Female	0.38	-0.0027	3	8671	-17316	47	0
Rut Hypothesis									
Rut		Mix	0.38	-0.00070	3	8678	-17330	11	0
Null			0.38		2	8667	-17318	23	0

Appendix S Continued

RCP Covariate			Intercept	Beta	df	LL	BIC	Δ	*w*
Between-Male Hypothesis									
Winter	Between	Male	0.39	0.0026	3	8694	-17363	0	1
Summer	Between	Mix	0.39	-0.0039	3	8687	-17349	15	0
Rut		Mix	0.38	-0.0007	3	8678	-17330	33	0
Winter	Between	Mix	0.38	-0.00028	3	8677	-17329	34	0
Null			0.38		2	8667	-17318	45	0
Summer	Between	Male	0.39	-0.0013	3	8671	-17317	46	0
All Contacts Hypothesis									
Winter	Within	Male	0.39	0.051	3	8742	-17458	0	1
Winter	Between	Male	0.39	0.0026	3	8694	-17363	95	0
Summer	Between	Female	0.38	0.010	3	8692	-17357	101	0
Summer	Between	Mix	0.39	-0.0039	3	8687	-17349	110	0
Summer	Within	Male	0.38	-0.0021	3	8683	-17341	118	0
Rut		Mix	0.38	-0.0007	3	8678	-17330	128	0
Winter	Between	Mix	0.38	-0.00028	3	8677	-17329	129	0
Winter	Within	Female	0.38	-0.0047	3	8674	-17323	135	0
Winter	Within	Mix	0.38	-0.0015	3	8673	-17321	137	0
Summer	Between	Male	0.39	-0.0013	3	8671	-17317	141	0
Winter	Between	Female	0.38	-0.0027	3	8671	-17316	142	0
Summer	Within	Female	0.38	-0.00016	3	8667	-17309	149	0

APPENDIX T. GLOBAL RCP MODELS BIC OUTPUT TABLES

TABLE T.1. Complete results of model selection for general liner regressions relating relative contact probabilities at known contact locations from collared deer in 2019-2020 and randomly generated locations across WMU 234 in eastern Alberta, Canada.

	RCP β Estimates								
	Winter		Summer	Rut					
	Within	Between	Between						
Intercept	**Male**	**Male**	**Female**	**Mix**	**df**	**LL**	**BIC**	**Δ**	***w***
0.39	0.037	0.0020	0.0080		5	8763	-17516	0	1
0.39	0.046		0.0060		4	8750	-17491	25	0
0.39	0.046		0.0060	-0.000044	5	8750	-17489	27	0
0.39	0.046	0.0014			4	8749	-17489	27	0
0.39	0.050			-0.00018	4	8742	-17477	39	0
0.39		0.0033	0.013		4	8732	-17456	60	0
0.39		0.0026			3	8694	-17383	133	0
0.38			0.009	-0.00043	4	8695	-17382	133	0
0.38			0.010		3	8692	-17377	139	0
0.38				-0.00070	3	8678	-17349	166	0
0.38					2	8678	-17330	185	0

APPENDIX U. RCP PREDICTIVE MAPS

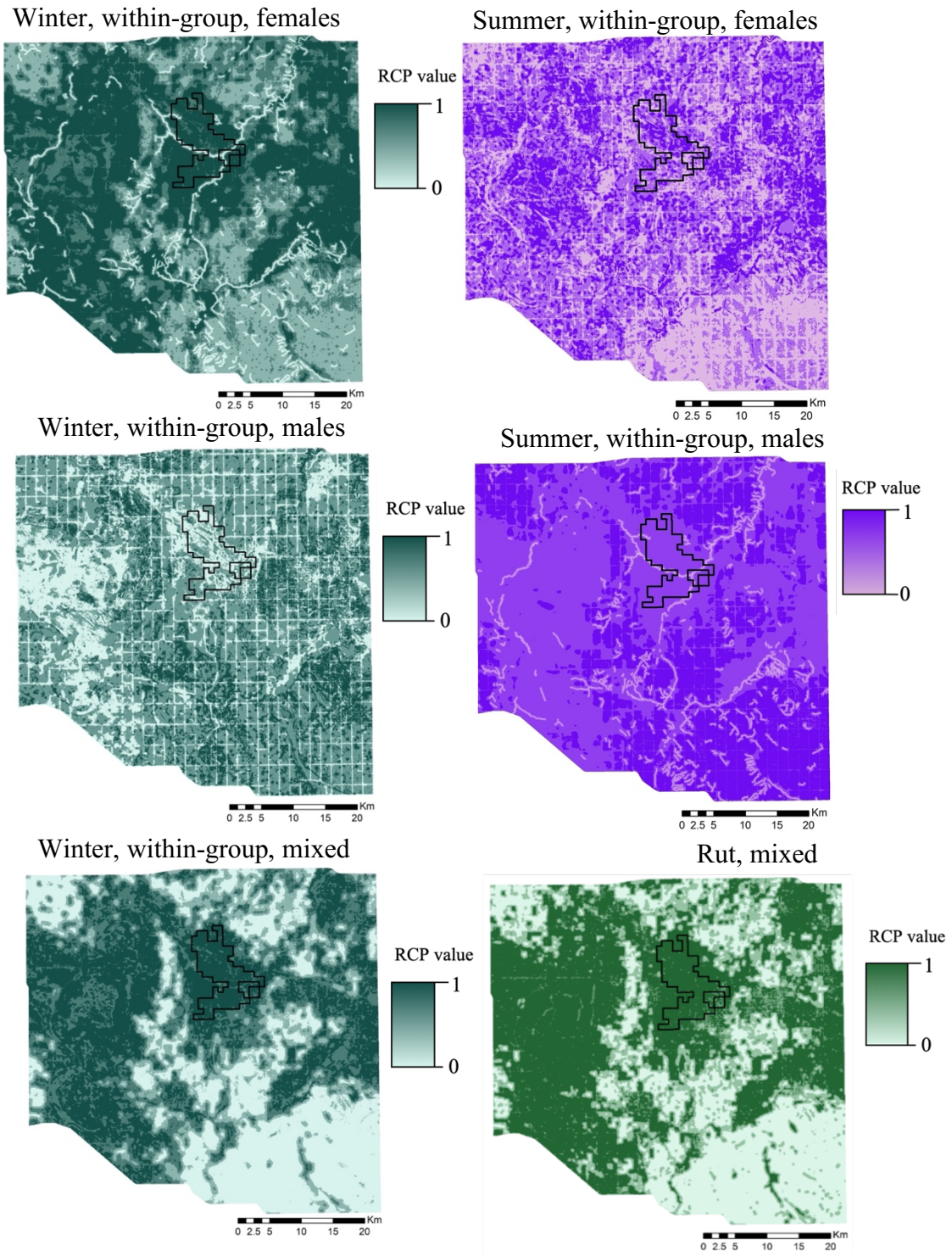

FIGURE U.1. Predictive maps depicting normalized values of relative contact probability across Wildlife Management Unit 234 for season, group types and dyad types of mule deer collared in the Cresthill Grazing Lease (black outline) in central eastern Alberta, Canada (2019-2020).

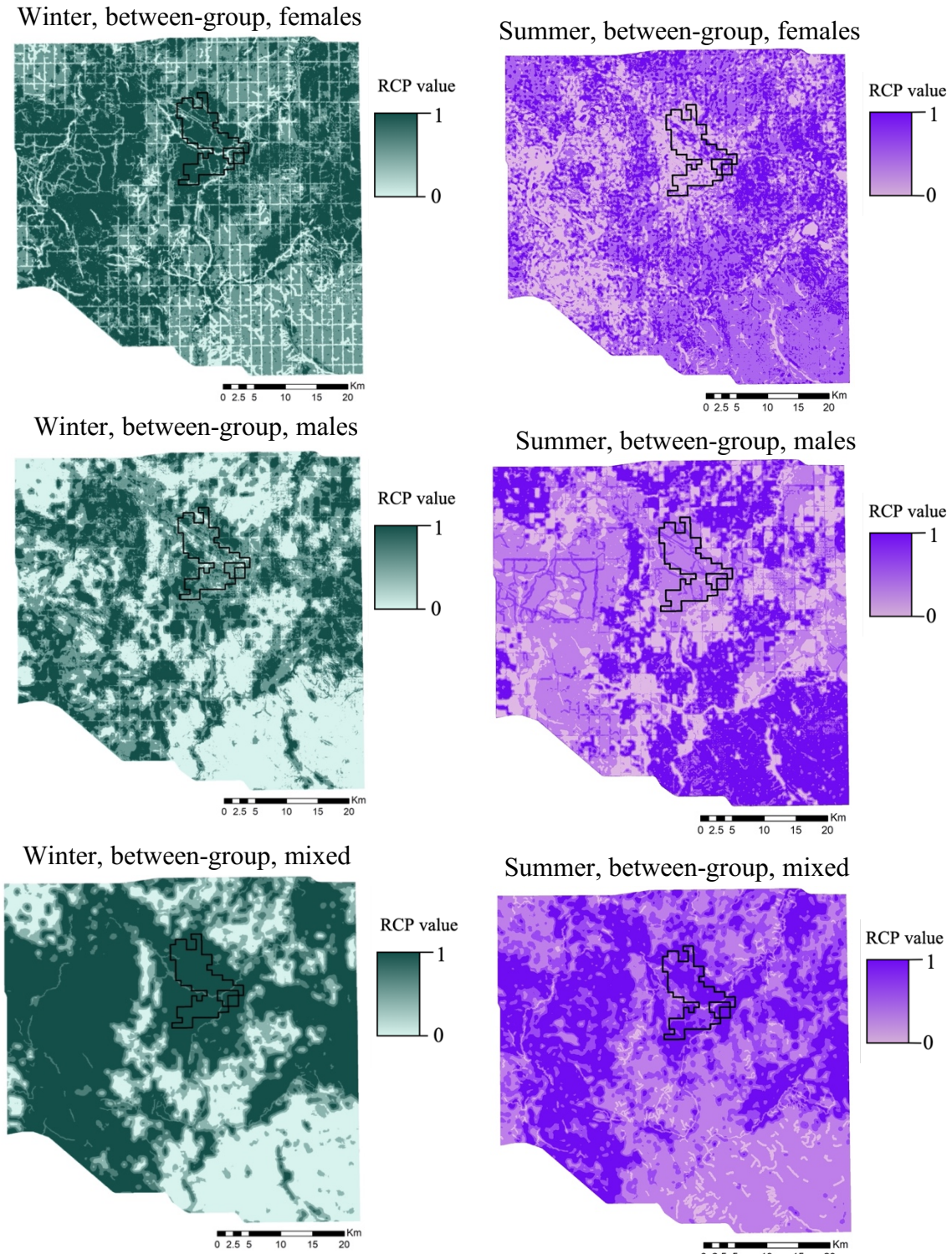

FIGURE U.2. Predictive maps depicting normalized values of relative contact probability across Wildlife Management Unit 234 for season, group types and dyad types of mule deer collared in the Cresthill Grazing Lease (black outline) in central eastern Alberta, Canada (2019-2020).